Transient Modeling and Control of

Split Cycle Clean Combustion Diesel Engine

BY

Keshav Sud

THESIS

Submitted as partial fulfillment of the requirements
for the degree of Doctor of Philosophy in Mechanical Engineering
to the Graduate College of the
University of Illinois at Chicago, 2013

Chicago, Illinois

Defense Committee:

Dr. Sabri Cetinkunt, Chair

Dr. Elisa Budyn

Dr. Michael J. Scott

Dr. Saeed Manafzadeh

Mr. Eric C. Fluga (Caterpillar Inc.)

Dr. Scott B. Fiveland (Caterpillar Inc.)

Table of Contents

Acknowledgements

I take immense pleasure today in looking back and having the opportunity to thank everyone who contributed towards the culmination of my research.

I will begin with expressing my gratitude to my advisor Prof. Sabri Cetinkunt who has not only guided me with his technical acumen and encouraged me at all times, but also influenced me in so many more ways that further fueled my passion for the subject.

I am also grateful to my mentors Dr. Scott B. Fiveland and Eric C. Fluga at Caterpillar Inc. for providing strategic direction to my work and reviewing it. My work was generously funded by Caterpillar Inc. and the University of Illinois at Chicago and I thank both the organizations for their support and allowing the use of their facility and resources. I would like to thank all my colleagues at Caterpillar Inc. who have directly or indirectly contributed towards my research by providing insights based on their vast experience.

Last but not the least; I would like to thank my parents, who kindled the dream in me and for their unfaltering faith, my very beautiful and perceptive wife, Malavika, who ensured I remained on the track for success, and her family for all their prayers and support for my intellectual pursuits.

This would not have been possible with even one of these people being absent, and the blessings of the almighty.

List of Figures and Tables

Figures

Tables

Abbreviations

SCCC – Split Cycle Clean Combustion

HCCI – homogeneous Charge Compression Ignition

CI – Compression Ignition

NOx – Nitrous Oxide family

DOE – Design of Experiments

HEX – Hydraulic Excavator

DPF – Diesel Particulate Filter

SCR – Selective Catalytic Reduction

TDC – Top Dead Center

BDC – Bottom Dead Center

CHEMKIN – Chemical Kinetics software

DYN – Dynamic

STAT – Static

HRR – Heat Release Rate

VPD – Virtual Product Development

BSFC – Brake Specific Fuel Consumption

IMT – Intake Manifold Temperature

IMP – Intake Manifold Pressure

1-D – One-Dimensional

R&D – Research and Development

NPI – New Product Introduction

CRDI – Common Rail Direction Injection

Cat® – A brand owned by Caterpillar Inc.

ESPD – Engine Speed

CA’ – Crank Angle Degrees

Abstract

Split Cycle Clean Combustion (SCCC) concept is a combustion process that results in reduced gaseous and particulate emissions while maintaining high engine efficiency when compared to the current state of the art diesel engine combustion process. Currently, some manufacturers have been commercially producing gasoline engines based on a similar Homogeneous Charge Compression Ignition (HCCI) concept, there are currently no diesel fuel powered SCCC engine existing in the market. This is due to the fact that the performance of these engines at various load conditions has not been completely evaluated.

The objective of this thesis is to design and evaluate the performance of a new diesel engine based on Split Cycle Clean Combustion (SCCC) concept for clean diesel combustion using one-dimensional simulation techniques. This study covers the engine and plant modeling of the SCCC engine using diesel fuel and comparison of its performance to a standard diesel engine of similar geometric size, to evaluate it performance and emission improvement claims.

A standard 4.4 liter displacement in-line four-cylinder engine model based on the compression ignition (CI) cycle, which is commercially available in Caterpillar Hydraulic Excavator 316, was modeled as per the dimensions. The engine model performance results were compared to the simulated test data obtained from Caterpillar and the engine model was satisfactorily validated.

A second model with similar geometry was developed on the SCCC concept with practically feasible geometry, compression ratios and air system dimensions. The design was improved

using “design of experiments” (DOE) method. The model was simulated in various configurations under part load and full load condition to obtain data for key variables such as gross power, fuel consumption, soot production, NOx production and engine controllability. This study does not include modeling of emissions for the SCCC engine, and relies on published claims of various studies and experiments for soot and NOx predictions.

Results were compared to claims of various studies in published literature, as well as to simulation results from Caterpillar’s Cat® C4.4 current production engine in their hydraulic Excavator 316. The results confirm that SCCC engine operating on diesel fuel can be designed to have similar thermal efficiency and power density to a conventional compression ignition cycle based engine of the exact same displacement, while also substantially reducing the presence of unburned hydrocarbons, NOx and Soot particles in the exhaust.

Chapter 1

1.1 Problem Statement

The objective of this study is to design and model a diesel engine based on the Split Cycle Clean Combustion (SCCC) concept, determine its steady state and transient performance and compare results to an in-line 4-cylinder 4.4 liter diesel engine which is used on Caterpillar hydraulic excavator (HEX) machine model 316, as well as to results reported in the published literatures.

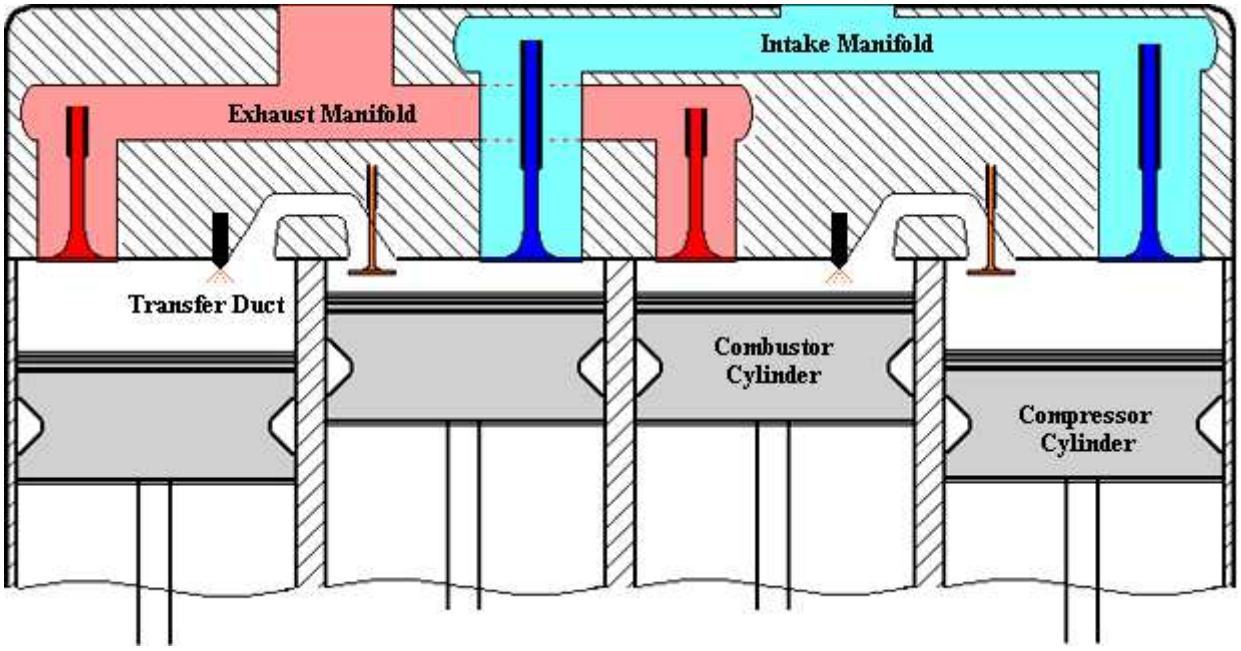

Fig. 1 Split Cycle Clean Combustion Engine (SCCC) Concept.

The transient performance of the entire engine system, i.e. engine and its air management system together, has never been evaluated before and is crucial to understand and accurately predict in order to ensure successful practical application of this concept.

Fig. 1 illustrates the basic geometric design of a Split Cycle Clean Combustion (SCCC) engine concept. The main difference compared to a conventional compression ignition diesel engine is that the exhaust valves are absent in adjacent cylinders, instead adjacent cylinders are connected together by a transfer duct that carries a high pressure charge of fuel air mixture from the "compressor cylinder" to the "combustor cylinder". Cylinders 2 and 4 are compressor cylinders and cylinders 1 and 3 are combustor cylinders. The compressor cylinder gets in fresh atmospheric air (or compressed air in turbocharged applications) via the intake valve, it then compresses the air which then travels to the combustor cylinder through the "transfer duct". Fuel is injected using a fuel injector into the combustor cylinder that vaporizes and mixes with the incoming high speed compressed air before it reaches the point of ignition. The combustion process then takes place in the combustor cylinder and the exhaust gasses are let out via the exhaust valve from the combustor cylinder. In this design, two cylinders (compressor and combustor cylinders) work as a pair for a complete combustion cycle.

This thesis study uses a one-dimensional computer modeling and simulation approach to predict split cycle clean combustion (SCCC) engine performance in both a naturally aspirated and a turbocharged configurations, and then compare its steady state and transient performance characteristics to a commercially available comparable sized compression ignition diesel engine.

In this process, a Caterpillar's 4.4 liter displacement compression ignition engine that is currently in production in their 316 HEX, in one-dimensional simulation software called "Dynasty" (a proprietary one-dimensional modeling software owned by Caterpillar Inc.). This model is run at multiple steady state points and transient operating conditions with continuous engine rpm sweeps at varying fueling and load conditions. Results are compared to simulated test data available from Caterpillar engine testing facility. A good correlation confirms and validates our 4.4 liter compression ignition based engine model which is being used as a baseline for our study.

In order to confidently model a SCCC engine, we first validated our modeling methodology by replicating the work presented by *University of Pisa* in their SAE paper "Clean Diesel Combustion by Means of the HCPC Concept 2010-01-1256" by Ettore Musu, Ricardo Rossi, Roberto Gentili and Rolf D. Reitz. Their Computational Fluid Dynamics (CFD) based model was reproduced as a one-dimensional model in Dynasty and results were compared back to validate the accuracy of our modeling approach.

A 4.4 liter compression ignition based engine model in Dynasty is modified to run on the SCCC concept. Modification are made within the packaging constraints discussed with Caterpillar's engine research team to achieve a realistic geometry, while remaining within dimensional and volumetric constraints of the 4.4 liter engine block. Various versions of this model were built with different transfer duct configurations to exploit difference control strategies and evaluate their impact.

SCCC engine model was simulated at various steady state points and transient conditions to obtain results that were compared to results obtained from running Caterpillar's Cat® C4.4 compression ignition engine model under similar conditions. Feasibility and performance of SCCC engine in real world applications was predicted.

1.2 Significance

SCCC engine operating on diesel fuel boasts of a significant reduction in unburned hydrocarbons, soot and NOx levels in the exhaust by providing a cleaner combustion with similar performance to compression ignition diesel engines. Lower exhaust emission levels will help in meeting the emissions requirement without the extensive use of after-treatment technologies.

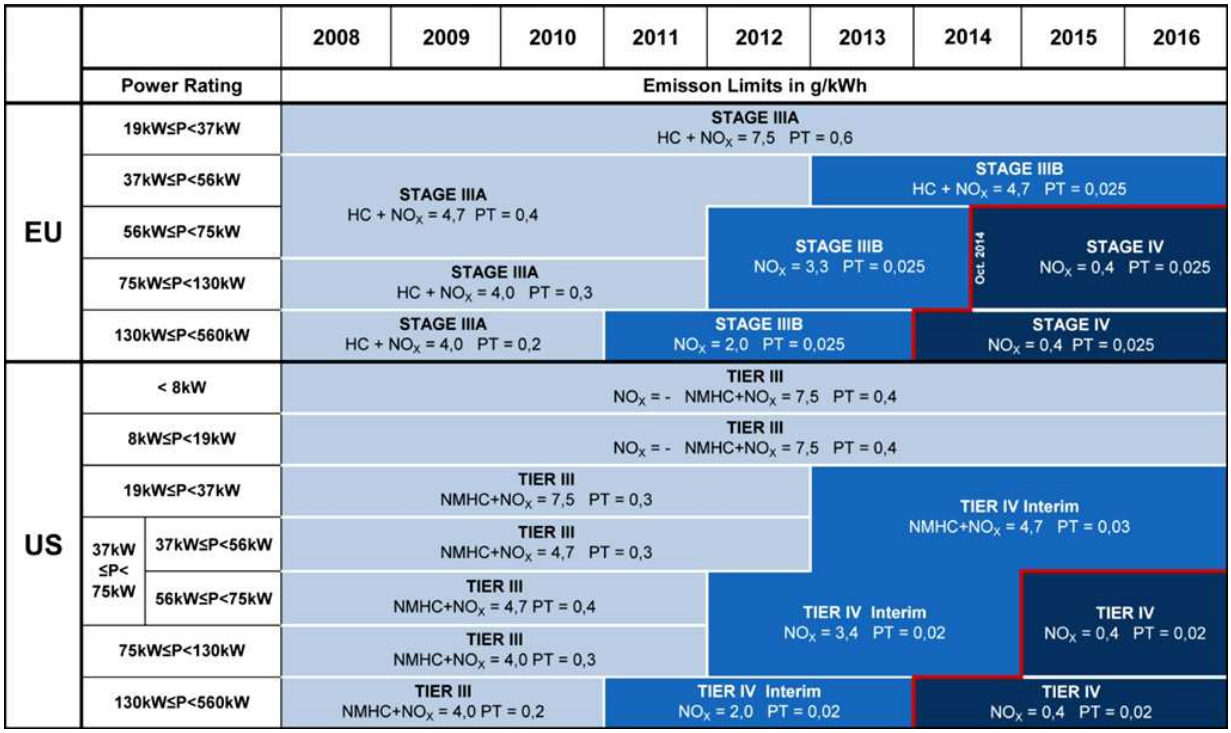

Fig. 2 USA and Europe emissions limits. (Sourced from www.boschrexroth.com)

The emission limits in g/kWh of the controlled pollutants as set by the U.S. Environmental Protection Agency (EPA) a showing in fig. 2. Continental Europe and the United States of America have the stricter emissions limits compared to other nations. Emission limits are

categorized based on the power the engine is certified for. For the 130-560kW category soot and NOx pollutant limits would have reduced to 1/10th by the year 2016 from the permissible limits that existed in 2008. To meet the emission requirements the current industry is heavily dependent on after-treatment technology. After-treatment is defined as the treatment of exhaust gasses once they exit the engine to either a filter or by chemically neutralization of the controlled polluting elements. This technology utilizes a "diesel particulate filer" (DPF) to filter soot particles, and "selective catalyst reduction" (SCR) with UREA liquid injection to chemically neutralize NOx species to nitrogen and water vapor. Fig. 3 illustrates the significance of after-treatment technology in reducing emissions to meet Tier 4 Interim requirements.

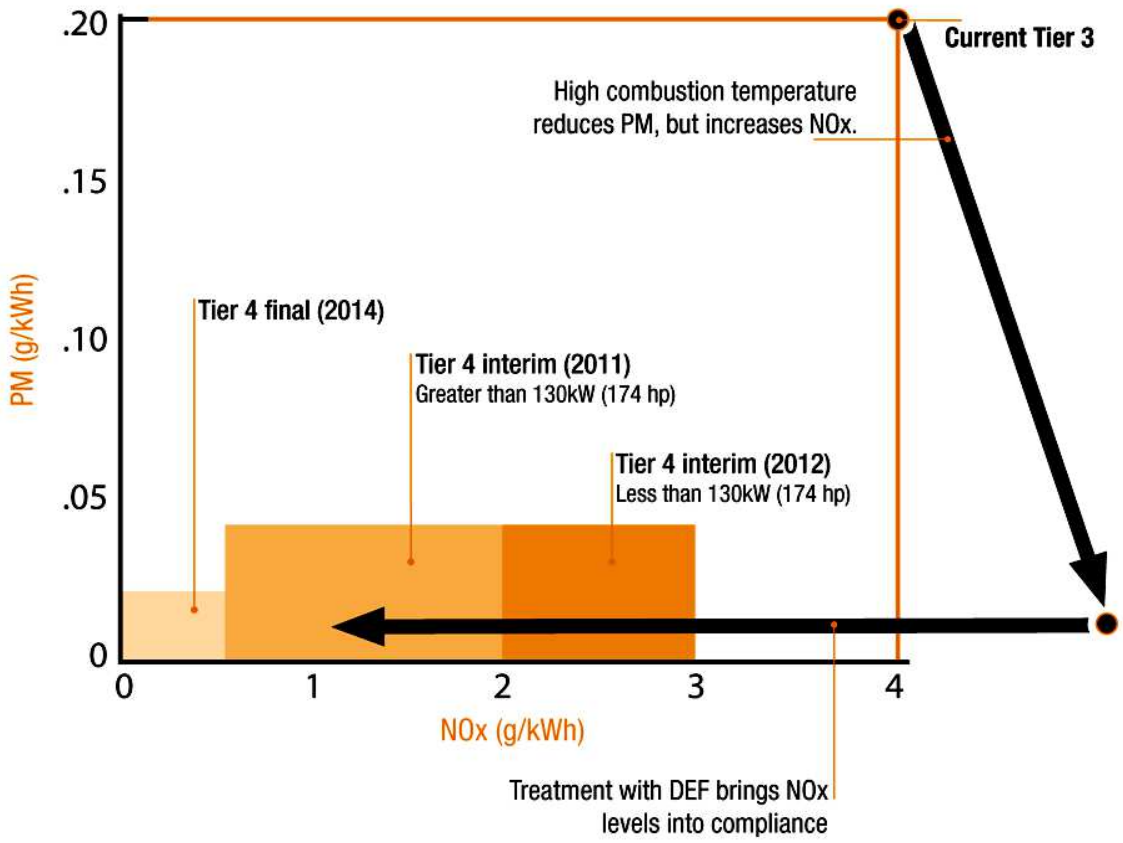

Fig. 3 Impact of after-treatment technology. (Sourced from www.cnh.com)

Fig. 4 describes the basic schematic of a six cylinder turbo-charged diesel engine with after-treatment. The diesel particulate filter (DPF) and selective catalyst reduction (SCR) are added as an after-treatment package to the exhaust end of the engine system.

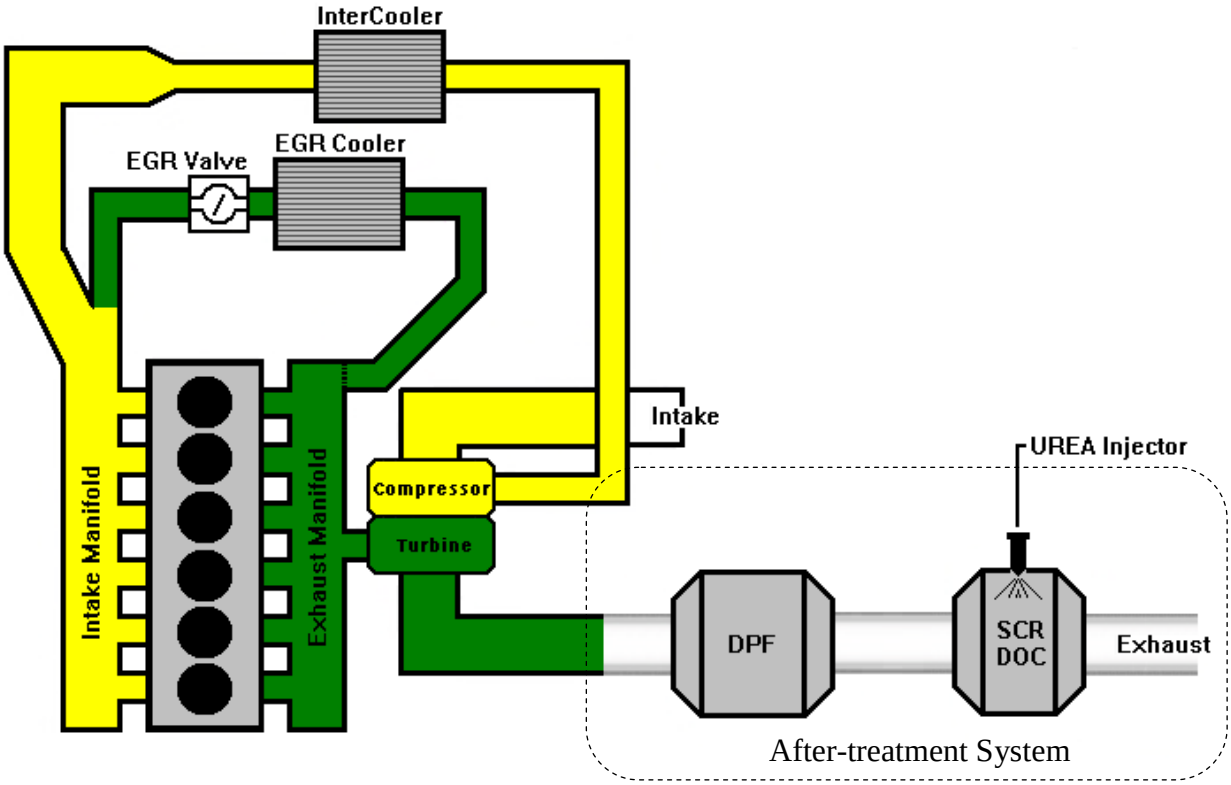

Fig. 4 Schematic of six cylinder turbo-charged diesel engine with after-treatment.

After-treatment technology has some major drawbacks which is forcing the industry to research alternatives of reducing emissions using other means. This was one of the major factors encouraging this thesis study. DFP and SCR in principle try to eliminate the unwanted emission from the exhaust gasses once they have already been produced inside the combustion chamber.

The after-treatment components required by the current engine design add a lot of bulk to the engine size and thus cause limitations to engine applications.

A Diesel Particulate Filter (DPF) is a non-restrictive mesh with channels parallel to direction of exhaust flow, the mesh is made of precious metals (such as Platinum, Palladium and other metals) that attract Soot (carbon) particles by property, the rest of the exhaust gas passes without any restriction. The DPF add significant cost to the engine. Over time the filter gets clogged due to the buildup of soot particles and has to go through a periodic regeneration process (during which the engine is inoperable), which involves injection and burning of raw fuel in the DPF cavity to oxidize the adhering soot particles into CO_2 and blow them out the exhaust. The injection of extra fuel into the DPF adds to cost of fuel to operate the engine and also causes engine down time.

Selective catalyst reduction (SCR) is the injection of UREA fluid $CO(NH_2)_2$ into the exhaust flow which chemically reacts to the NOx species in the exhaust and converts them to neutral nitrogen and water vapor. The injection of UREA fluid demands the existence of separate urea injector and its controls. To maintain a continuous supply of UREA fluid, an additional storage tank is needed which add to bulkiness of the engine and replenishment of UREA adds cost related to storage and procurement of an additional fluid. In summary, the after-treatment technology adds significant cost and complexity to an engine system. Thus, the industry is in need of an alternate less complex method of emissions reduction.

This thesis study demonstrates the potential of meeting the lower emission requirements set by EPA by using the Split Cycle Clean Combustion (SCCC) diesel engine concept. SCCC lowers emissions produced in the combustion chamber comparing to a conventional diesel engine by developing a better and more uniform charge composition. This improved the fuel burn during the combustion process, produces much less soot and NOx in the exhaust. Thus SCCC can eliminate the need for any after-treatment system.

This study is a significant contribution to all applications employing diesel engines as a power source and fall under the emissions regulations. Heavy industrial equipment and engine manufacturers will benefit from this thesis study by gaining insight and a better understanding of the transient behavior and performance of a SCCC engine under various fueling and load conditions. Further study of the SCCC engine concept tailored to their respective applications could lead to its wide commercial applications.

1.3 Split Cycle Engine Concept

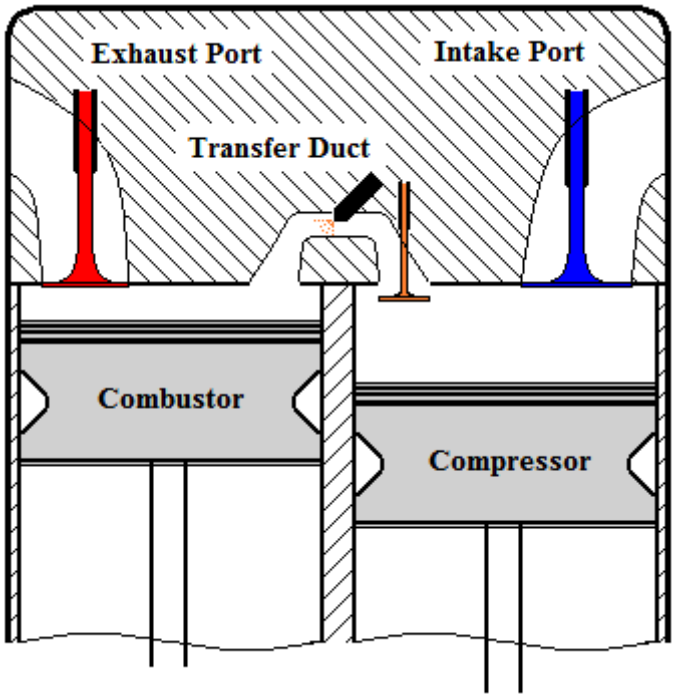

Fig. 5 Schematic of simple two-cylinder split cycle clean combustion engine.

The SCCC engine is different from the conventional diesel engine, as it has a separate cylinder for compression of air and another cylinder for combustion of the fuel air mixture. In a conventional diesel engine, each cylinder does both compression and combustion. In an SCCC engine air enters into the compression cylinder of the engine, it then gets compressed and transferred into the combustor cylinder of the engine through the transfer duct. During transfer fuel is injected into the combustor cylinder right at the end of the transfer duct, so the fuel injection utilizes the temperature and velocity of incoming charge and also gets more time that a

conventional diesel engine to produce a more uniform fuel air mixture. This mixture is understood to be a partially homogeneous mixture which then auto-ignites after the physical and chemical delays of combustion are passed. Another key difference between the conventional diesel engine and SCCC engine is that the compression ratio of the compression and combustion cylinders differ from each other to assist in maintaining a positive pressure bias between the compression and combustion cylinders which aids in the charge transfer through the transfer duct.

The SCCC engine explained in this thesis study operates on a two-stroke cycle. Fig. 5 shows two cylinders working as a pair in the SCCC engine with the fuel injection taking place into the transfer duct instead of in the combustor cylinder.

Fig. 6 explains the operation of a SCCC engine on the two-stroke cycle by segmenting a 360 degree revolution into four key stages.

The four stages are described as the

a) Intake stage,
b) Compression stage,
c) Combustion stage,
d) Exhaust Stage,

Stage 1: Intake: Fresh air enters the compression cylinder through the intake port when the intake valve is open, once the piston reaches close (dependent on valve timing) to bottom dead center (BDC), intake valve closes and Stage 2 of the naturally aspirated operation of the engine beings.

Stage 2: Compression: While the intake valve closes, the piston now moves upwards compressing the air within the compression cylinder, a little before the piston reaches top dead center (TDC), the smaller transfer valve opens and the charge (compressed air) rushes into the combustor cylinder through the transfer duct. During the charge transfer fuel is injected into the transfer duct, which mixes rapidly with the high temperature compressed air and makes a relatively homogeneous compressed fuel air mixture.

Stage 3: Combustion: Once the piston in the compression cylinder crosses TDC, the transfer valve closes and stage 3 begins. The compressed fuel air mixture in the combustor cylinder has crossed the temperature and pressure thresholds required for auto-ignition and the combustion starts with a very high heat release rate being typical of SCCC.

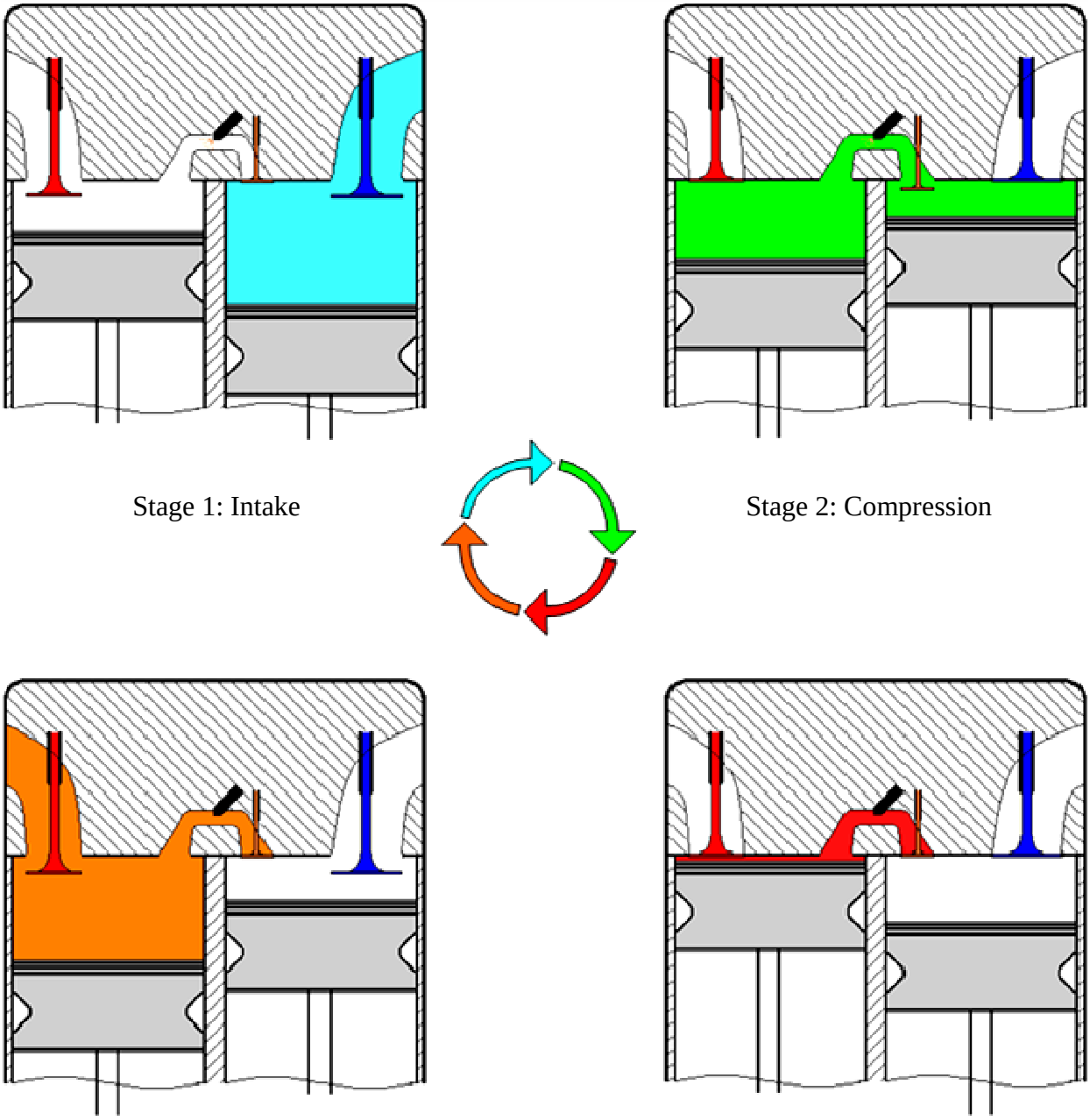

Fig. 6 Staged operation of a two-cylinder split cycle clean combustion engine concept.

Stage 4: Exhaust: The energy released during combustion is absorbed and converted into rotational motion by the piston and crank shaft in the combustion cylinder on its way down. Once this piston reaches BDC the exhaust valve opens and the exhaust gasses escape.

The energy release and absorption during combustion in a SCCC engine differs from that in a conventional compression ignition engine. Fig. 7 shows the pressure-volume (PV) diagram of the SCCC engine and CI engine. The area highlighted in blue is the work done in the compression cylinder and the area in red is the total available work which is different to the available work highlighted in red in the plot on the left.

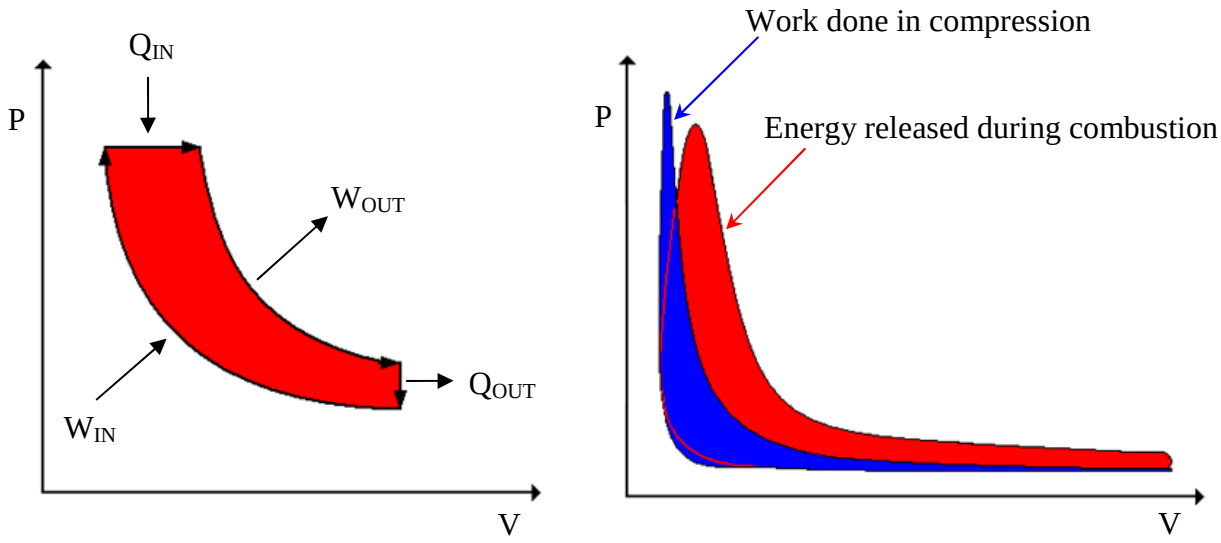

Fig. 7 a) PV diagrams of CI engine. *b) PV diagram of SCCC engine.*

1.4 Literature Review

Assanis et al [49] provided a schematic of the methodology to analyze transient heat release in subsequent cycles in a diesel engine. Techniques were described to infer mass of air trapped in a cylinder and mass a fuel injected along with the predicted growth in accumulated residual burnt gasses. Their parametric effects were studied under pressure gradients, piston motion and short circuiting by valve overlap. The mass of fuel injected was deduced by integrating injection pressure and injection duration, this mass of fuel along with the above mentioned parameters were used to accurately define the instantaneous thermodynamic state of a mixture and a characteristic heat release was developed for transient engine operation.

Fiveland et al. [12] studied a four stroke HCCI Engine using simulation. They used CHEMKIN libraries for mass, species and chemical modeling, CHEMKIN libraries were then coupled with gas exchange, turbulence and heat transfer models and integrated over an entire engine cycle to complete one HCCI simulation. A variable volume bomb was used for computations. Variation in ignition versus temperature, pressure, equivalence ratio and composition were evaluated. Also a cumulative affect on output parameters was examined as input parameters such as inlet air pressure and temperature were varied.

Babajimopoulos et al. [3] presented a detailed study of the gas exchange processes in HCCI combustion as a function of valve events. The study is based on a full cycle simulation of an HCCI engine in steady state, the engine cycle is segmented into two stages which are coupled together but solved using two individual codes. KIVA-3V a multi-dimensional fluid mechanics

code was used to simulate exhaust, intake and compression up to the transition point after which chemical reactions became important, the KIVA-3V results were then used as initial conditions for the a thermo-kinetic code to compute the combustion and expansion part of the cycle. After validation of results against experimental data an application method was described with respect to variable valve actuation.

Fiveland et al. [10] studied a quasi-dimensional thermodynamic simulation model of a turbocharged homogeneous charged compression ignition (HCCI) concept employing three thermodynamic zones within the cylinder to predict heat exchange and emission by accurately modeling the development of chemical species over the period of combustion. The combustion volume was modeled into three thermodynamic zones like the physically based core, boundary layer and crevice zones. The study described a method to integrate a complete chemical kinetics combustion model with a complete physical model of a turbocharged homogeneous charge compression ignition engine.

Simescu et al. [4] performed an experimental investigation of a partial premixed charge compression ignition (PCCI) diesel engine for combustion characteristics and emissions in a heavy duty application. In this study PCCI was used along with direct fuel injection on a Cat® C-15 heavy duty engine. Fuel was sprayed into the intake manifold and also directly into the combustion chamber. Impact on engine performance, emissions and efficiency was characterized as a function of various manifold injector geometries, percentage of total fuel quantity into the manifold. The test results also discussed the production of NOx species and incomplete products of combustion such as carbon monoxide and unburned hydro carbons (UHC) with respect to

partial premising. This study emphasized the severe need of optimization of spontaneous ignition of the premixed charge.

Khalid et al. [5] analyzed the relation between mixture formation during the time between period of ignition delay and the beginning of burning process in diesel combustion. Emissions are largely dependent on the mixture formation before combustion, to simulate the combustion chamber this study used a rapid compression machine with changing experimental parameters like ambient density, swirl velocity and injection pressure. A high speed digital camera was used to construct Schlieren (i.e. optical in-homogeneities in transparent material not visible to the human eye) photographs and to investigate mixture formation. This study provided a clear overview of outputs like spray evaporation, spray interference, mixture formation, ignition process and flame development. The study also articulated that high pressure injection is the key to improvement in mixture formation and reduce emission levels under high ambient density, as in engines with forced induction.

Kang et al. [9] at General Motors (GM) produced two test vehicles powered by gasoline HCCI engines. This paper explained the controls used on the test vehicles, by outlining the control strategy most feasible for the HCCI's flameless combustion process. The parameters being controlled were:

a.) EGR rate,

b.) Air fuel ratio,

c.) Variable valve timing,

The engine controller was designed to keep these parameters with the preset limits while monitoring combustion efficiency and emissions. The controller was tested and demonstrated on a single cylinder and multi-cylinder engine operating in dual SI-HCCI mode.

Musu et al. [1] used CFD modeling to evaluate the performance and characteristics of naturally aspirated homogeneous charge progressive combustion engine. Their study was based on a steady state analysis using CFD through various equivalence ratios. They tested three different transfer duct geometries trying to improve the flow efficiency and reduce the speed of air through the duct. Their study described the benefits of having a different compression ratio in the combustion and compression cylinders, the impact on Soot and NOx emission under high load conditions.

There are studies that articulate a concern of HCCI combustion losing efficiency under higher equivalence ratios and high engine loads, thus studies of possibly having a dual mode engine operation like SI-HCCI and CI-HCCI mode shift are floating in the industry. Etheridge et al. [51] studied a fast running yet detailed chemistry model focusing on capturing the transition state going from Spark Ignition (SI) to HCCI combustion as operating load requirements dropped in their four stroke, inline four cylinder, direct injected engine model. The study was based on a Stochastic Reactor Model (SRM) coupled with a one dimensional simulation software GT-Power. The study also explained tuning parameters to optimize the SI-HCCI mode transition while keeping the NOx emission low.

Mo et al. [50] studied the HCCI combustion in detail in his PhD dissertation and provided information to fill in some gaps unfilled by current experimental knowledge. The study explains the cylinder temperature distribution, analysis the instability and misfire mechanism. The study isolated many key variables and produced a parametric study around them providing a clear impact that each of those variables play in the operation of an HCCI engine. This study used a relatively new KIVA-MZ model with a new mapping scheme between CFD cells and thermodynamic zones as a virtual experimental setup to validate the combustion process. A one-dimensional model was also built to facilitate fast iterative processes of evaluating the impact of change in each variable. A variable combination of nine engine geometric and operating parameters was investigated with respect to their impact on ignition timing. The effect of ignition timing was subsequently evaluated on combustion efficiency and burn rate. Results showed that engine geometric parameters influenced in-cylinder temperature distribution more than the operating parameters and that ignition timing cannot be controlled independently. The study also explained that ignition timing is the most important variable of the HCCI combustion process along with other influential parameters such as equivalence ratio, engine speed and crevice volume. A direct relationship between crevice volume and combustion efficiency was established. This parametric study in CFD yielded trend correlations which were introduced into a one-dimensional simulation software GT-Power and was used to evaluate combustion instability and misfire.

Chapter 2

2.1 One Dimensional Modeling Approach

Below is a high level comparison between the benefits and drawbacks of choosing one dimensional over three-dimensional or computational fluid dynamics (CFD) based modeling. The primary concern amongst researchers is loss of results fidelity using one-dimensional simulation, which often drives them away from using it despite of all its benefits. If the correct approximations are made, the model geometry is constrained, one-dimensional simulation can yield very high fidelity results when compared to CFD.

CFD

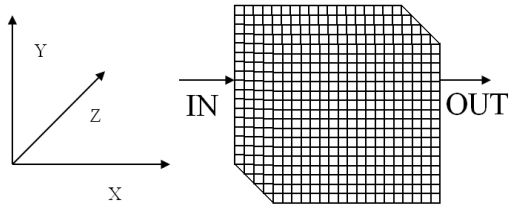

1. Slow simulation time
2. Better port modeling
3. Full descriptive geometry
4. High fidelity results
5. Limited by memory
6. Not feasible for iterative analysis.

One-Dimensional

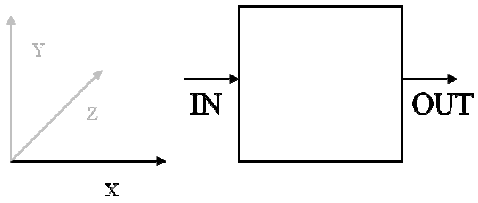

1. Fast simulation time
2. Ability to model the entire engine and air system.
3. Ability to examine plant balance
4. Evaluate overall engine efficiency.
5. Capture air system behavior.

2.2 Split Cycle Clean Combustion Engine

HCCI combustion has been studied using limited geometry models with CFD modeling, as the concept has so far shown promising results, a lot of interest is expressed in developing it further. For significant contribution to the HCCI concept a CFD model is found to be very slow thus not feasible for iterative analysis, parametric studies, design and controls development. Due to the computational overhead created by CFD models, researchers try to simplify their geometry or model only the minimal required components to save as much time as possible, as a result the outputs of the CFD model are based on many assumed boundary conditions and the behavior of HCCI combustion in conjunction with all its air systems has been very difficult to explore.

In this thesis study it was decided to model the entire Split Cycle Clean Combustion Engine along with all its air systems in one-dimension to determine/develop the entire engine operation efficiency and feasibility. For modeling purposes, Caterpillar's proprietary one-dimensional simulation software, "Dynasty" was used. All essential engine components such as air cleaner, intake manifold, intake valves, compression cylinder, transfer duct, combustion cylinder, crankshaft, exhaust valve, exhaust manifold and muffler were modeled. Many variants of the SCCC engine model including few turbocharged variants were built. The turbo charging, cooling package and intercooling ducts were also modeled.

2.2.1 Geometric Model

The entire engine comprising all air system (naturally aspirated and forced induction), crank shaft, engine cylinders, turbocharger, heat exchanger and air to air after cooler components were modeled. Fig. 8 shows a one-dimensional plant model of a naturally aspirated SCCC engine with one combustion cylinder and one compression cylinder. Turbocharged variants of the SCCC Engine were also modeled but not shown to aid ease of understanding.

Fig. 8 contains the following engine components and later in this thesis, the turbocharged version of SCCC engine also shows the turbocharging components.

a) Air Intake

b) Intake Manifold

c) Intake Valve and Port

d) Compressor Cylinder

e) Transfer Valve and Port

f) Transfer Duct

g) Combustor Cylinder

h) Exhaust Valve

i) Exhaust Manifold

j) Muffler

k) Crankshaft and Timing Components

Fig. 8 One dimensional SCCC engine model schematic in Dynasty.

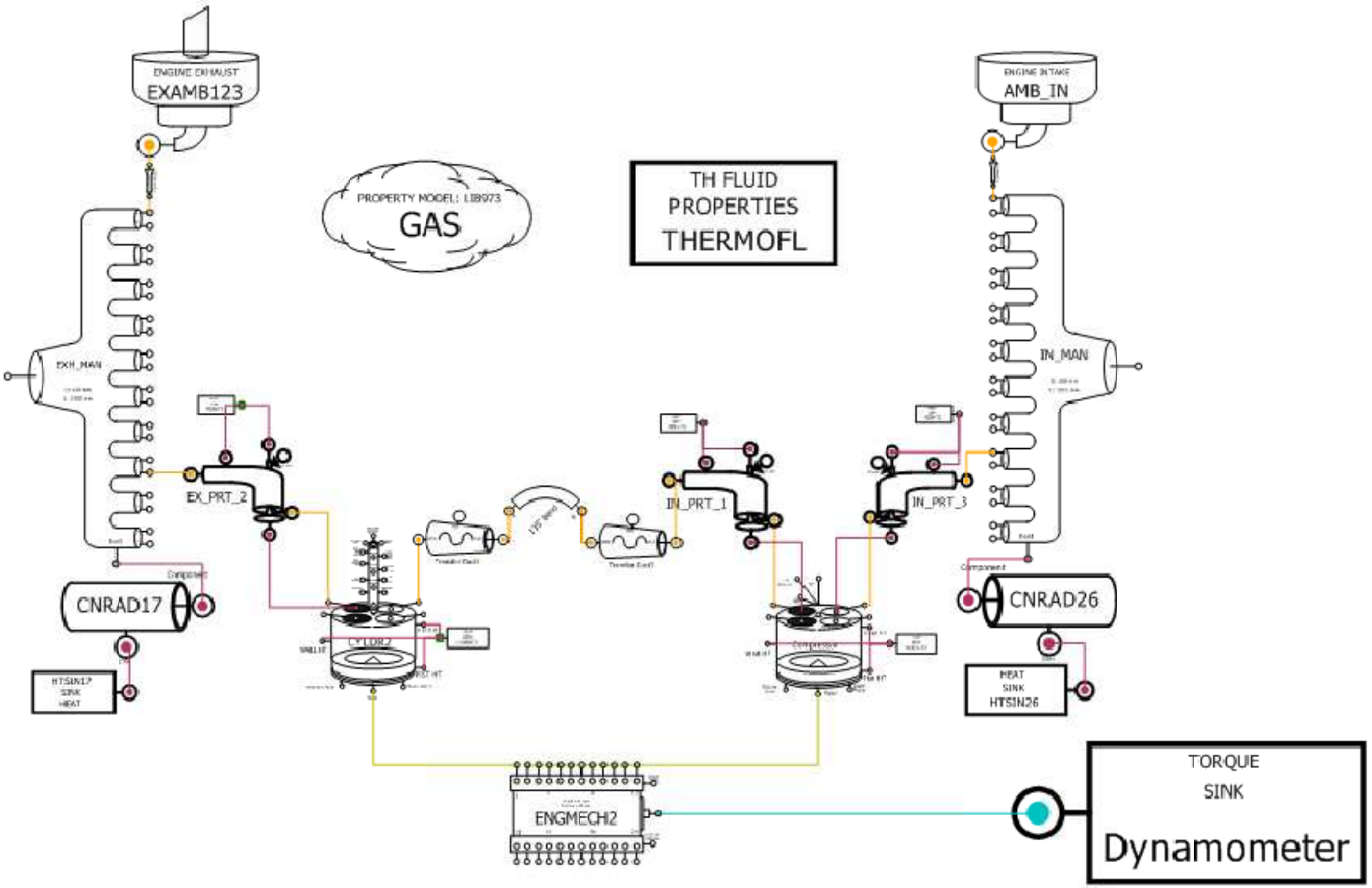

2.2.2 Air Systems Model

2.2.2.1 Air Cleaner

This component acts as an air passage from the atmosphere into the intake manifold. It was modeled to impose the appropriate restrictions and efficiency of filtration. Composition of intake gas as well as atmospheric temperature and pressure boundary conditions can be defined in this component.

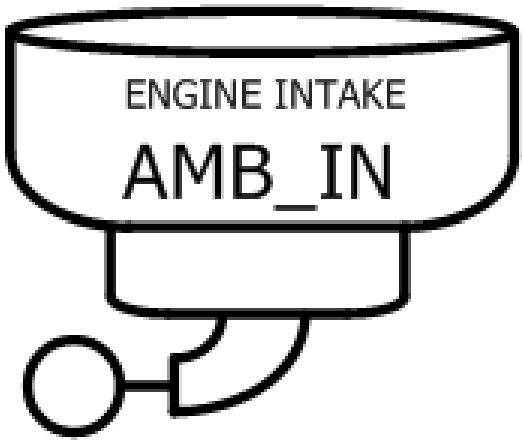

Fig. 9 Air cleaner subsystem.

Unless the filter is specified as clogged in percentage, it is assumed that the gas passing through the component passes through an infinite area and thus carries zero velocity at point of inlet, however an intake mass flow rate is computed based on manifold vacuum. The simulation code begins tracking the mole fraction of Oxygen and Carbon Dioxide in the system from this point.

$$V_{IN} = 0 \quad (1)$$

$$H_{IN} = f(P_{IN}, T_{IN}, \phi_{IN}) \quad (2)$$

Where:

V_{IN} = Velocity

H_{IN} = Energy

P_{IN} = Pressure

T_{IN} = Temperature

ϕ_{IN} = Equivalence Ratio

2.2.2.2 Intake/Exhaust Manifold

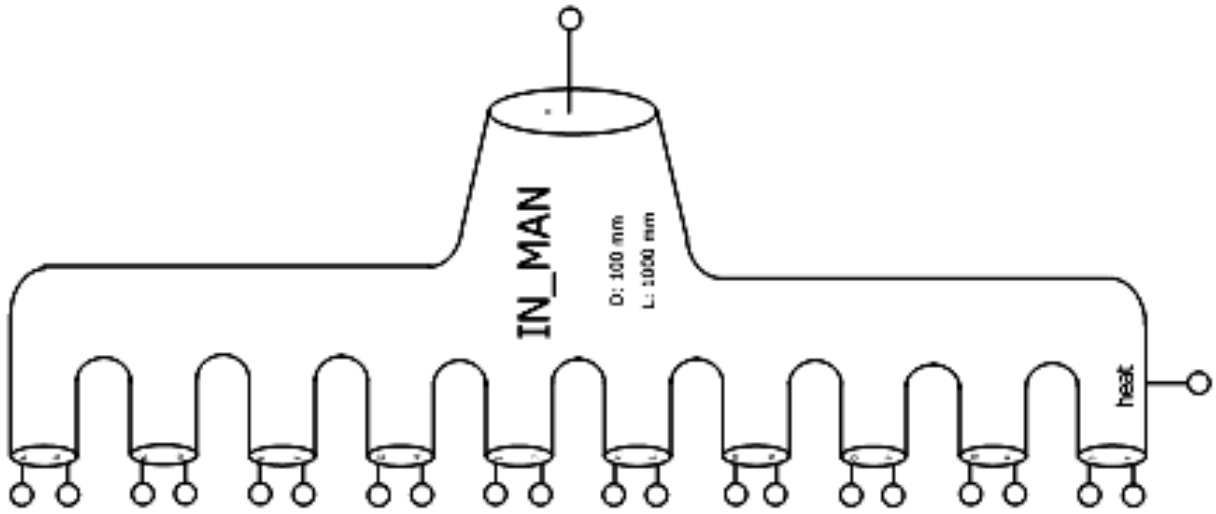

Fig. 10 Intake/Exhaust manifold subsystem.

This component acts as a constant volume for compressible fluid flow to represent intake and exhaust manifolds in engines. It also allows setting constant temperature condition if required.

Convection based heat transfer is modeled to dissipate or absorb heat from a surrounding jacket of coolant or water.

It is assumed that the gas properties are homogeneous throughout the gas volume, the component walls are rigid implying a rigid volume boundary condition and for all heat transfer calculations the component is considered to be cylindrical in shape.

$$\frac{dm}{dt} = \sum_i \dot{m}_i - \dot{m}_{WC} - \dot{m}_{AC} \tag{3}$$

Where:

M_i = Mass of air species

M_{WC} = Mass of condensed water

M_{AC} = Mass of condensed sulfuric acid

$$P = f(\rho, T, \phi_b, \phi_{ub}) \tag{4}$$

Where:

ρ = Air density

T = Temperature

ϕ_b = burnt equivalence ratio

ϕ_{ub} = unburned equivalence ratio

$$\dot{q}_{Heat} = h_c A_{surf} (T_{Heat} - T) \quad (5)$$

Where:

$\dot{q}_{Heat}$ = Rate of surface heat transfer.

h_c = Heat Capacity

A_{surf} = Surface Area

T_{Heat} = Temperature of heat sink

T = Temperature

2.2.3 Compressor/Combustor Cylinder Model

This component model is a simple single-zone, compression-ignition, direct-injection combustion chamber with heat transfer through the head, valves, piston and liner of the cylinder. The chamber solves for three characteristic variables: gas, heat and translational. Fuel can be introduced into the cylinder by either specifying a heat release in kJ/deg by using the connectors at the top to inject Fuel (kg/s) using an “injector component”.

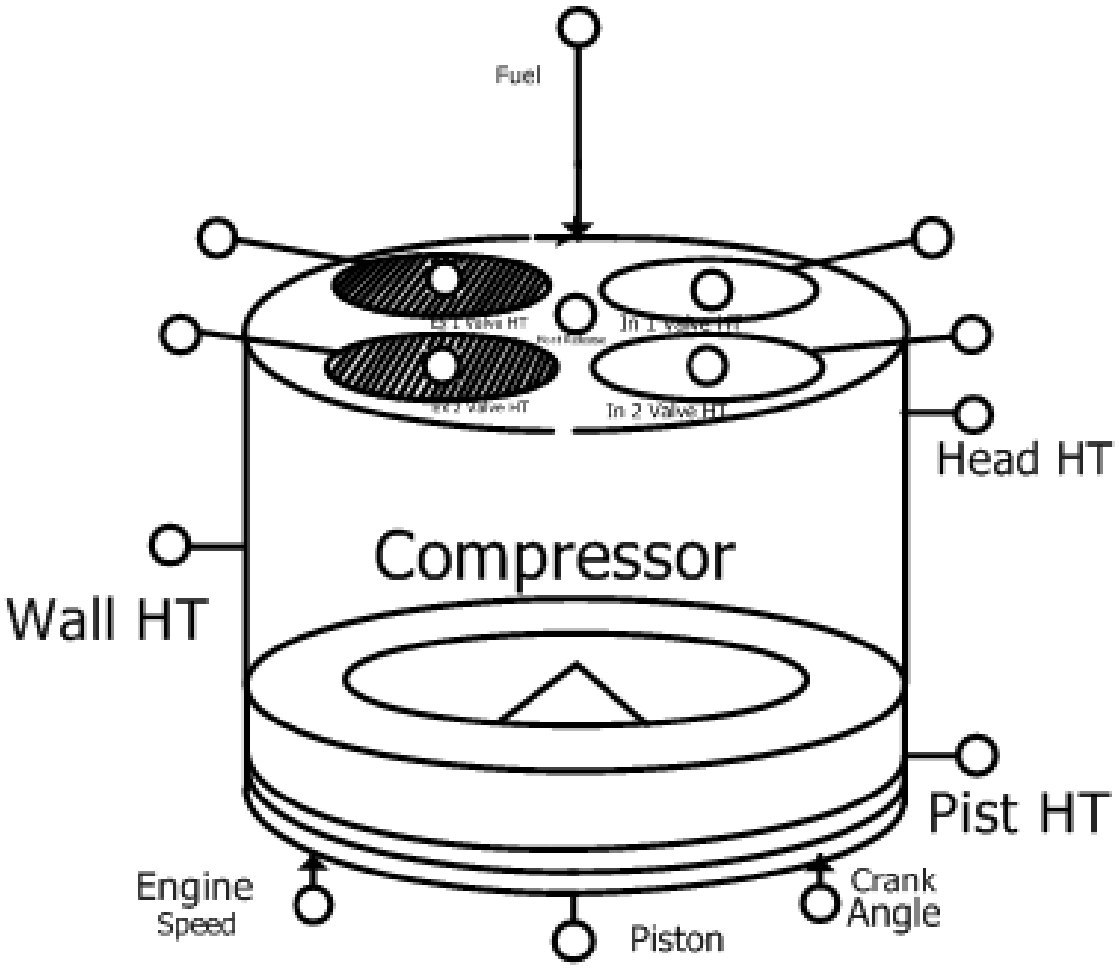

Fig. 11 Cylinder subsystem.

As can be seen in the fig. 11, heat transfer is calculated at three nodes, wall, head and piston using *Woschni* heat transfer model for the convective heat transfer modeling. It is assumed that

a) The mixture obeys the ideal gas equation of state, PV = mRT

b) The system is a closed system when the valves are closed.

c) Kinetic and potential energies are neglected in energy equation.

d) There is no blowby.

e) All fuel energy is released to cylinder.

g) Combustion is modeled for a single zone.

Conservation of Mass:

$$\frac{dm_{Total}}{dt} = \dot{m}_{Intake} + \dot{m}_{Exhaust} + \dot{m}_{FuelInjected} \tag{6}$$

Where:

$\dot{m}_{Intake}$ = Rate of change of intake gas mass.

$\dot{m}_{Exhaust}$ = Rate of change of mass exiting in exhaust

$\dot{m}_{FuelInjected}$ = Rate of change of inject fuel mass

Conservation of Energy:

$$\frac{dT}{dt} - \frac{\left[\left(\left(\dot{m}^{*} h_i\right)_i + P_{cyl} Area_{Piston} V_{Piston} + \dot{q}_{Total} + \dot{m}_{FuelInj} h_{FuelInj}\right) - \frac{dE_{part}}{dt}\right]}{m^{*} \frac{du}{dT}} = 0 \tag{7}$$

where: $$\frac{dE_{part}}{dt} = m \frac{du}{d\phi_b} \frac{d\phi_b}{dt} + m \frac{du}{d\phi_{ub}} \frac{d\phi_{ub}}{dt} + (u + KE) \frac{dm}{dt} + m \frac{dKE}{dt} \tag{8}$$

where: ϕ_b= Burnt Equivalence Ratio; ϕ_{ub}= Un-burned Equivalence Ratio

KE = Kinetic Energy

Calculation of Heat Release and Ignition Delay using Arrhenius Reaction Rate Expression:

$$\frac{d\tau}{dt} = 1375\left(FuelCetane^{b}\right)\left(P_{cylinder}{}^{a}\right)\left\{e^{\left[\frac{const}{T_{cylinder}}\right]}\right\} \quad (9)$$

$$IgnitionDelay_{Main,Pilot} = \int \frac{d\tau}{dt} dt \quad (10)$$

Compression Ratio:

$$CompressionRatio = \frac{ClearanceVolume + DisplacementVolume}{ClearanceVolume} \quad (11)$$

$$DisplacementVolume = \frac{\pi * BORE^{2}}{4} * STROKE \quad (12)$$

2.2.4 Duct and Bend Model

This component model represents the transfer duct. It models an unsteady compressible fluid flow through a section of straight or conical pipe, capturing pressure and mass flow rate variations mimicking the ducts in an engine.

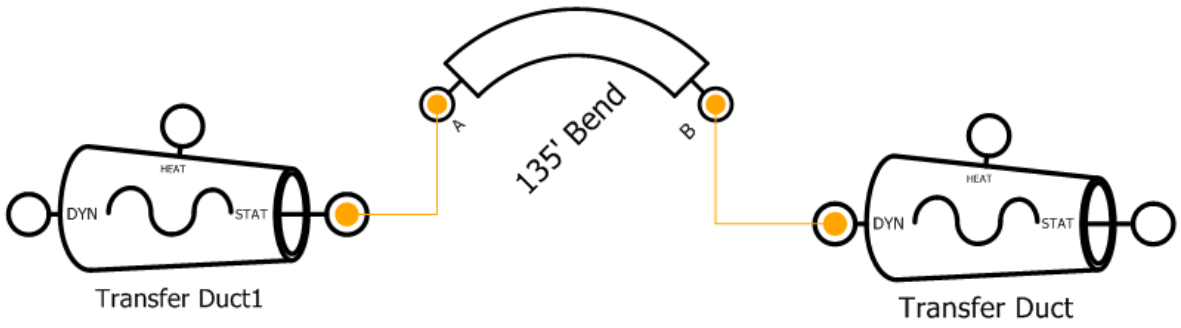

Fig. 12 Air duct subsystem.

It is assumed that:

a.) Mass flow rate is constant throughout the duct from x=0+ to x=L.

b.) All momentum changes in the duct are calculated only at *Dyn* end.

c.) Friction force between the fluid and duct walls is included in conservation of momentum equations, but do not add any thermal effects.

d.) Unless there is a "heat sink" connected to the HEAT connector of the duct, no heat transfer is assumed through the duct walls and flow is assumed to be isentropic.

Conservation of Mass:

$$\frac{dm}{dt} = \sum_i \dot{m}_i - \dot{m}_{condense} \tag{13}$$

Internal Pressure:

$$P = P(\rho, T, \phi_b, \phi_{ub}) \tag{14}$$

$$\rho = \frac{m}{Area} \tag{15}$$

Where (*refer fig.14*): $$Area = \frac{1}{12} L\pi(D_{stat}^2 + D_{stat}D_{dyn} + D_{dyn}^2) \tag{16}$$

Heat Transfer:

$$\dot{q}_{Heat} = CA_{surface}(T_{Heat} - T) \tag{17}$$

Radial Bend:

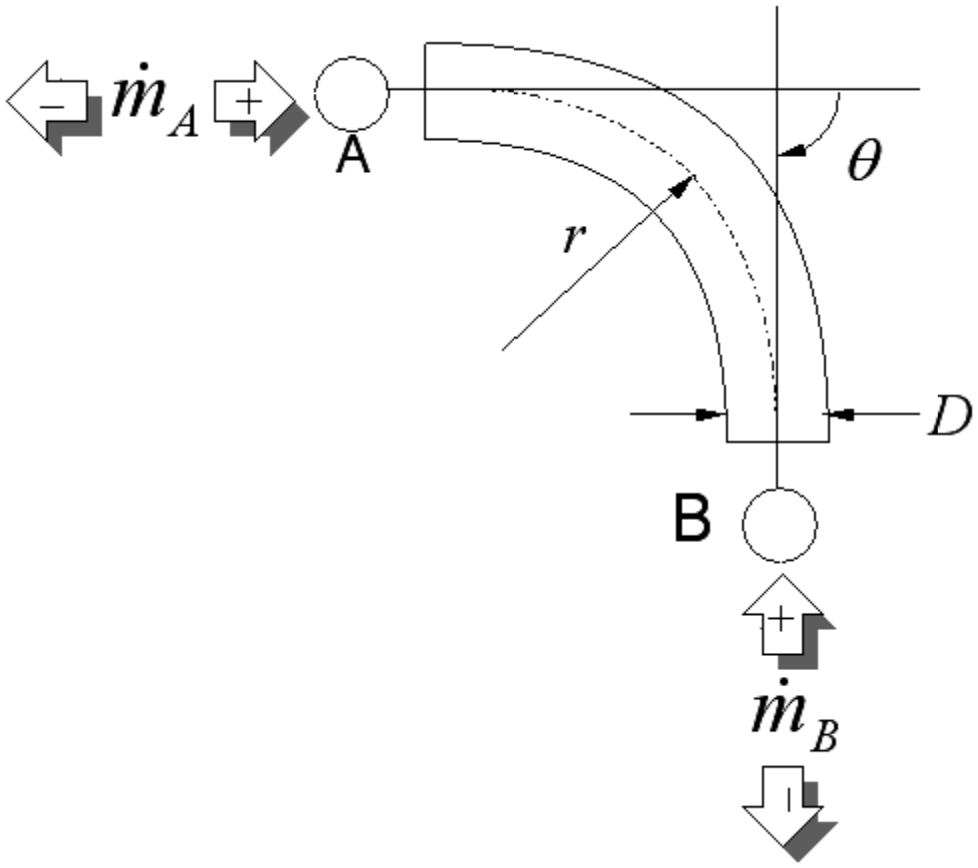

Fig. 13 Circular duct joints subsystem.

$$\dot{m}_A + \dot{m}_B = 0 \tag{18}$$

To calculate bend resistivity a constant K is calculated. A table is populated for a 90" bend stated as K_{90}, and then all other K values for different bend angles are a linear interpolation using K_{90} from the table.

$$K_{Angle}=K_{90}*\text{Angle} \tag{19}$$

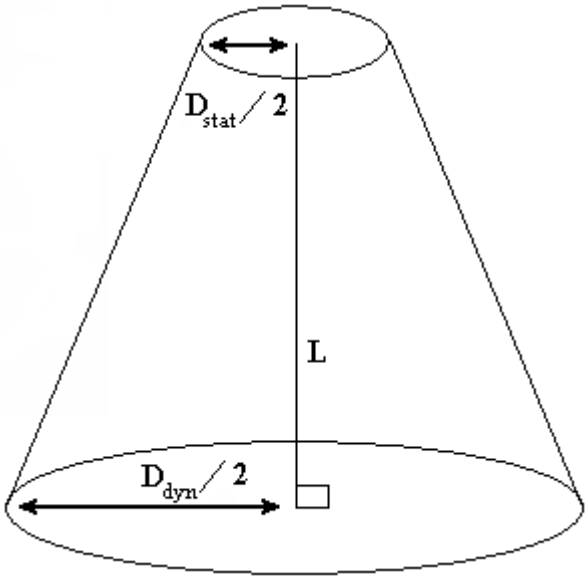

Fig. 14 Conical air duct section.

It is important to take into account some well known constraints while modeling high pressure and high speed flow though a duct in one-dimensional modeling.

The ratio of duct length to average duct diameter (= 1/2 (D_{STAT} + D_{DYN})) should in general be greater than about 1.5 for good convergence characteristics of average wall pressure and momentum equations. To achieve high fidelity in capturing high-frequency pressure oscillations the ratio should be kept to a minimum and the duct should be segmented into more number of grids for staggered solving.

The ratio of ducts “stat” end diameter to the “dyn” end diameter must be between 3/4 and 4/3 to prevent sharp transitions in area that could lead to flow separation from the duct walls.

2.2.5 Turbocharger

This component models a turbocharger turbine and compressor component. Equations are modeled to calculate rotational, thermal and gaseous characteristics. The turbine shaft powered as the exhaust gas expands and does the work on the turbine wheel. The turbine wheel power is based on turbine maps generated from steady state gas stand data obtained from a supplier. The power from the turbine shaft which is connected to the compressor shaft acts upon the inlet gas stream to raise its pressure and temperature according to the compressor maps generated from steady state gas stand data obtained from a supplier.

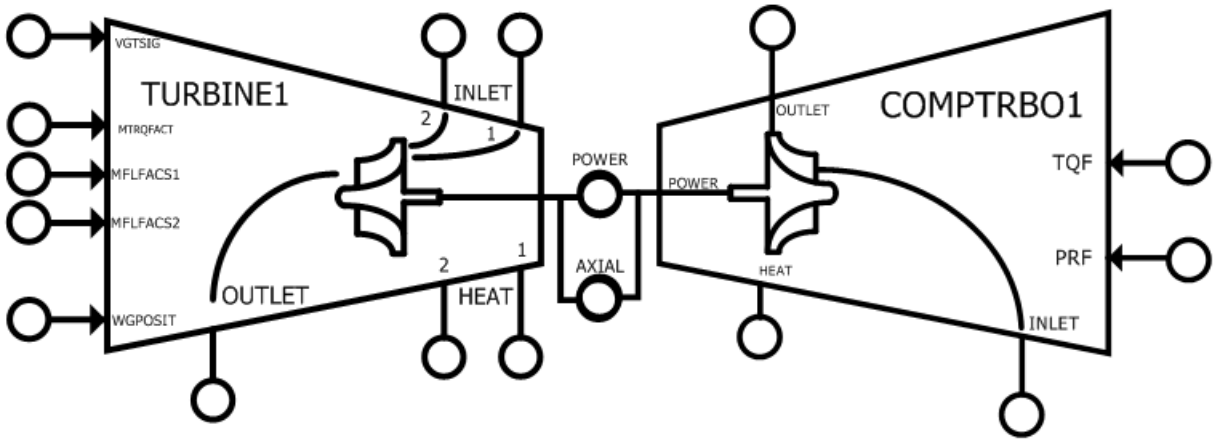

Fig. 15 Turbocharger subsystem.

It is assumed that:

a.) The gas obeys the ideal gas equation of state, $PV = mRT$

b.) The flow is steady, there is no gas storage within the turbo housing.

c.) Turbine and Compressor maps are provided from the manufacturer.

Conservation of Mass:

$$\dot{m}_{inlet} + \dot{m}_{outlet} = 0 \tag{20}$$

Conservation of Energy:

$$(\dot{m}\,h)_{inlet} + (\dot{m}\,h)_{outlet} + P_{shaft} + \dot{Q}_{wall} + \dot{Q}_{b.h.} = 0 \tag{21}$$

$$Q_{wall} = \dot{hc} * Area_{wall} * (T_{wall} - T_{gas}) \tag{22}$$

Gas Velocity:

$$V_{outlet} = \frac{\dot{m}_{outlet}}{\frac{\pi}{4} * D_{outlet}^{\ 2}} * \rho \tag{23}$$

Turbine wastegate flow:

$$\dot{m}_{wg} = C * Area_{wg} * P_{total} * (PHI / R / T)^{0.5} \tag{24}$$

Pressure Ratio:

$$PR = 1 + (PR_{map} - 1) * Tuning_{factor} \tag{25}$$

$Tuning_{factor}$ = Varies from 0-1 to account for modeling tolerances.

$$P_{outlet} = P_{inlet} + PR \tag{26}$$

Chapter 3

3.1 Compression Ignition (CI) Cycle

To understand the nuances of split cycle combustion it is important that we recollect how a conventional diesel ignition engine works. Diesel engines have been in production for the better part of the last century and they work on the Compression Ignition (CI) cycle.

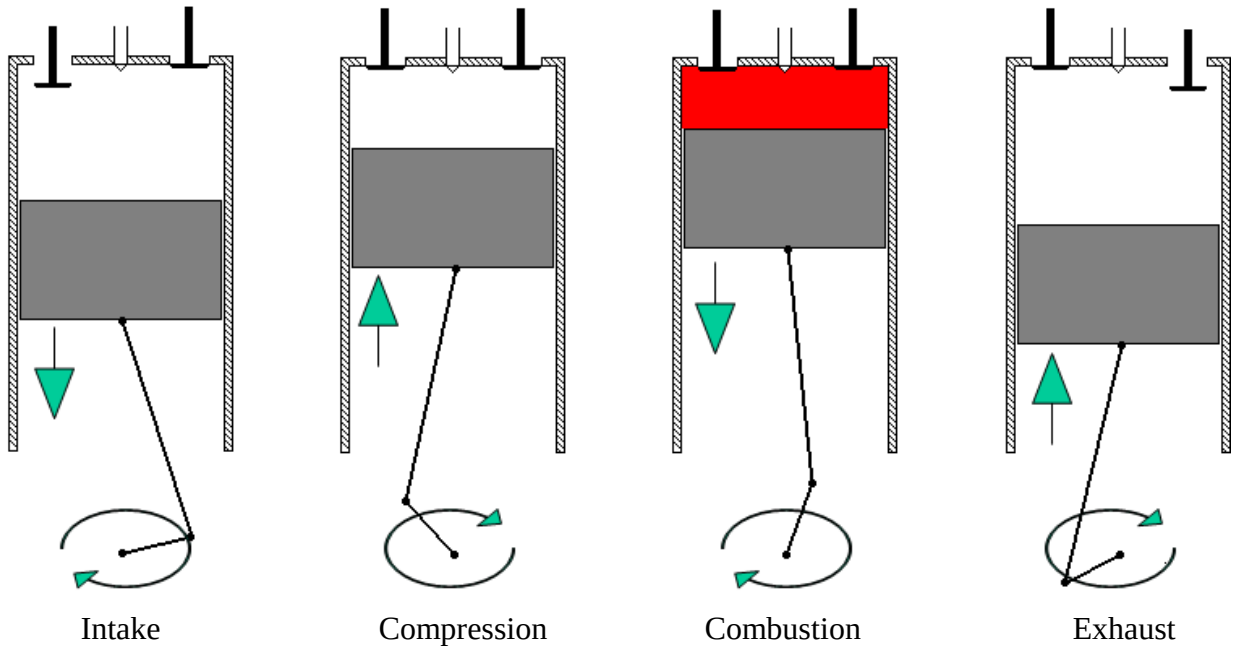

Fig. 16 Stages in a compression ignition cycle.

Almost all diesel engines operate on 4-storke. Fig. 16 describes these 4 strokes, the intake stroke, compression stroke, combustion stroke and exhaust stroke. There is one power stroke every 720’ rotation of the crank shaft. In a multi cylinder diesel engine every cylinder goes through all the 4-

strokes. Only pure air enters the engine in the intake stroke, fuel is injected into the combustion chamber when temperature and pressure conditions are just right (the ignition timing is controlled by specifying the time of injection or by using pilot injection). The fuel is injected at a very high pressure through a multi hole injector nozzle which helps in atomizing and mixing of fuel and air just prior to combustion and once the chemical and physical delays of combustion are crossed the mixture ignites.

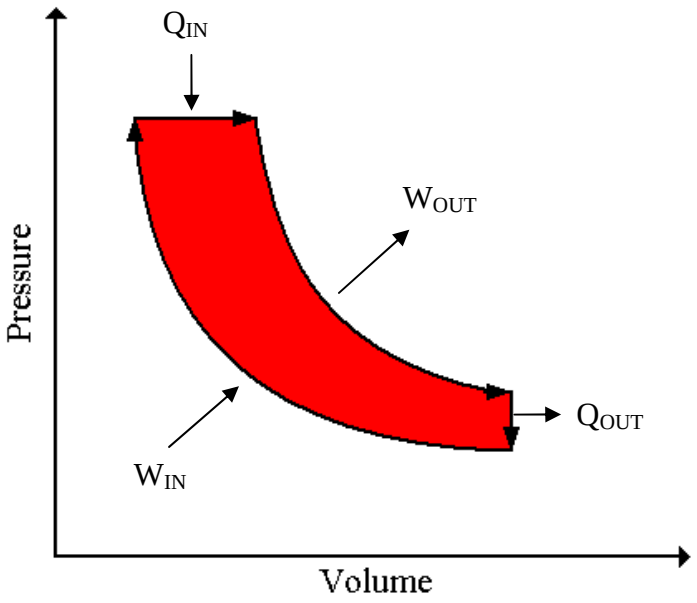

Fig. 17 PV curve for a CI cycle.

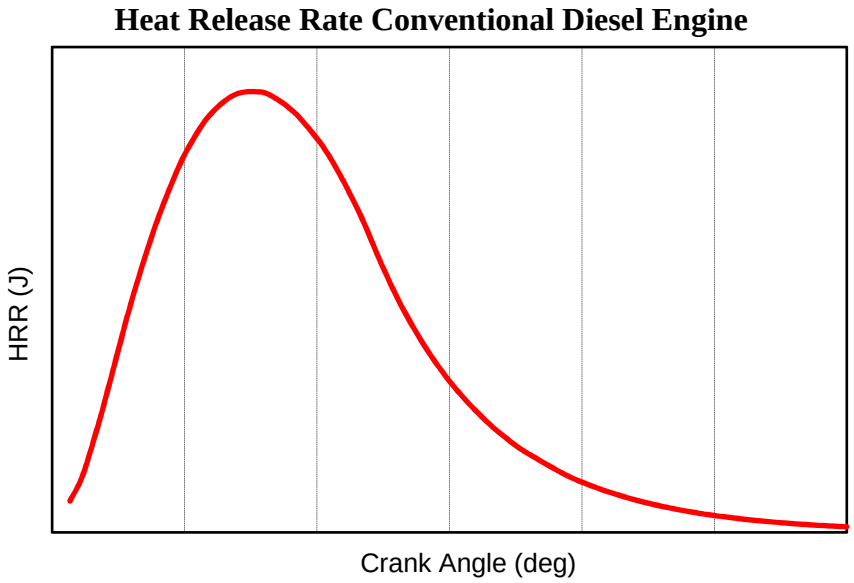

Fig. 18 General heat release profile for a conventional diesel engine.

Fig. 17 shows the pressure volume diagram for a compression ignition cycle showing that work is done in compression and work is realized in the same piston during combustion. Fig. 18 shows the characteristic shape of heat release with respect to crank angle and it should be noted that the heat release spans over a wide crank angle range and range to about 70’CA typically. Heat release in a spontaneous combustion is much faster in comparison to a conventional diesel engine as shown in fig. 22.

3.2 Compression Ignition Engine Control

Over time compression ignition engines have evolved and various strategies have been developed for control of combustion and heat release. The primary objective of controlling combustion is to drive engine efficiency while controlling emissions. However these

requirements are tailored to different engine applications, for example military engines are bound by relatively less strict emission requirements so the controls on those engines are focused to derive maximum engine performance with less focus on controlling emissions. In another case if the engine is being used to power a generator in a hospital the primary emphasis will be to control engine noise and emission levels with some compromise on engine performance.

Compression ignition diesel engines can be controlled by varying fuel injection and valve timing with respect to crank position. A turbocharged configuration is impacted more by valve timing than a non-turbocharged application. Fuel injection controls the timing and quantity of fuel being injected into the combustion chamber. Fuel injection into the combustion chamber can either be in one go or in partial injections throughout the combustion process, these partial fuel injections are named pilot injection, main injection and post injection based on the time of injection with respect to the combustion process.

The control of valve timing comprises of controlling the opening and closing of intake and exhaust valves in a cylinder with respect to crank position, valve timing can be segmented further into variable valve timing and constant valve timing both of which are highly researched areas in the engine development field.

Pilot Injection: When a small quantity of total fuel is injected into the combustion chamber prior to the onset of combustion with the primary purpose of elevating in-cylinder temperature and pressure and overcoming chemical and physical delays in combustion it is referred to as pilot injection. Pilot injection is a very popular knob that engine designers turn to prepare in-cylinder

conditions for an ideal combustion process and maximum heat release. In very special and highly complex engines pilot injection may not be of the same fuel type as the main fuel. For instance the pilot injection might be of diesel in an engine actually running on natural gas. Optimal time of pilot injection that allows for sufficient but not too much time gap between pilot and main injection will ensure optimal conditions

Main Injection: This comprises of the majority of total fuel being injected into a combustion chamber during one power stroke. Main injection pressure, time, duration and quantity is decided to yield the best heat release profile that gets converted to the power produced by the engine, these parameters are dependent on engine application and noise constraints.

Post Injection: When a small quantity of fuel is injected into the combustion chamber late in the combustion cycle it is called post injection. The primary purpose of post injection is to help reduce emissions by burning off the un-burnt hydrocarbons left over after the main combustion process.

Valve Timing: This involves varying the timing, lift and duration of the intake and exhaust valve with respect to the crank position in order to achieve the best volumetric efficiency out of the engine and to seal the combustion chamber at an appropriate time prior to the combustion process. Two strategies exist in this regards, constant valve timing and the variable valve timing strategy, and as the name suggests the latter one employs means to vary valve timing, lift, duration either continuously or step wise during engine operation.

3.3 Split Cycle Engine Control

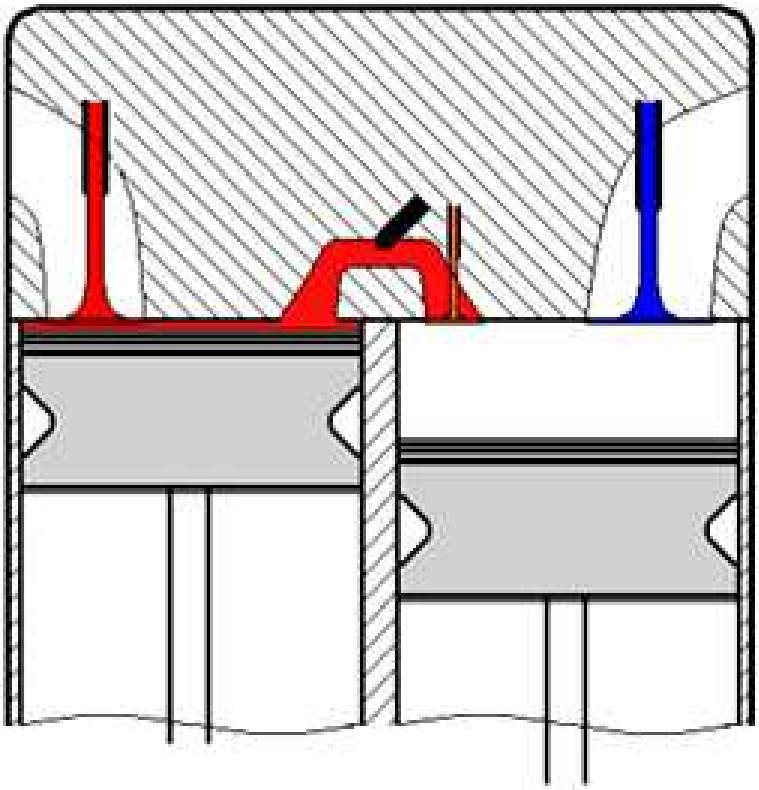

Fig. 19 A split cycle engine cylinder pair highlights the combustion chamber in red.

The aim in SCCC combustion is to compress the air charge before it is introduced in the combustion chamber and use the charge velocity and temperature during transfer to vaporize and mix fuel. SCCC engine benefits by the design of a flat head piston in the compression cylinder for high cycle efficiency during compression and also substantially more mixing time and swirl velocity than a conventional diesel engine.

In a conventional diesel engine fuel is injected at the peak of the compression stroke into the compression chamber, the injection needs to be at high pressure to be able to penetrate and mix in with the high pressure air. Typical characteristic of mixing in a conventional diesel engine are heterogeneous mixing and fuel spray reaching high temperature zones on the cylinder walls, this causes the production of soot and NOx. In the SCCC engine a low pressure fuel injection is sufficient as the fuel mixing is not dependent on spray penetration and rather fuel mixing relies on swirl, velocity and temperature of the transfer charge, this gives the fuel better mixing characteristics and also eliminates the disadvantage of the fuel spray reaching cylinder walls. This gives SCCC the ability to have a cleaner and more efficient combustion cycle with substantial reduction in soot and NOx.

Fig. 6 shows the stages in the operating cycle of the SCCC engine in 2-stroke. Thus a 4 cylinder SCCC engine with 2 compression and 2 combustor cylinders operating in 2-stroke produces the same number of power strokes and matches the power density of a conventional diesel engine where all four cylinders are firing in 4-stroke. The SCCC engine also has fewer moving parts.

The combustion chamber in an SCCC engine comprises of the squish volume in the combustor cylinder and the volume of the transfer duct, shown in fig. 19. The combustion chamber volume is bounded by the transfer valve on the intake end and the exhaust valve on the exhaust end. Pilot injection and a part of main injection begin before the transfer valve is fully closed thus the combustion process begins before the combustion chamber is completely sealed.

The existence of only one exhaust valve and the introduction of a transfer valve per cylinder pair in a SCCC engine required different valve timing than that of a conventional diesel engine. There are various strategies developed for the control of valve timing, lift and duration. The primary objective is to improve the volumetric efficiency of the engine and to create an optimum combustion chamber boundary to allow the conversion of heat release into cylinder pressure which is realized by the combustor cylinder piston to produce power.

Valve lift profiles were made by analyzing the results of the “design of experiment” runs. It was inferred that variable valve timing is not needed at this time. The basic idea behind valve timing is to open the intake valve when there is enough vacuum inside the cylinder to provide efficient intake air flow through the manifold, but waiting too long to open the valve can cause engine choking and decrease the overall engine efficiency. The transfer valve timing was designed to achieve a pressure gradient across the compressor and combustor cylinders, also reduce the turbulence of air and reduce velocity in the transfer duct. Exhaust valve timing was designed to use the input charge for scavenging while providing enough time for all burnt gas removal.

The DOE results showed that SCCC was not benefitting from variable valve timing and a fixed valve profile was identified that was yielding good mass flow rates across the intake, exhaust and transfer valves at all engine operating loads and engine speeds.

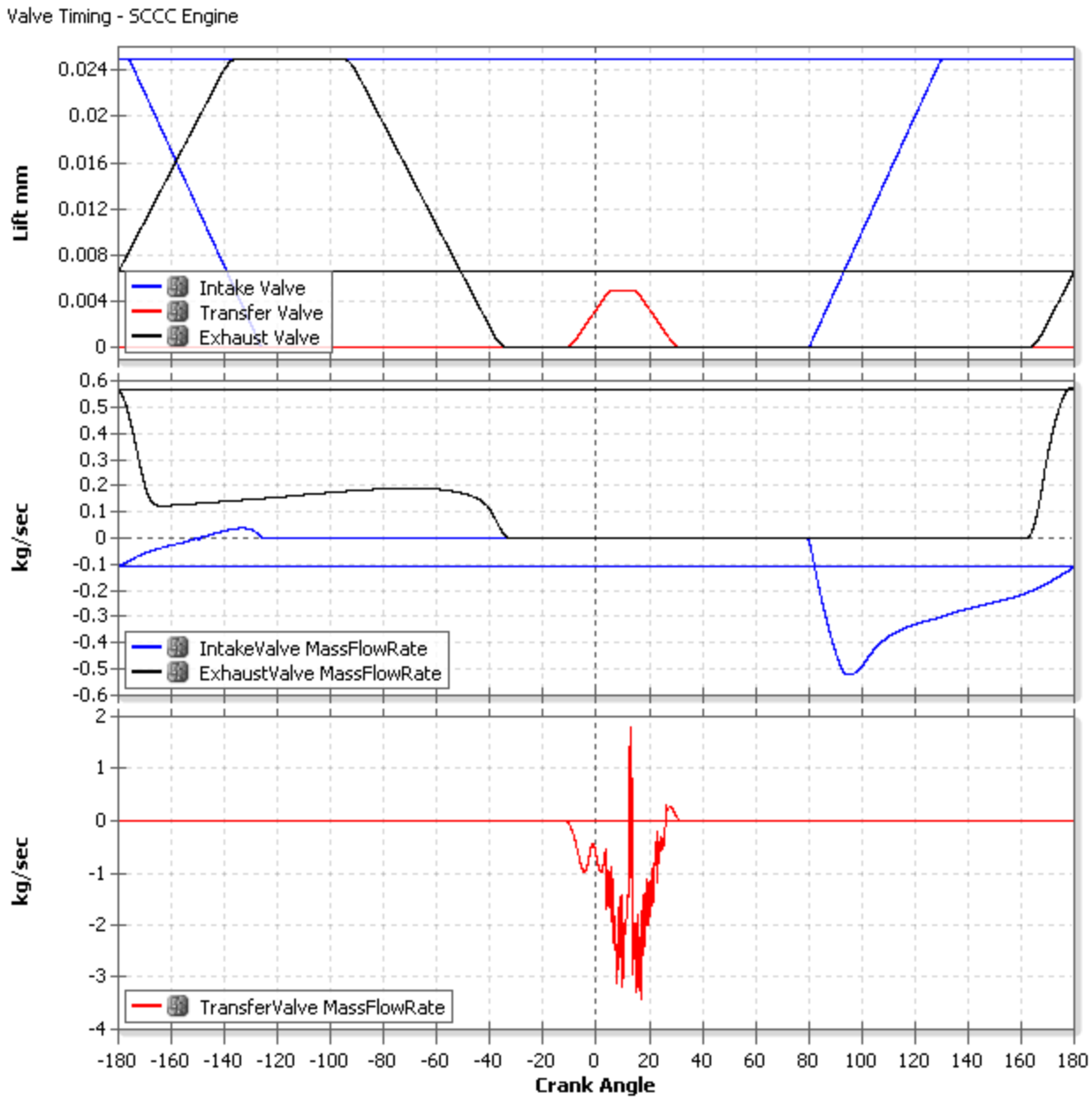

Fig. 20 Mass flow rate as a result of valve timing at full engine load.

Fig. 20 above shows mass flow rate during valve opening while the engine is operating at full load. Negative flow rate indicates mass entering into the intake cylinder and charge entering into

the combustor cylinder, whereas the positive flow rate indicated the mass of burnt gasses exiting the combustor cylinder.

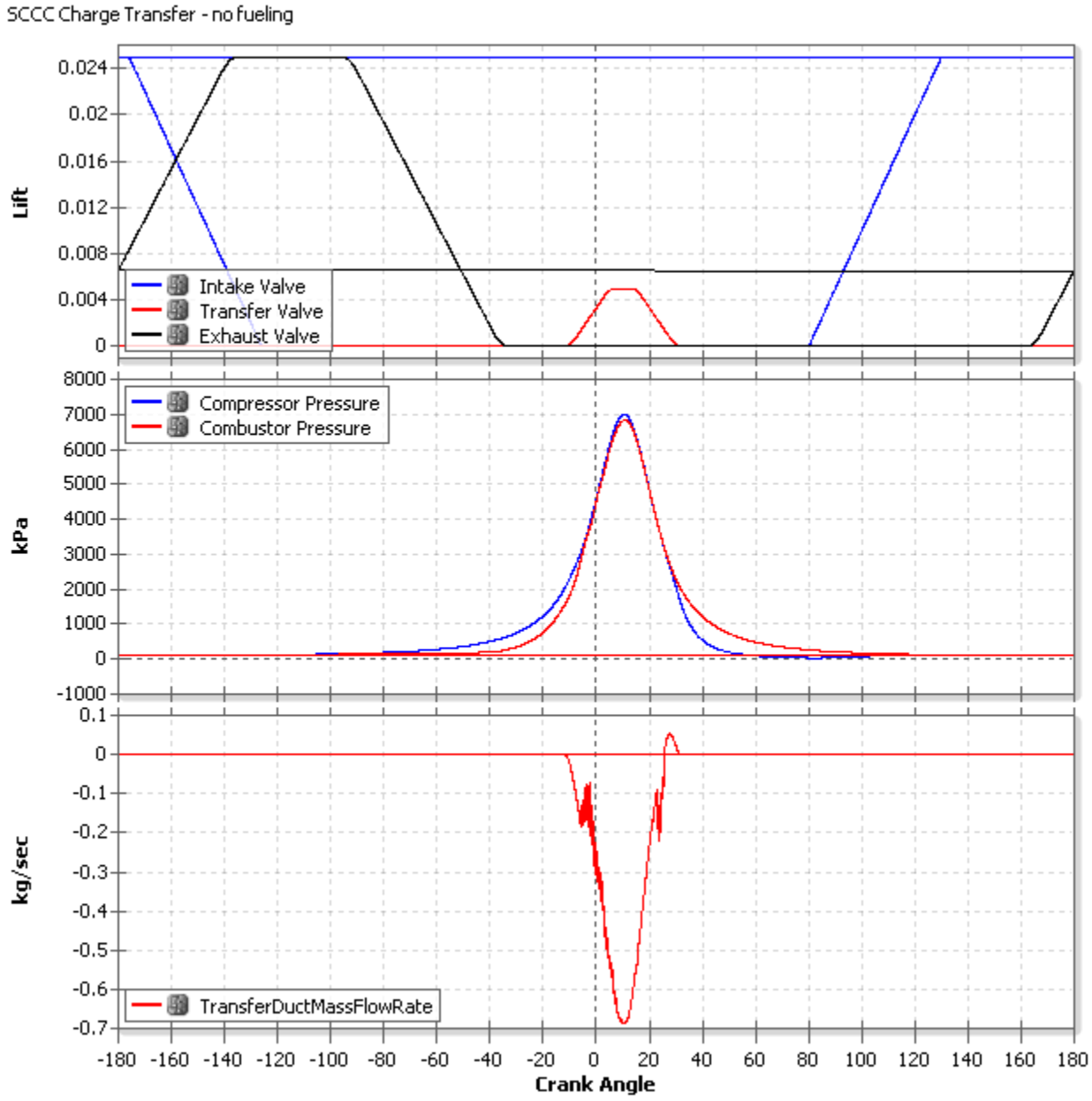

Fig. 21 Cylinder pressures and charge transfer in motoring mode.

When the valve cracks open the high pressure differential about the valve causes the high mass flow rate and as the pressure differential slowly decreases the mass flow rate decreases. The third row in fig. 20 shows a very high mass flow rate through the transfer valve which is favorable.

The transfer duct was designed to keep the velocity of charge in the transfer duct to its minimum while promoting smooth swirling charge transfer into the combustor cylinder. The reduction of velocity reduces turbulence in charge transfer. The shape of the duct as also improved on by analyzing results from the DOE to minimize the impact of pulsation during combustion on the incoming charge transfer. In SCCC operation combustion in the combustor cylinder begins before the charge transfer from the compressor cylinder to the combustor cylinder completes and the transfer valve closes, this created pressure waves in the opposite direction of charge flow, the impact of these pressure waves need to be minimized to achieve good engine volumetric efficiency and to prevent the equivalence ratio of the compressor cylinder from rising. Fig. 20 and fig. 21 elaborate the contrast in air mass flow rate across the transfer duct with and without combustion. The air profiles in fig. 21 show a smooth mass flow rate but the peak values a pretty low as compared to fig. 20 as there is no combustion energy going to the turbochargers thus there is no turbochargers spool to create significant intake manifold pressure into the compression cylinder. Fuel is injected into the entrance of the combustor cylinder and is timed to use incoming air charge for mixing, the combustion process begins after the chemical and physical delays are crossed while there is still incoming charge transfer. To accomplish this main fuel injection has to complete over very short crank angle duration and thereon the turbine like combustion progresses a lot faster than a compression ignition engine as seen in fig. 22.

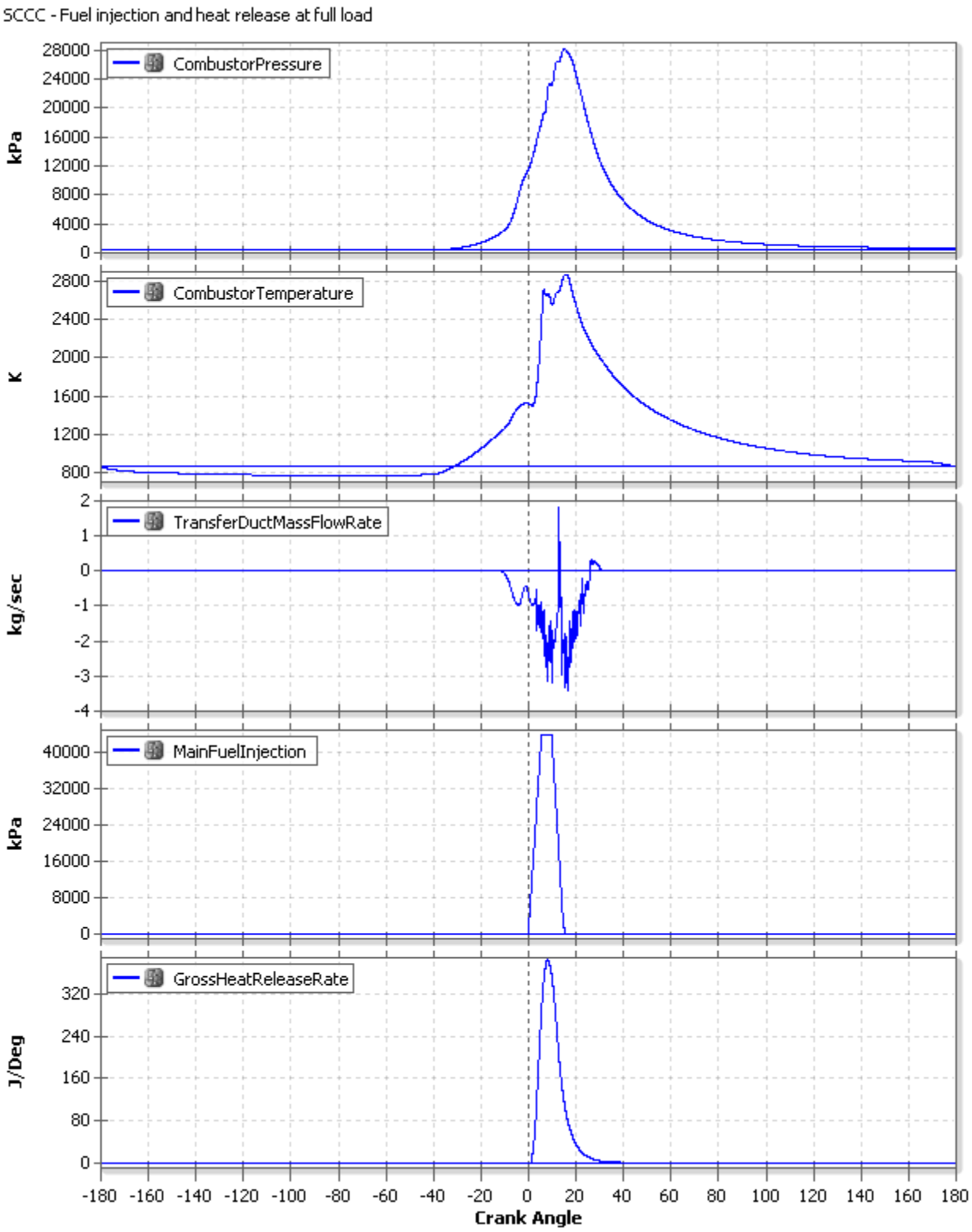

Fig. 22 SCCC main fuel injection and HRR.

Chapter 4

4.1 Results: Cat® C4.4 Hydraulic Excavator 316 Engine model validation using actual and simulated test data.

Part	Part	Description
ECM Software Version	-	Alpha12
Engineering Engine Model	-	C4.4 (4EDV1 plus *)
Piston	3242699	Q
Compression Ratio	-	16.5:1
Camshaft	3320989	C4.4 Tier 4i Camshaft
Turbo	3345339	GT22 C241 56mm 50trim
Fuel Injector Configuration	3240340	6hole x 130deg x 770cc/min
EGR Cooler	3466184	4 plate
Development Engine	-	12V

Table 1 Cat® C4.4 engine component part numbers (316 Excavator rating).

Cat® C4.4 is a 4.4 liter inline 4-cylinder turbocharged diesel engine that is used by Caterpillar in its Hydraulic Excavator Series 316. The C4.4 is one of the smaller and lower costing engines that the company makes, most other engines have more number of cylinders. Owing to its small size, relative simplicity of being an inline 4-cylinder and its constant speed application in the

excavator this engine provides the best platform to evaluate the benefits of SCCC, thus it was chosen for this research study.

Caterpillar's Virtual Product Development (VPD) division creates and validates these engine models in their one-dimensional modeling and simulation software *Dynasty*. All the modeling done for SCCC during this study is also in *Dynasty*.

As the C4.4 engine is being used as baseline for our study it is very important to validate model accuracy to the real engine. Thus to validate the C4.4 engine model accuracy it, a few important engine characteristics were compared to simulate test data. The parameters were chosen so that the engine model and the modeled turbo charging loop can be completely validated.

The parameters being evaluated are:

a) Lug Curve Power check
b) Part load Power check
c) Brake Specific Fuel Consumption
d) Exhaust Manifold Temperature
e) Turbocharger Speed
f) Boost Pressure
g) Engine transient response via block load testing.

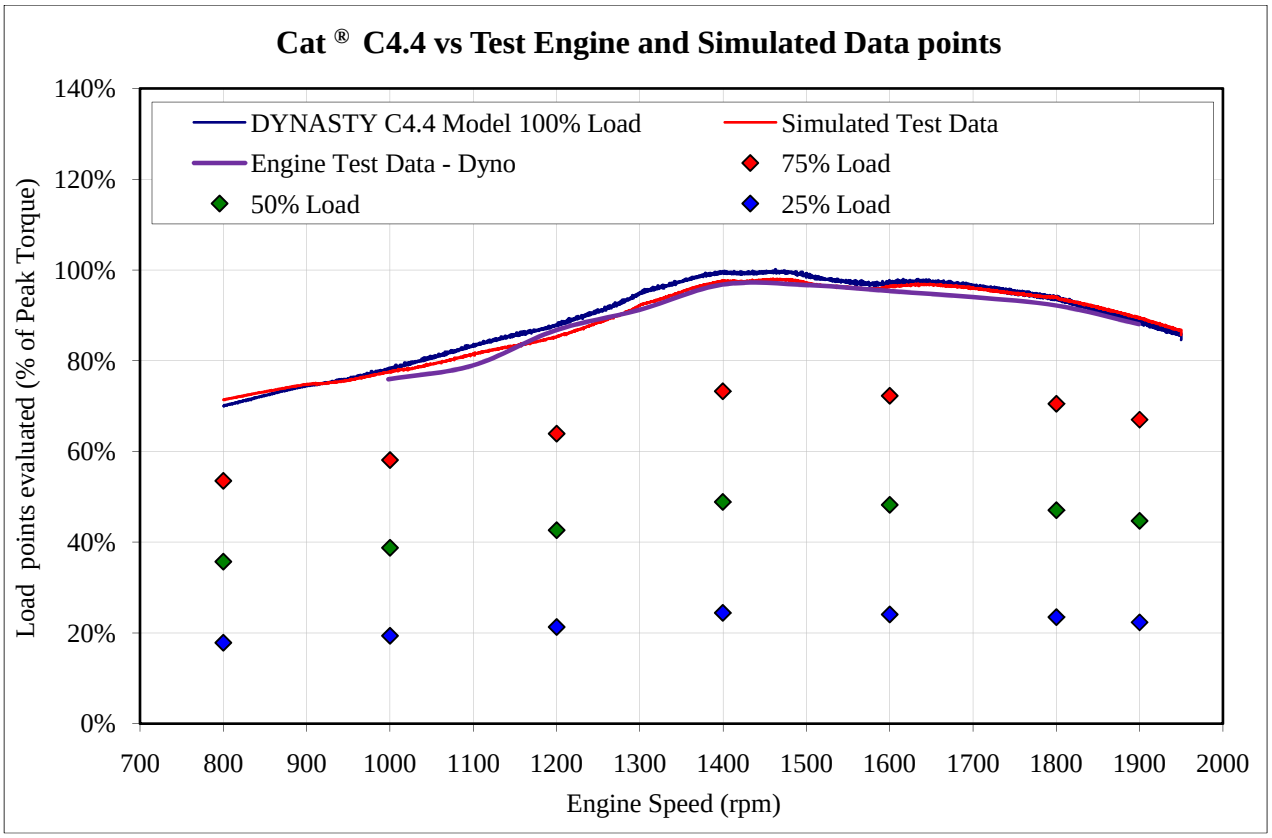

Fig. 23 Cat® C4.4 engine model lug curve comparison.

Fig. 23 above shows the lug curve and part load evaluation points used to validate the C4.4 Dynasty model using simulated test data. Power was checked at steady state at every 200 rpm interval including peak torque (1400rpm), rated power (1800rpm) speed and the engine rating high idle (1950rpm) speed.

Fig. 23 also shows the comparison between simulated test data lug curve power to the Dynasty model power at lug curve. The maximum deviation in lug curve power was found to be within ± 3%, thus we can say that the model is producing power accurately at lug curve.

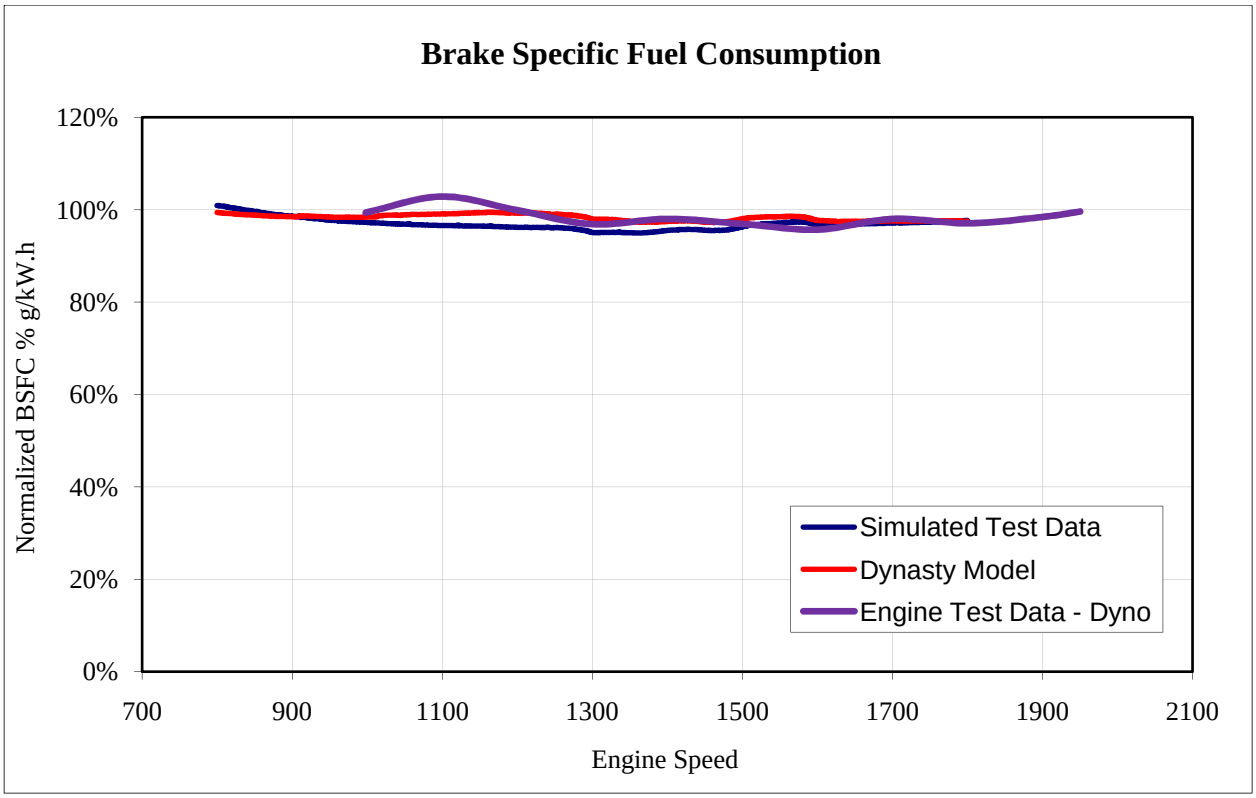

Fig. 24 Cat® C4.4 engine – BSFC.

Fig. 25 shows the overall brake specific fuel consumption error percentage between the simulated test data and the model, fig. 24 highlights the absolute brake specific fuel consumption at lug curve. It can be seen the model results show upto 3% better BSFC at full load while operating in the mid of the rpm range and at low and very high rpms the result accuracy increases with the model claiming upto 2% better BSFC.

The regions shaded in green to yellow to red are the regions where the model is under predicting BSFC by 1- 4% with the accuracy worsening as engine rpms get lower than 1000rpm. At these low engine speeds the fuel quantity being injected into the engine is very low and even though there is a good amount of gross power being produced the net power is very low since most of it

is being used to overcome the friction and pumping losses of the engine. It is very difficult to predict the friction and pumping losses of an engine, and yet engineers at Caterpillar do a remarkable job but as the internal loss to gross power ratio increases the BSFC prediction becomes difficult as can be seen from fig. 25.

Overall the model results show a 3% over to 4% under prediction in BSFC and thus the model is showing a very high accuracy to simulated test data.

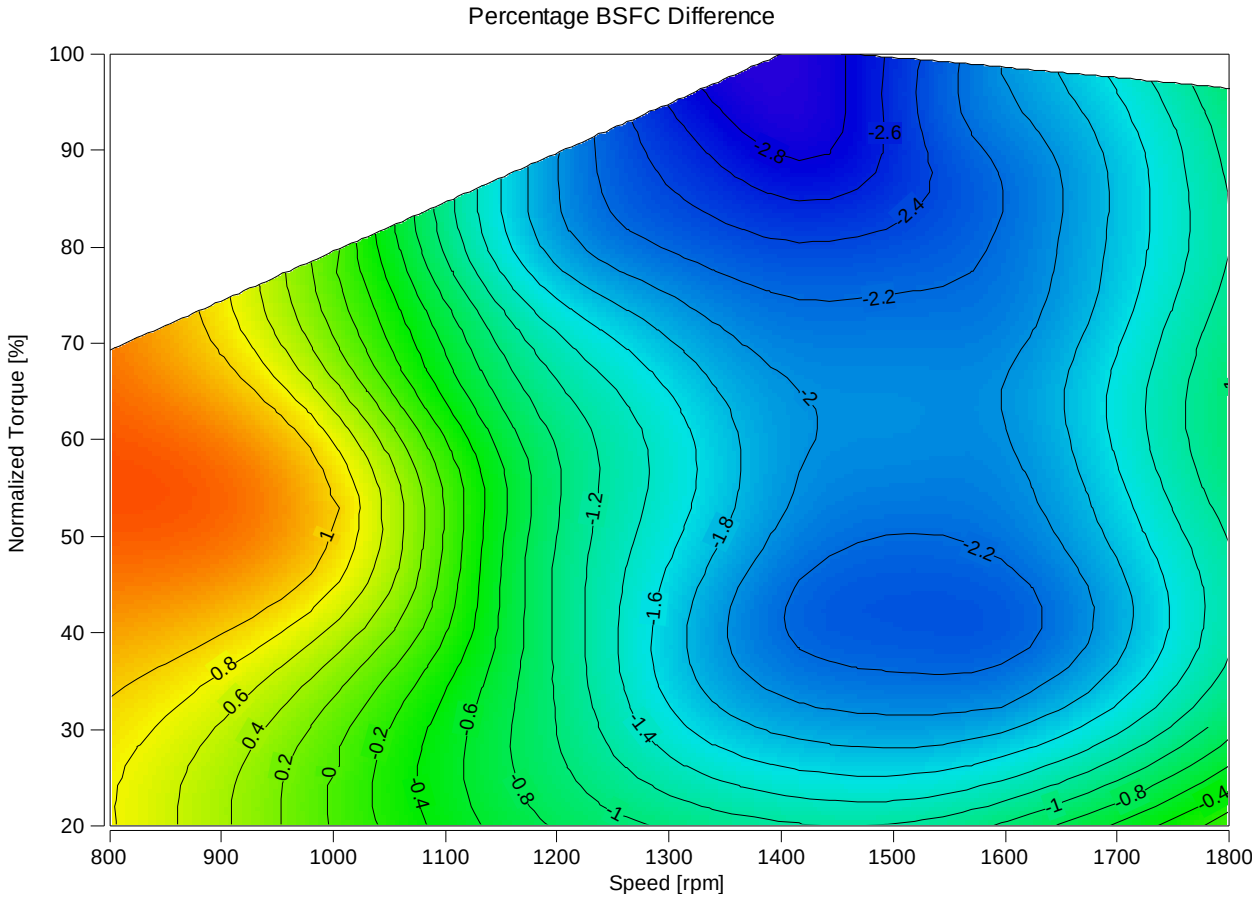

Fig. 25 Cat® C4.4 engine – part load BSFC.

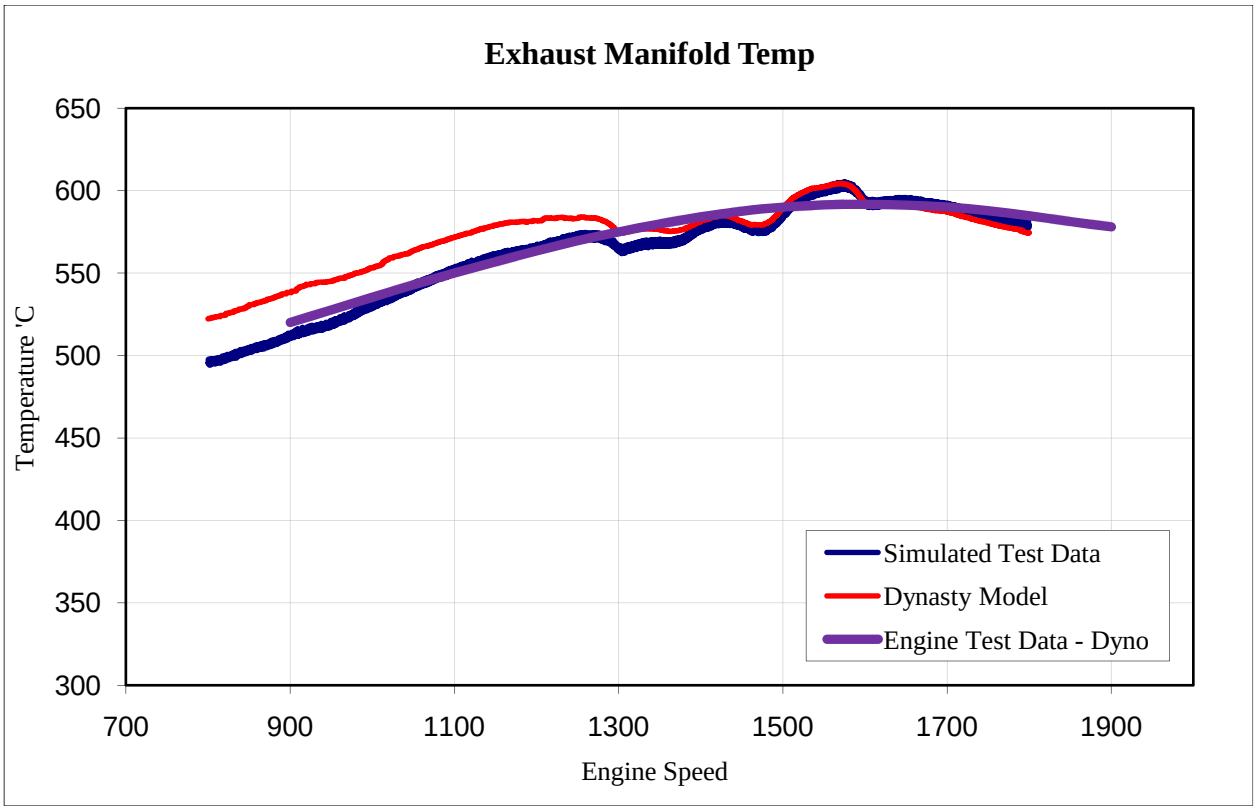

Fig. 26 Cat® C4.4 engine – exhaust manifold temperature.

Fig. 27 shows the percentage error in exhaust manifold temperature (EMT) of the engine and fig. 26 highlights the absolute error at lug curve. Exhaust manifold temperature is a good measure to compare engine performance as it an indication of in-cylinder combustion conditions, valve timing and the energy that is being thrown at the turbine of the turbocharger.

It can bee seen that at lug curve the model predictions are very accurate in the mid to high rpm range and then the error starts to increase and the model over predicts the exhaust manifold temp by upto 6% at low idle. Exhaust manifold predictions are ranging from 6% over prediction to 4% under prediction with an exceptionally good match in the mid operating speeds and medium to high engine load conditions.

Overall the model results show a 6% over to 4% under prediction in EMT and thus the model is showing a very high accuracy to simulated test data

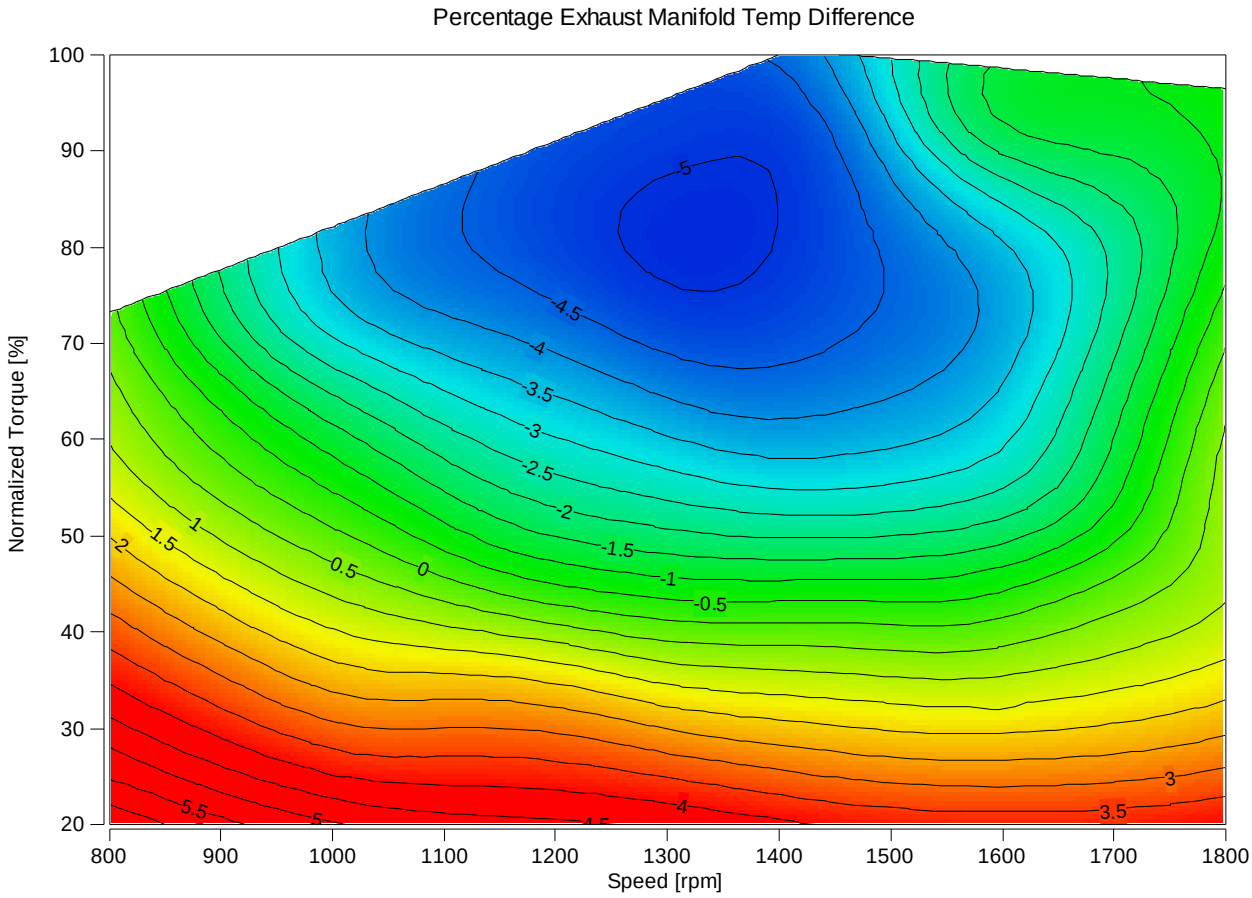

Fig. 27 Cat® C4.4 engine – part load exhaust manifold temperature.

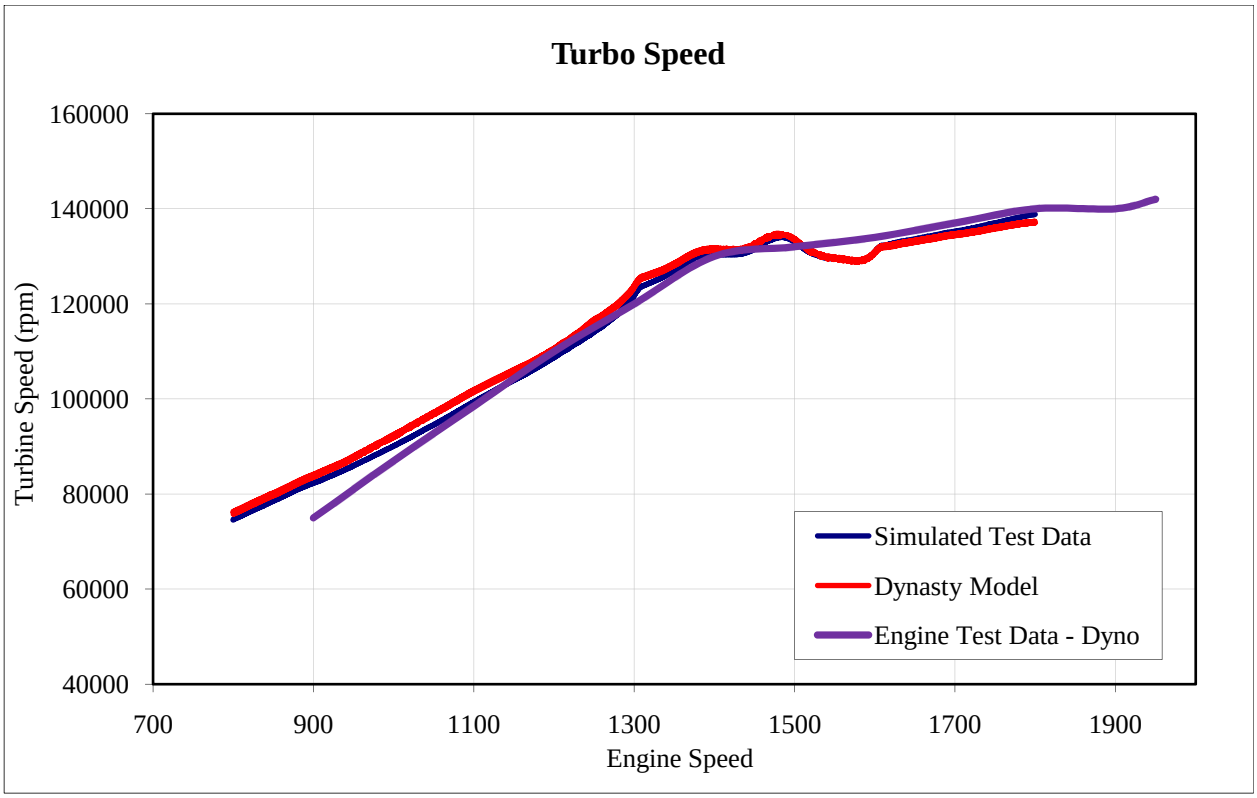

Fig. 28 Cat® C4.4 Engine model – turbo speed.

Fig. 29 shows the percentage error in turbocharger shaft speed and fig. 28 highlights the absolute error at lug curve. Turbocharger speed is a good measure for mass flow rate of exhaust gasses coming out of the each cylinder and also the wastegate operation.

It can be seen that at mid to high engine operating speeds and at mid engine loads at low engine speeds and at low engine load the model predictions are dead on. The model is over predicting turbo speed by upto 2% at high load and mid engine speeds and the error increases to 4% over prediction at low engine speeds. Trends in error change at high engine speeds and low load conditions are shown by regions shaded in yellow to red with the error increasing to upto 4% under prediction of turbo speed by the mode as the engine speed approaches high idle.

Overall the model results show a 4% over to 4% under prediction in turbo speed and thus the model is showing a very high accuracy to simulated test data

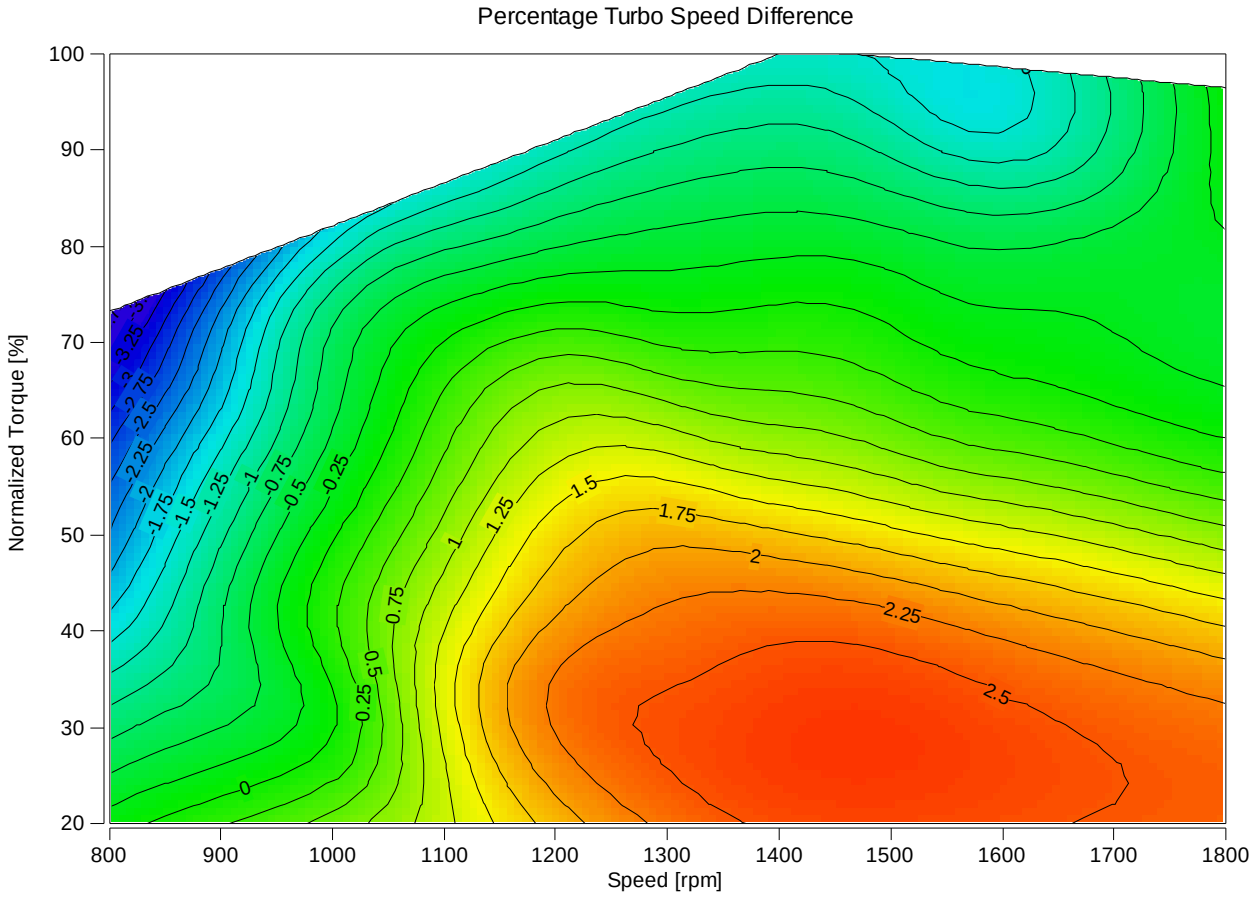

Fig. 29 Cat® C4.4 engine model – part load turbo speed.

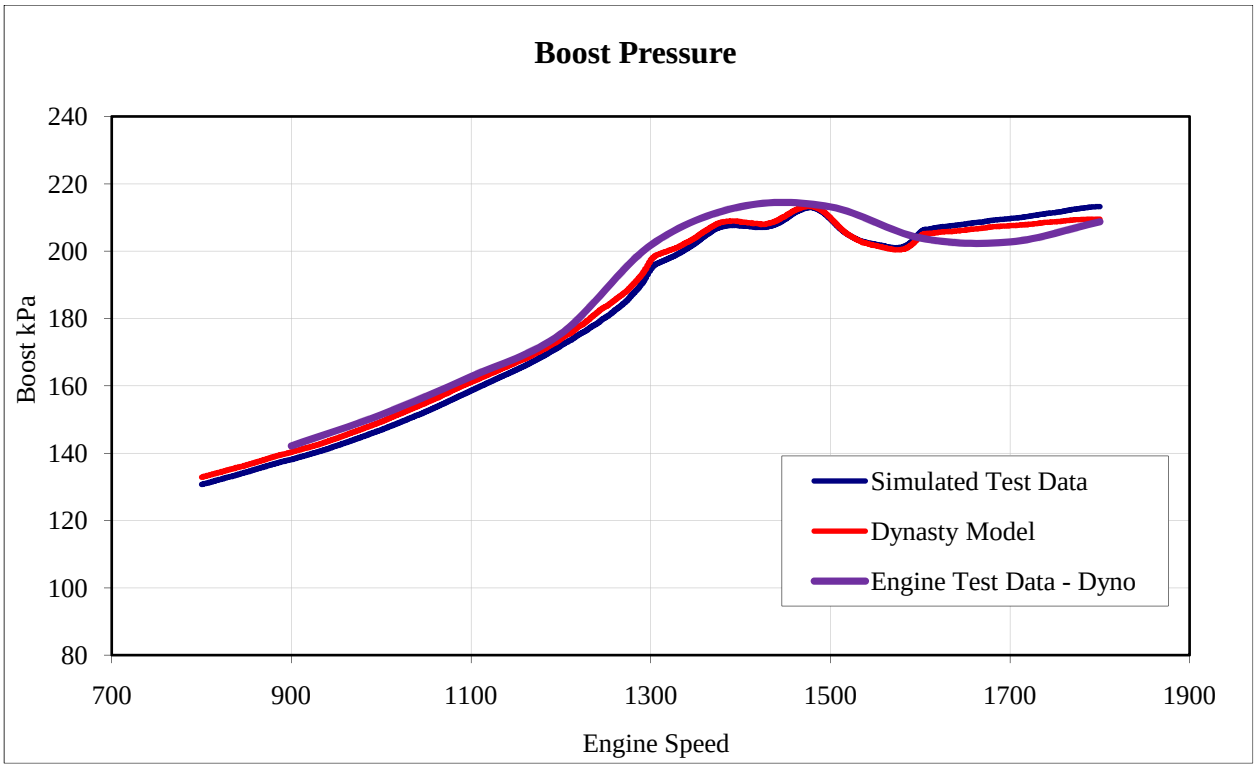

Fig. 30 Cat® C4.4 engine model – boost pressure.

Fig. 31 shows the percentage error in boost pressure and fig. 30 highlights the absolute error in boost at lug curve. Boost pressure is a good measure to compare engine performance as it is critical in maintaining the required equivalence ratio in the combustion chamber. The ECM measures the amount of air going into the combustion chamber and thus alters the injection pressure and injection duration to deliver the fuel quantity required to reach the desired equivalence ratio. The equivalence ratio has to be optimum for good combustion and to meet emission requirements, if the combustion is too rich (high equivalence ratio) or too lean (low equivalence ratio) then it is detrimental to the piston head surface, reduces power, lowers in cylinder temperature and increases Soot (unburnt hydrocarbons) or NOx (nitrous oxide species) emissions.

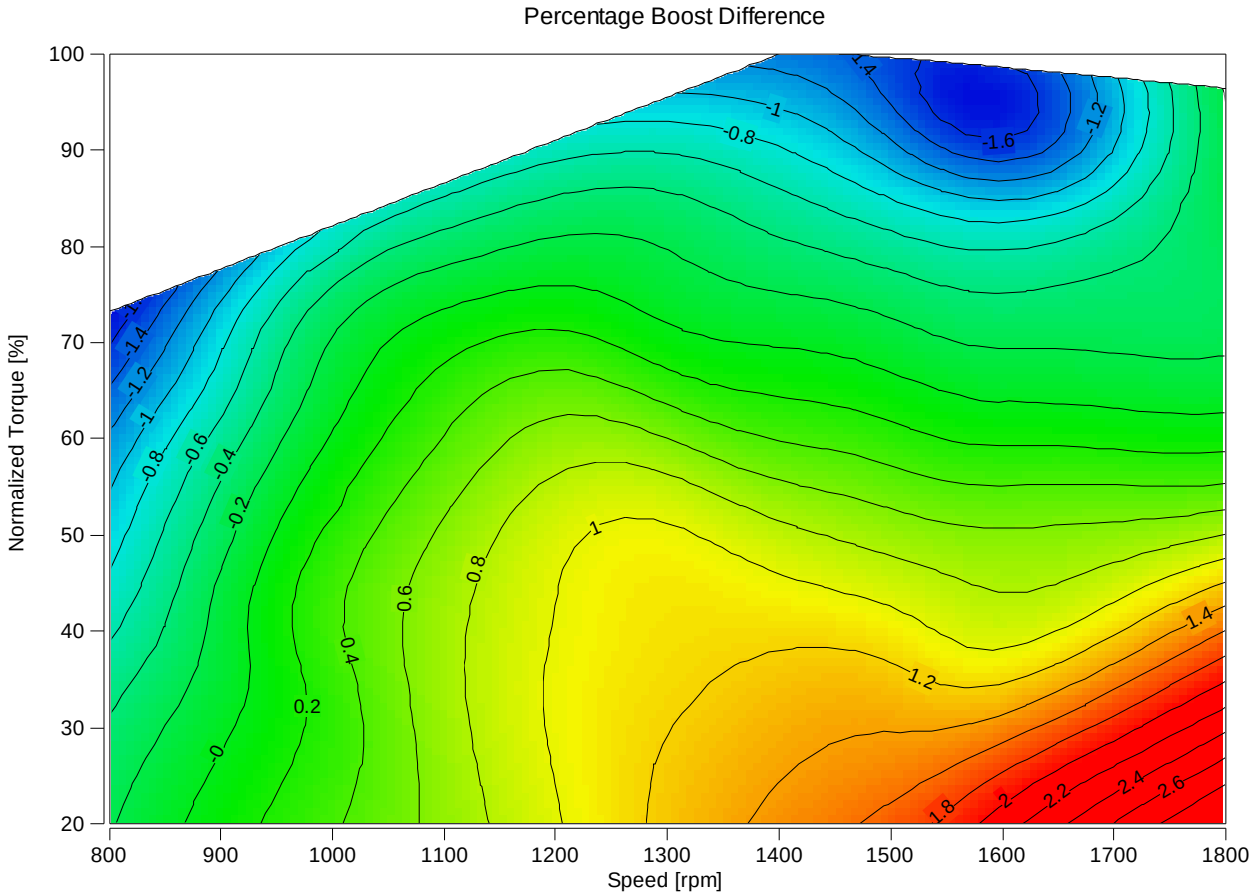

Fig. 31 Cat® C4.4 engine model – part load boost pressure.

It can be seen that in the mid to high operating speeds and high engine operating loads and all throughout the low operating speeds the model is over predicting boost pressure by 1% with the error increasing to 2% at low speeds and high loads. From 1000rpm up all the way to high idle and at low to mid engine operating loads the engine and the model predictions are dead on and then the error climbs to upto 2% under prediction at high engine speeds and really low engine operating loads.

Overall the model results show a 2% over to 2% under prediction in turbo speed and thus the model is showing a very high accuracy to simulated test data.

Fig. 32 shows the transient response testing by means of block load test which is an industrial standard for evaluating engines transient performance. Engine speed is held constant at 1800rpm and a sudden load is applied and held steady for a period of time and then released. The engines response to load application and removal is evaluated to determine engines transient response.

Row 4 in fig. 32 shows load transition from 50 Nm to 420 Nm and then back during testing, where 420 Nm is 85% of engines peak torque load. Looking at curves in rows 1 to 4 it can clearly be seen that engine speed droop and overshoot results show a very good match with error being within 3%, engine boost and exhaust manifold temperature also show a very good match with simulated test data.

Overall the model results are within 3% error prediction for all results evaluated during transient response testing and thus the model is showing a very high accuracy to simulated test data.

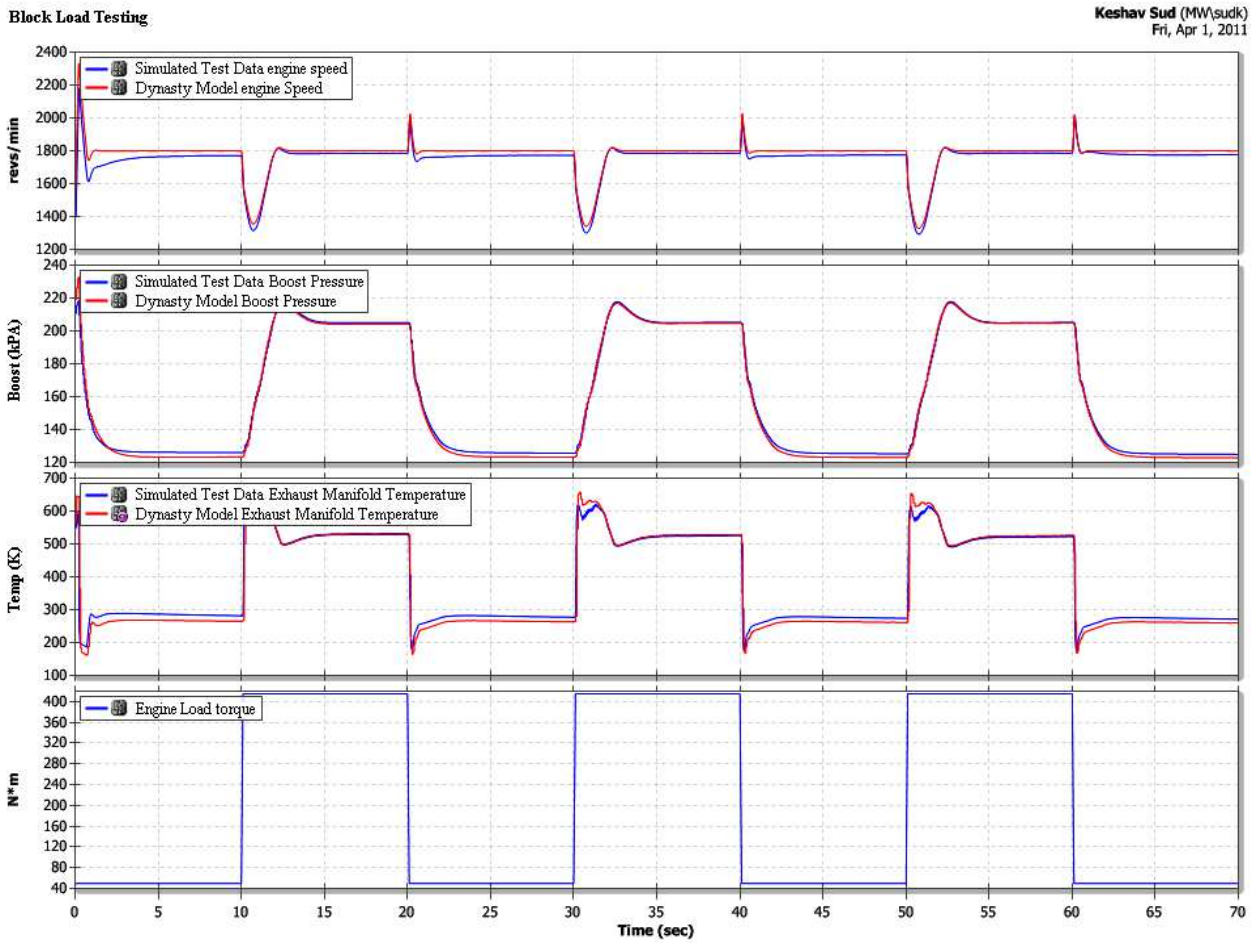

Fig. 32 Cat® C4.4 engine model – transient response.

4.2 Results: 1-D Modeling Approach Validation with University of Pisa Results.

As mentioned before, we validated the fidelity of our 1-D simulation engine by replicating the engine geometry, boundary and injection characteristics presented by University of Pisa in their SAE paper “Clean Diesel Combustion by Means of the HCPC Concept 2010-01-1256” by Ettore Musu, Ricardo Rossi, Roberto Gentili and Rolf D. Reitz. Their Computational Fluid Dynamics (CFD) based model was simplified and remodeled in 1-D and then a few key engine characteristics were compared between the two to verify a good match.

The modeling activities were segmented into 5 sections and the parameters in each section were modeled to match University of Pisa’s specifications:

a) General Parameters
b) Compressor Parameters
c) Combustor Parameters
d) Valve Profiles and Lifts
e) Transfer Duct Parameters

	General Parameters	Uni. of Pisa	Dynasty
1	Modeling Technique	CFD - 3D	1D
2	Fuel	C14H28	Diesel
3	Fuel Temp	363K	363K
4	Pilot Start of Injection	8' BTDC	8' BTDC
5	Pilot End of Injection	6' BTDC	6' BTDC
6	Main Start of Injection	0' BTDC	0' BTDC
7	Main End of Injection	20' ATDC	20' ATDC
8	Injector	7 - Hole	7 - Hole
9	Fuel Injected	27 mg/stroke	27 mg/stroke
10	Nozzle Diameter	0.14 mm	0.14 mm
11	Injection Rate	square profile	square profile
12	Cone Angle	14'	14'
13	Engine Speed	2000	2000
14	Combustor Initial Temperature	750 - 850 K	750 - 850 K
15	Combustor Initial Pressure	280 - 350 kPa	280 - 350 kPa
16	Compressor Initial Temperature	480 - 530 K	480 - 530 K
17	Compressor Initial Pressure	480 - 520 kPa	480 - 520 kPa
18	Ambient Temperature	323K	323K
19	Ambient Pressure	100kPa	100kPa
20	Simulation Start (TVO)	330' ATDC	0' ATDC
21	Simulation End (EVO)	1050' ATDC	steady state
	Compressor Parameters	Uni. of Pisa	Dynasty
22	Displacement	499cm3	499cm3
23	Bore	86 mm	86 mm
24	Stroke	86 mm	86 mm
25	Squish Height	0.5 mm	0.5 mm
26	Geometric Compression	117:1	117:1
	Combustor Parameters	Uni. of Pisa	Dynasty
27	Displacement	598 cm3	598 cm3
28	Bore	86 mm	86 mm
29	Stroke	103 mm	103 mm
30	Squish Height	0.5 mm	0.5 mm
31	Geometric Compression	85:1	85:1

	Valve Profiles and Lifts	Uni. of Pisa	Dynasty
32	Intake Valve Open	60' ATDC	60' ATDC
33	Intake Valve Close	54' BTDC	54' BTDC
34	Transfer Valve Open	33' BTDC	33' BTDC
35	Transfer Valve Close	52' ATDC	52' ATDC
36	Exhaust Valve Open	165' ATDC	165' ATDC
37	Exhaust Valve Close	9' BTDC	9' BTDC
38	Intake Valve Lift	15mm	15mm
39	Exhaust Valve Lift	15mm	15mm
40	Transfer Valve Lift	3mm	3mm
	Transfer Duct Parameters	Uni. of Pisa	Dynasty
41	Displacement	4.8 cm3	4.8 cm3
42	Type	Conical	Conical
43	No. of main duct segment	1	4

Table 2 University of Pisa vs Dynasty modeling differences.

To meet our goal it was very important that modeling be done as accurately as possible with the fewest possible assumption and approximations. All geometric parameters of the two cylinder engine and the control parameters were aligned to achieve a similar combustion profile and heat release rate. For simulation purposes the initial conditions of temperature, pressure and calculated equivalence ratio were also aligned.

There were slight deviations in modeling that had to be done to increase the fidelity of our 1-D model and to capture results at a high resolution during the gas exchange process. These model changes were primarily dependant on our *Dynasty* simulation solver characteristics and my past project experience using *Dynasty*. The most important amongst these changes was segmenting the transfer duct into four sections rather than having it as one big duct. *Dynasty* solves for

temperature, pressure and mass flow rate and the entrance and exit of every section within the dynamic duct, based on the nature of the cycle I expected high velocity and pressure waves to be travelling as a result of high compression on the compressor end and also expected some rebound waves being forced back into the transfer duct by the combustion cylinder as a result of progressive combustion, thus to capture the wave form it was important that the duct be segmented. Understanding the nature of charge from within the transfer duct is important to make a successful SCCC engine.

Some of the key features of the 2-cylinder SCCC model derived from *University of Pisa* specifications are in the cylinder geometry, transfer duct and transfer valve design. These features are also the basis on which a SCCC engine differs from a conventional CI engine. In a conventional CI engine whether two cylindered or multiple cylindered, all cylinders have the same bore, stroke and overall cylinder volume. This SCCC engine has a larger stroke on the compressor cylinder than that on the combustor cylinder thus enabling it to produce a charge of higher volume and density. All cylinders in a conventional CI engine have the same compression ratio where as this SCCC engine has a higher compression ratio on the compressor cylinder than that in the combustor cylinder enabling it to create a positive pressure gradient in the desired direction of charge flow. In a conventional CI engine the compression phase precedes the combustion phase so the air in the combustion chamber attains optimal temperature and pressure for efficient combustion, where as in the current SCCC engine setup the combustor cylinder is phased ahead of the compressor cylinder, but because the combustor cylinder has lower compression ratio than the compressor cylinder a positive pressure gradient can still be maintained for charge flow.

It was presumed that going from three dimensional CFD based model to a one dimensional model we were going to lose some result fidelity, but the objective was to create a one dimensional model in Dynasty that yields results within acceptable error tolerance to *University of Pisa* CFD model and also gives us the benefit of fast computational times and expanded component modeling.

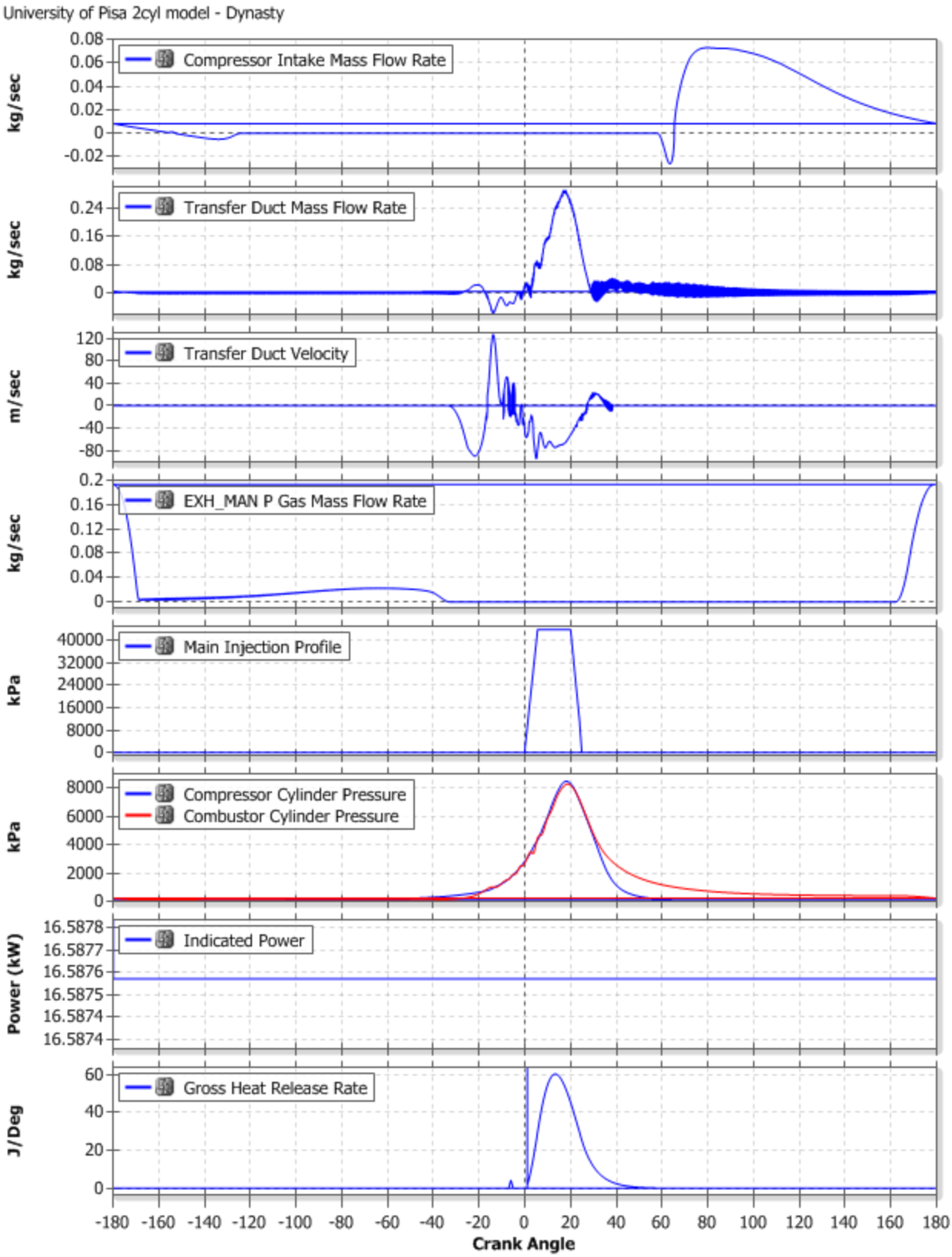

Fig. 33 Dynasty model of University of Pisa geometry characteristics at 27mg/stroke.

During our comparison, a few key engine characteristic and variables were chosen that were attributing to the engine's geometric modeling and combustion process and simulation accuracy. The variables were very carefully chosen to compare complete engine operation while also highlighting detailed combustion and gas exchange simulation results.

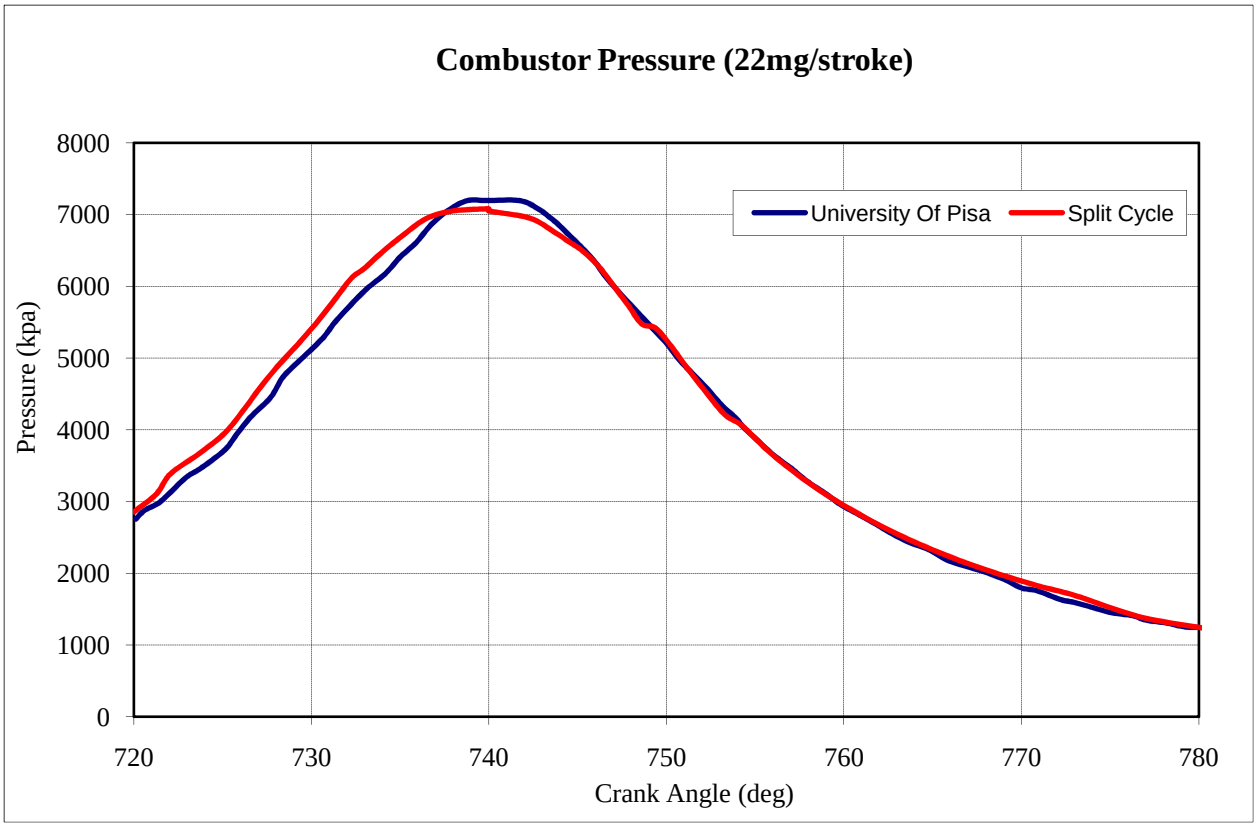

Fig. 34 Combustor pressure vs crank angle at 22mg/stroke.

The combustor peak in-cylinder pressure results show a very good match confirming that the pressure growth in the combustion chamber as a result of charge compression and heat release is modeled with comparable fidelity to a three dimensional model. Rise is in-cylinder pressure is a direct results of the universal gas equation, $PV = mRT$ and is dependent on the heat release Q and also the heat release rate profile. It can be noticed that from 740CA' to 750CA' the blue

curve is above the red curve and from 750CA' onwards it is below, which aligns with the trend seen in the heat release rate seen in fig. 37. In-cylinder pressures are also impacted by valve opening and closing times as the combustion chamber is only completely sealed after the transfer valve closes and the exhaust valve opens.

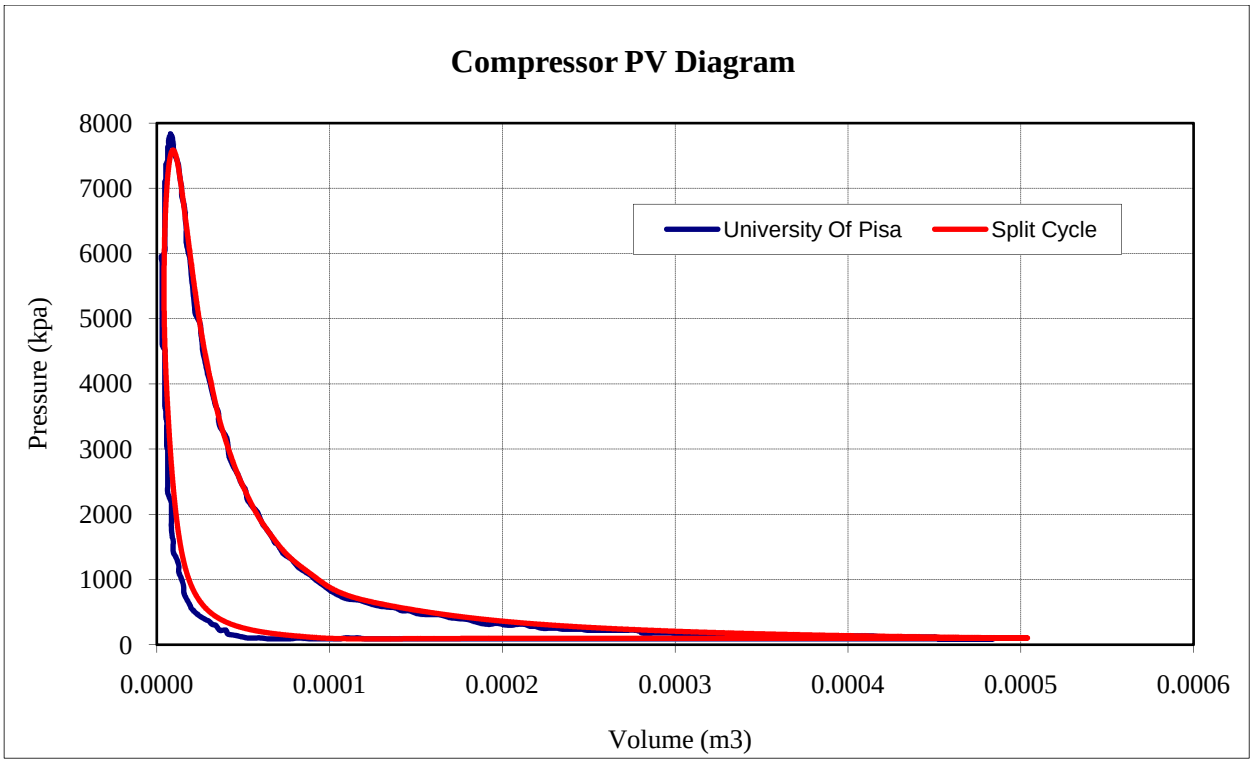

Fig. 35 Compressor PV diagram.

The area contained within the curve of the pressure volume diagram of the compressor cylinder indicates the work done by the piston during air intake in the intake stroke and also the work done during compression stroke. Intake work plus compression work is the total area under the curve. As it can be seen in fig. 35 a good match is seen in the compressor PV diagram, this validates that boundary conditions were accurately established on the compressor side in the model. Piston position versus valve timing relationship and volumetric efficiency of the intake

side controls the shape of this PV diagram, and as both PV curves lay right on top of each other, the modeling of the intake loop has been validated to have not lost any significant modeling accuracy as a result of one dimensional simplification.

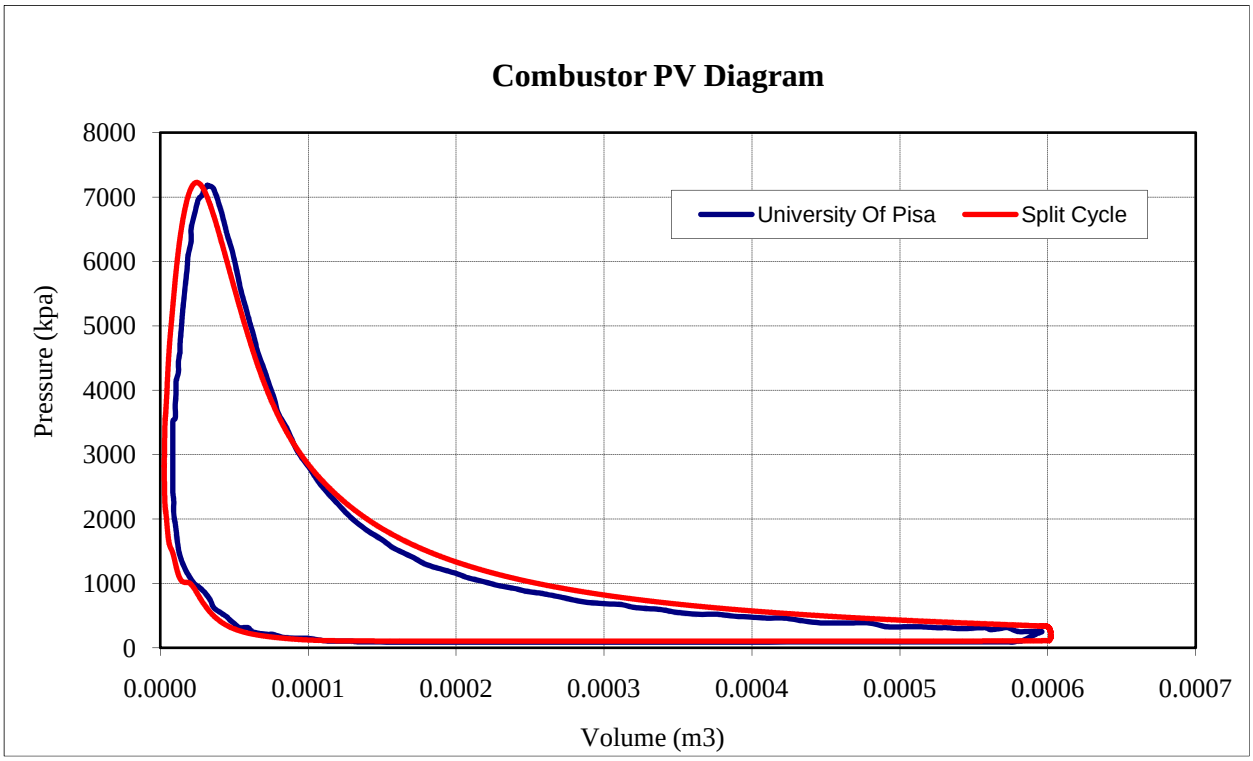

Fig. 36 Combustor PV diagram.

The combustor PV diagram show that the curves superimpose almost perfectly with very slight variation in when SCCC reaches peak in cylinder pressure with respect to the combustion camber volume, this is due to rate of heat elevating in cylinder pressures. The left leg of the red curve in fig. 36 is a result of the left leg of the HRR seen in fig. 37. The pressure decay rate matches very well with University of Pisa results. Overall fig. 36 shows a very good match confirming good combustion characteristics and a good combustor cylinder boundary conditions match.

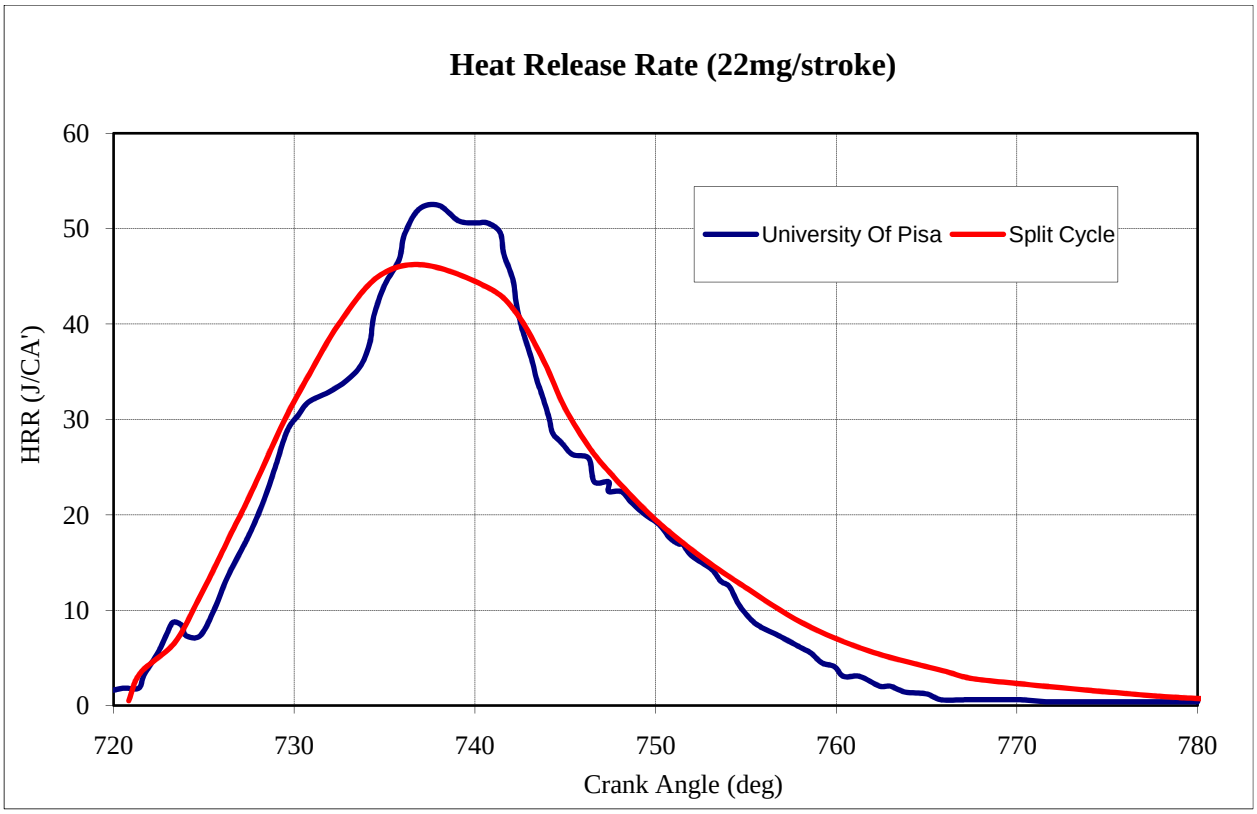

Fig. 37 Heat release rate vs crank angle.

Heat release rate is defined by the chemical reaction going on in the combustion chamber after the physical and chemical delays of combustion are passed. Once the characteristics of a particular combustion process are identified there are many commercially available chemical combustion models to be used with for CFD and 1D solvers. Fig. 37 shows a good match between the heat release rate profiles vs crank angle however there is a difference in heat release rate, this due to difference in the Dynasty solver vs the CFD solver and also due to the exact chemical composition assumed for diesel fuel. As results in fig. 34 and fig. 36 show a very good match to University of Pisa results and these results are a direct consequence of HRR, we can infer that fig. 37 is a good match with results within the accuracy of one-dimensional modeling.

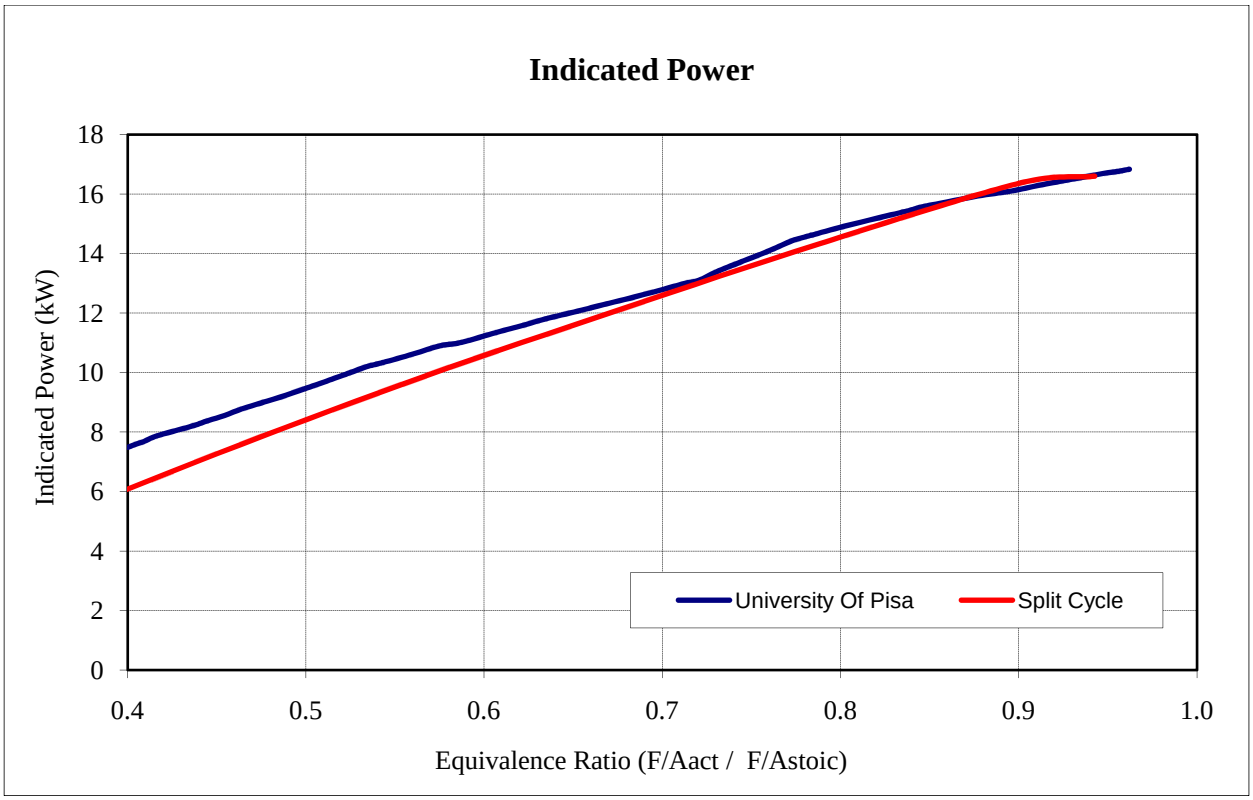

Fig. 38 Indicated power vs equivalence ratio.

The indicated power produced by the University of Pisa CFD model and one dimensional Dynasty model show a good match at various equivalence ratios with a slight difference at low equivalence ratios due to expanded one dimensional modeling abilities. At low equivalence ratios the ratio of work used in overcoming pumping losses to the work produced by combustion becomes more dominant so even a slight change in pumping losses can be clearly captured in indicated power. Since our one dimensional model had the air system actually modeled it eliminated all associated assumptions that have to be made in case of CFD modeling and reflects pumping losses more accurately.

4.3 Results – Cat® C4.4 Liter Split Cycle Clean Combustion Engine.

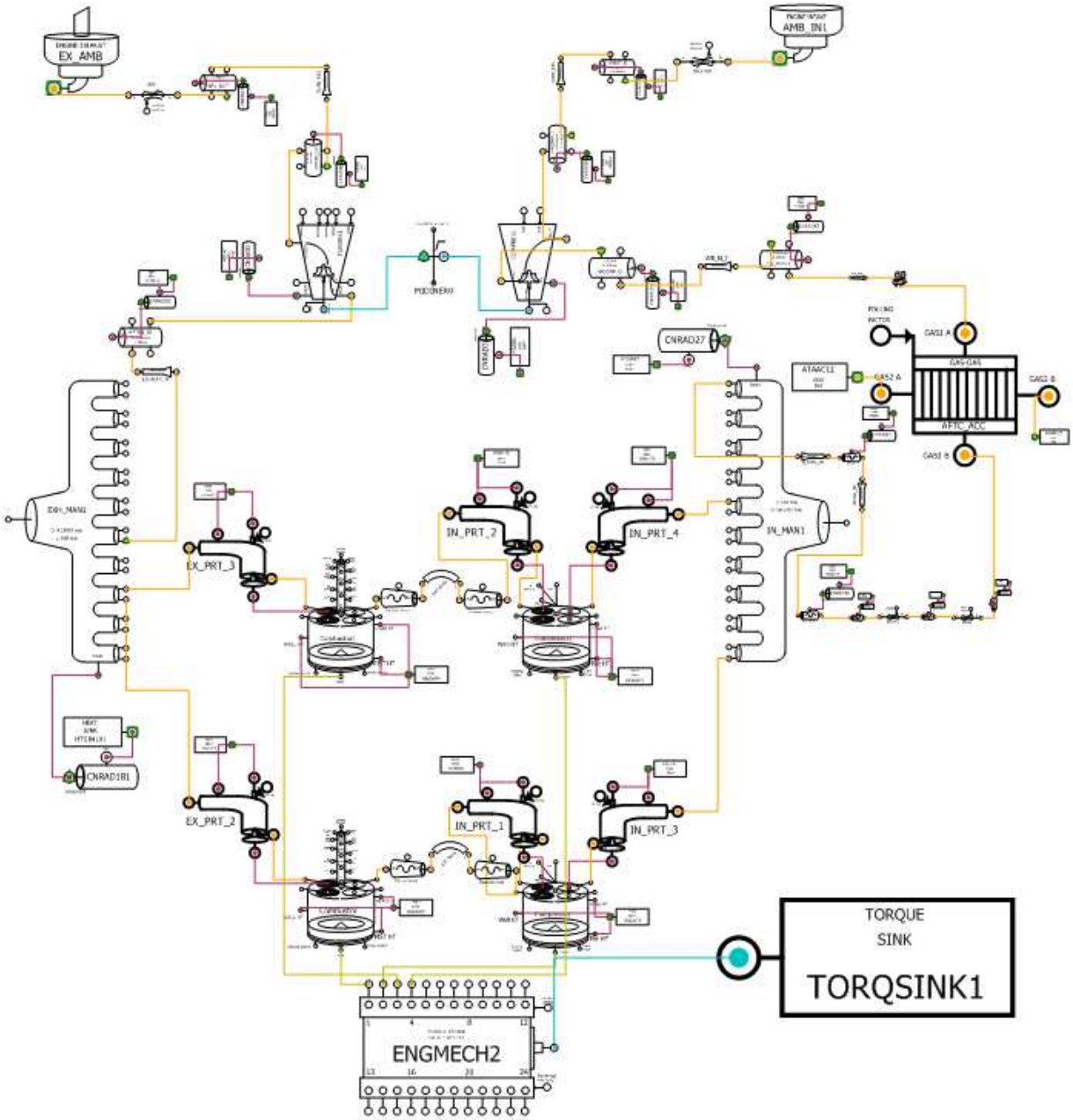

Fig. 39 a. Complete plant model of a Split Cycle Clean Combustion 4.4 liter 4 cylinder engine.

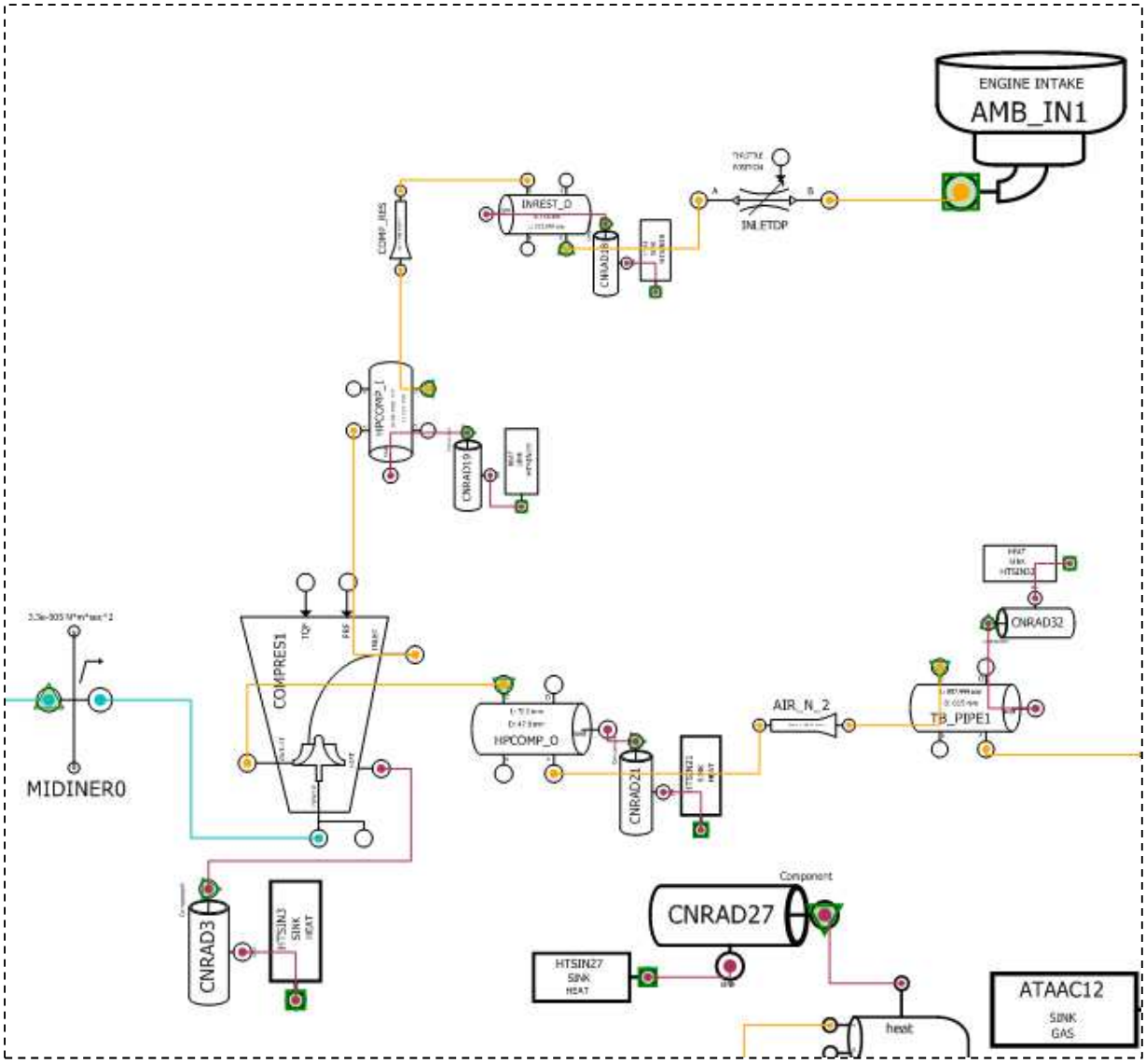

Fig. 39 b. Intake and Compressor loop of Split Cycle Clean Combustion 4.4 liter 4 cylinder engine.

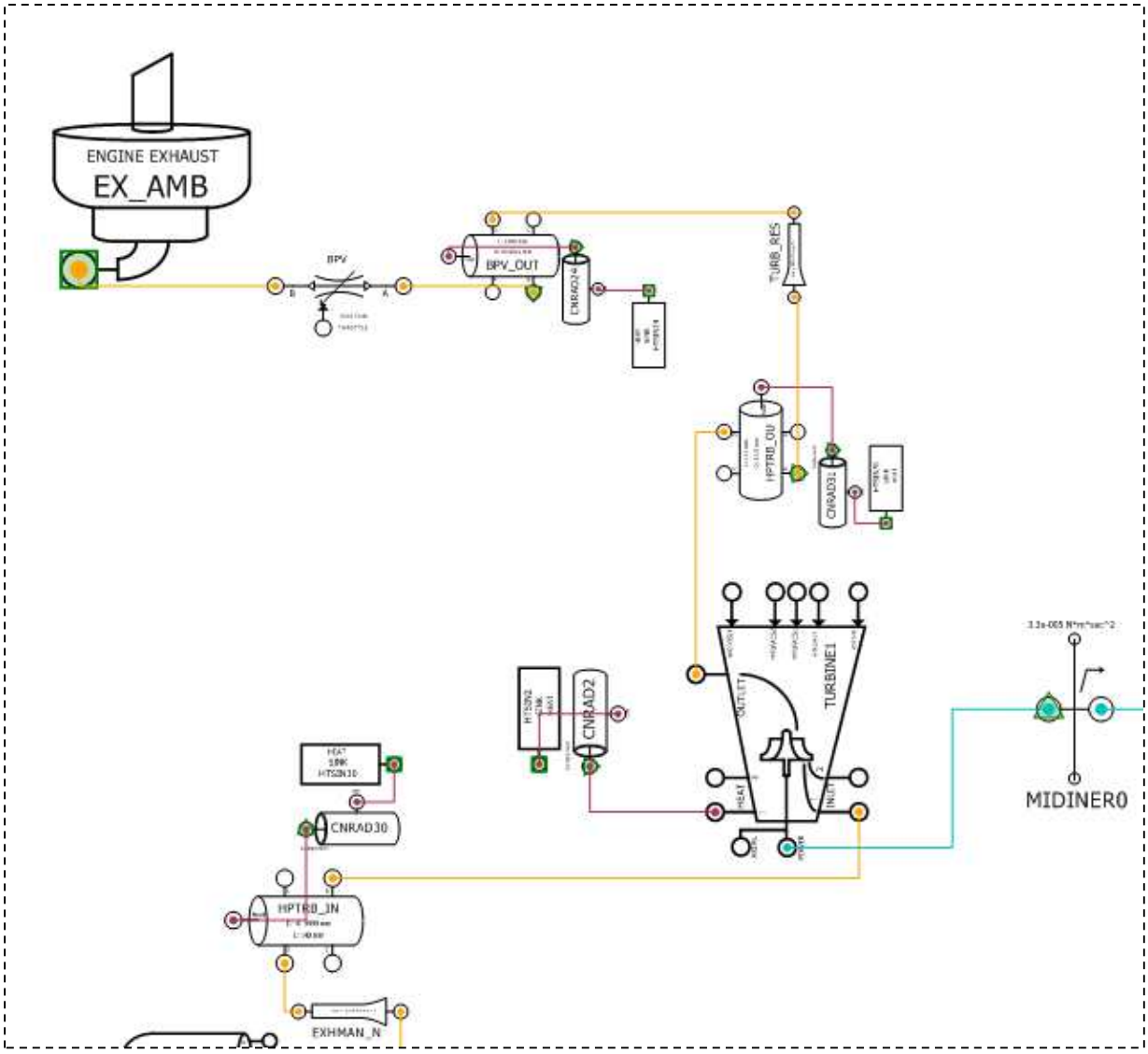

Fig. 39 c. Exhaust and Turbine loop of Split Cycle Clean Combustion 4.4 liter 4 cylinder engine.

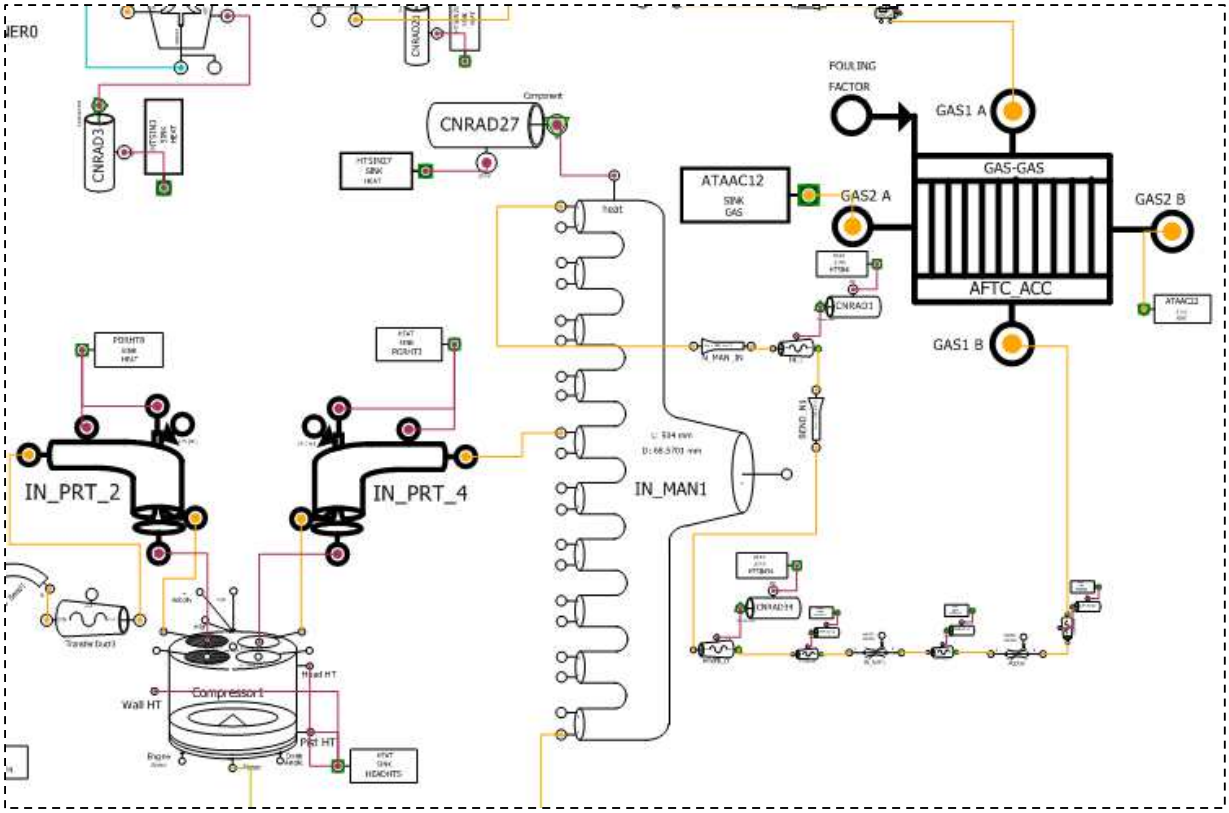

Fig. 39 d. Intercooler, Intake Manifold and Compressor Cylinder of the Split Cycle Clean Combustion 4.4 liter 4 cylinder engine.

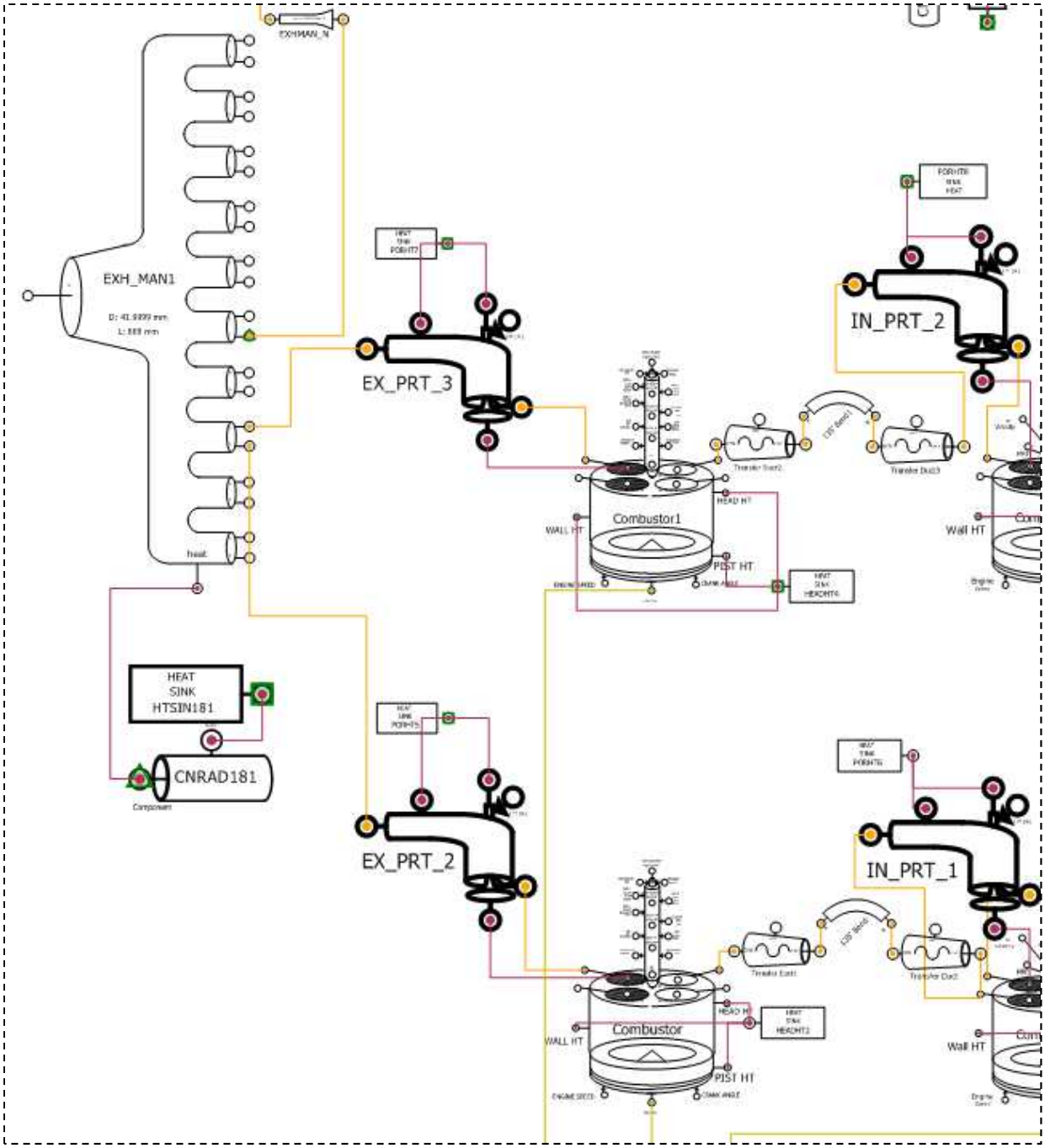

Fig. 39 e. Transfer Duct, Exhaust Valve and Exhaust Manifold of the Split Cycle Clean Combustion 4.4 liter 4 cylinder engine.

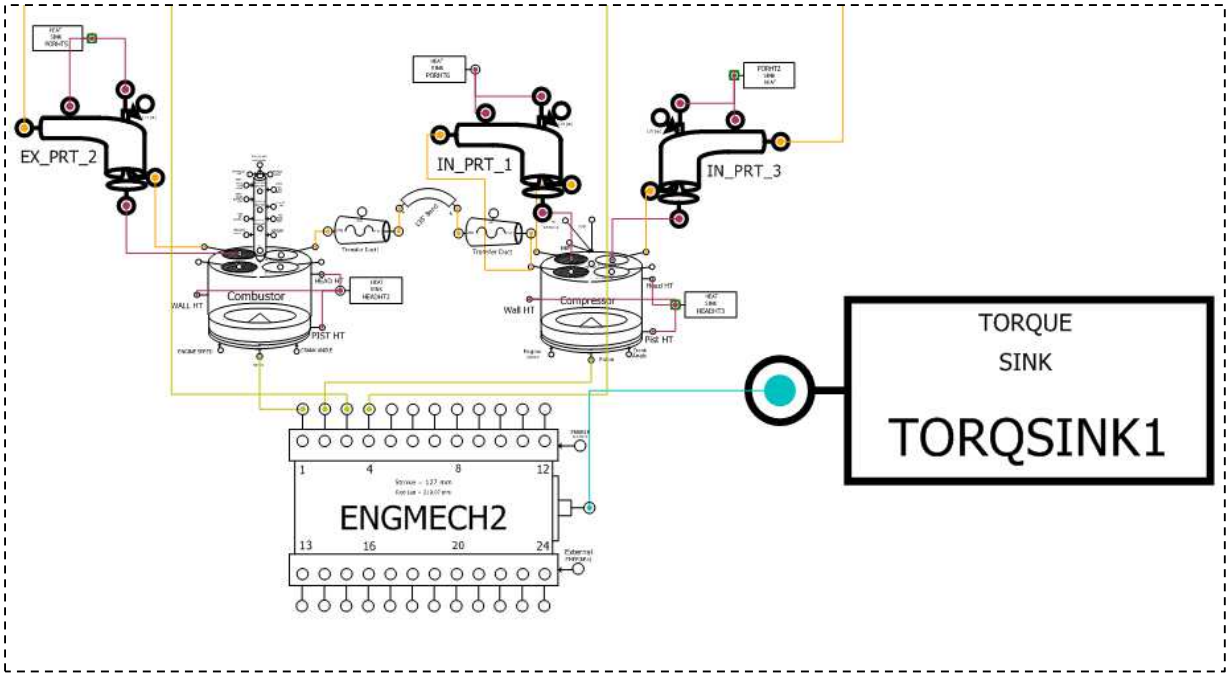

Fig. 39 f. Crank Shaft and Dynamometer of the Split Cycle Clean Combustion 4.4 liter 4 cylinder engine.

For developing the SCCC model of Caterpillar's C4.4 engine we leveraged their existing CI model and made component and control modifications to operate it on the SCCC concept.

Caterpillar Inc. invests a lot in Virtual Product Development (VPD) for R&D and NPI processes. They also do VPD in various levels of virtuality. They employ pure modeling based development, then hardware in the loop development followed by prototyping, lab testing and then field testing in the development of any new product.

For this study a one-dimensional model of Caterpillar's current production Cat® C4.4 engine used in their 316 Hydraulic Excavator was leveraged after validating it with simulated test data

obtained from obtained from dynamometer testing and field testing of the engine. The goals of this study had to be achieved while working within the constraints of feasibility and cost effectiveness, thus it was decided to leave the block and manifold geometry unchanged and the other components may be modified as needed to achieve efficient split cycle combustion.

In this effort the components comprising the forced induction loop such as the turbocharger, intercooler, etc were found to be sufficiently sized for the C4.4's split cycle clean combustion variant and thus were not changed. Changes were only made to the cylinder head, intake and exhaust valves, cam shaft, crank shaft, connecting rods and pistons.

Along the research process all modeling geometries were discussed with the engine packaging team at Caterpillar and all component sizing, machining and efficiency constraints were considered to ensure that a C4.4 engine could be converted to a real prototype SCCC test engine in the future without much tooling cost.

Fig. 39 shows all the components of the 4.4L SCCC four cylinder diesel engine.

a) Air Intake
b) Turbocharger
c) Intake Manifold
d) Intake Valve and Port
e) Compressor Cylinder
f) Transfer Valve and Port

g) Transfer Duct

h) Combustor Cylinder

i) Exhaust valve

j) Exhaust Manifold

k) Muffler

l) Crankshaft and timing components

m) Dynamometer.

The Dynamometer component will be used in maintaining a desired engine speed while measuring engine torque or defining an engine torque and measuring the speed at which engine delivers that torque instead. It is very helpful in capturing engine speed-torque characteristics at a constant speed or variable speeds.

	General Parameters	CAT C4.4	SCCC
1	Modeling Technique	1-D Validated	1-D
2	Fuel	Diesel	Diesel
3	Air Filter	Unclogged	Unclogged
4	Cat Turbocharger model	GT22 56/50mm	GT22 56/50mm
5	Intercooler Type	Air to Air	Air to Air
6	Intake Manifold Volume	1.86 L	1.86 L
7	Exhaust Manifold Volume	0.93 L	0.93 L
8	Diesel Particulate Filter	Partial rest.	No DPF
9	Muffler	No rest.	No rest.
10	Stroke	4 Stroke	2 Stroke
11	Firing Order	1,3,4,2	1,2,3,4
12	Firing Interval CA degrees	0-540-180-360	0-22.5-180-202.5
13	FMEP at Low Idle	60 kPa	60 kPa
14	FMEP at High Idle	133 kPa	133 kPa
15	Engine Low Idle & High Idle	800, 1950 rpm	800, 1950 rpm
16	Coolant Temperature	80'C	80'C
17	Ambient Air Temperature	25'C	25'C
18	Ambient Air Pressure	100 kPa	100 kPa
19	Common Rail	Yes	Yes
20	Variable Valve Timing	No	No
21	Injector Geometry - no. of holes	6	9
22	Injector Geometry - hole dia.	0.12 mm	0.12 mm
	Engine Block Parameters	CAT C4.4	SCCC
23	Displacement	4.4L	4.4L
24	Bore	105 mm	105 mm
25	Stroke	127 mm	variable
26	CR Compressor Cylinder	NA	105 : 1
27	CR Combustor Cylinder	16.5 :1	92.5 :1
	Camshaft and Valve Parameters	CAT C4.4	SCCC
28	No of Intake Valves	2	2
29	Intake Valve Area	1510 mm2	1510 mm2
30	No of Exhaust Valve	2	2
31	Exhaust Valve Area	1321 mm2	1321 mm2
32	No of Transfer Valves	NA	1

33	Intake Valve Open	355 CA'	80 CA'
34	Intake Valve Close	-150 CA'	-126 CA'
35	Transfer Valve Open	NA	-10 CA'
36	Transfer Valve Close	NA	30 CA'
37	Exhaust Valve Open	130 CA'	165 CA'
38	Exhaust Valve Close	-340 CA'	-36 CA'
39	Intake Valve Lift	9.33 mm	25 mm
40	Exhaust Valve Lift	9.0 mm	25 mm
41	Transfer Valve Lift	NA	5 mm
42	Transfer Valve Area	NA	500 mm2
	Transfer Duct Parameters	CAT C4.4	SCCC
32	Displacement	NA	12.7 cc
33	Type	NA	conical
34	No. of ducts constitute main duct	NA	2
35	Cone Diameter (large end)	NA	25.2 mm
36	Cone Diameter (small end)	NA	18.9 mm
37	Length	NA	16.5
38	Bend Angle	NA	135'
39	Bend Radius	NA	25 mm

Table 3 Cat® C4.4 and SCCC key model parameters.

Table 3 compares some of the major specifications of Cat® C4.4 and its SCCC variant engine. The major design differences are highlighted in blue. SCCC valve timings in Table 3 are with respect to combustor cylinder 1 at crank angle 0.

Lug curve of an engine is the max power the engine produces according to its certified rating. When an engine is being sold manufactures certify this lug curve and advertize the engine power according to it. Fig. 41 shows the lug curve for the Cat® C4.4 engine we are using in our study. It can be seen that SCCC makes significantly more power than C4.4 all throughout the operating range. Maximum performance advantage can bee seen between 1200-1600rpm range. As both

engines are of the same displacement, higher peak power and higher power all throughout the operating range improve the power to displacement ratio of the engine. The results show that a similarly sized SCCC engine can be used to support higher peak power rated applications than a conventional diesel engine. Looking at the SCCC lug curve from 1500-1950rpm it can be seen that the slope is negative, which is a favorable characteristic in applications where the engine gets impacted by sudden loads at high rpms. The negative slope supports a better engine rpm recovery to sudden loads or a better resistance to bogging due to block loads.

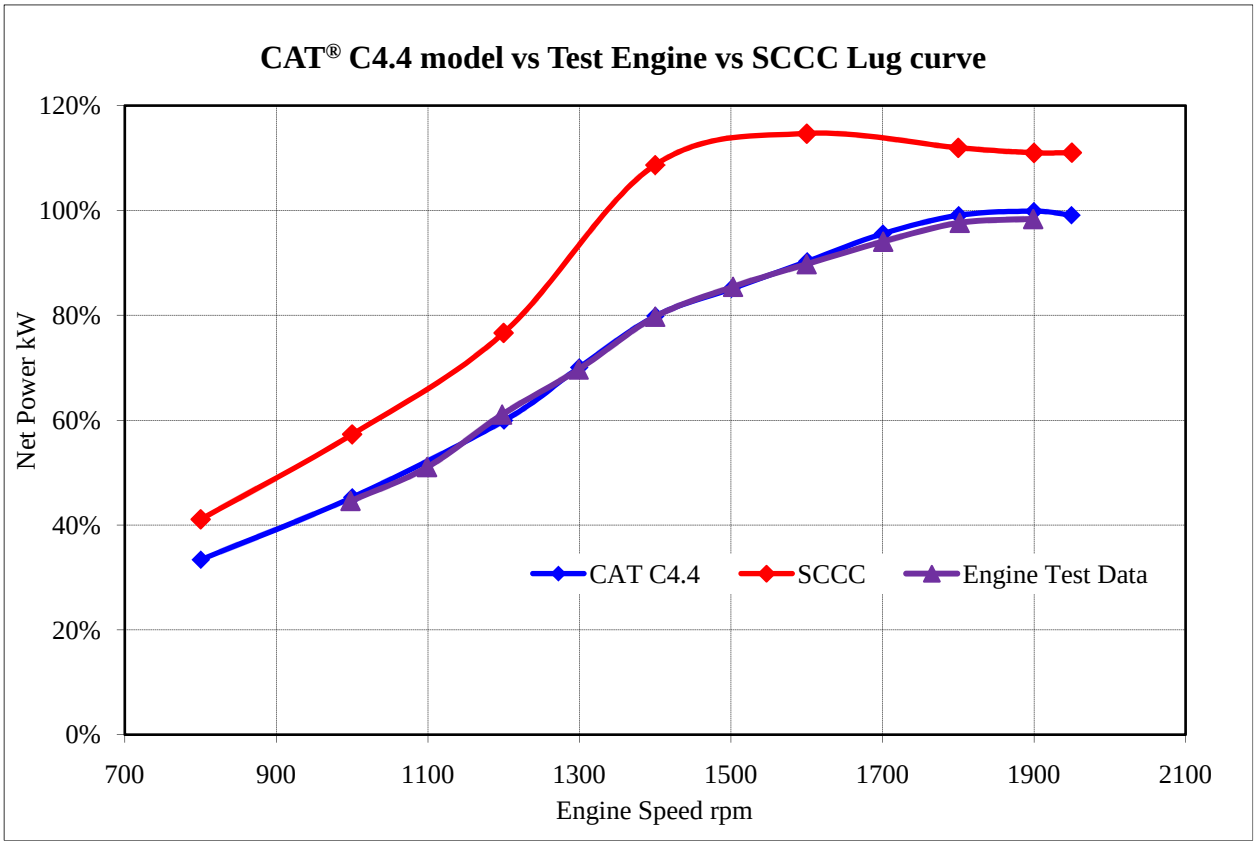

Fig. 41 Cat® C4.4 max power used in Excavator 316.

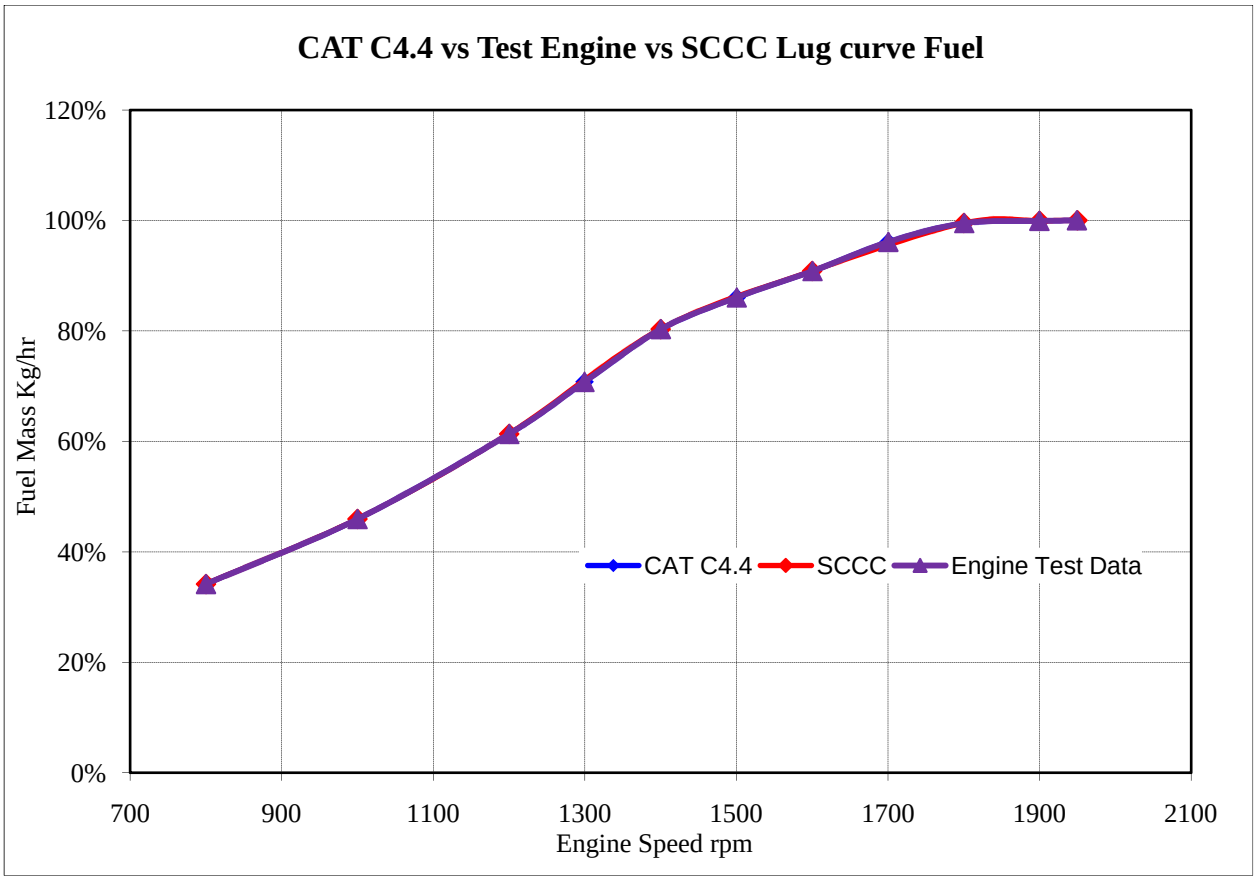

Fig. 42 Lug curve fuel.

Lug curve fuel or max fuel for an engine is defined as the fuel needed to produce the rated power of the engine. For part load testing a percentage of this total fuel is injected at various engine speeds and the engine's power, efficiency and other parameters are evaluated. As Cat® C4.4 engine is the measurement datum for our study we used its lug curve fuel and performance was measured with our SCCC engine performance. Fig. 42 shows lug curve fuel for Cat® C4.4 engine. So both Cat® C4.4 and SCCC engine were run with same fuel quantity and SCCC produced significantly more power as seen in fig. 41. By using the same fuel rate rather than trying to match SCCC peak power to Cat® C4.4 it became easier to compare the performance of the two engines with respect to changes in other internal and environmental variables.

Engine fuel is controlled by an electronic engine governor that resides in the engine ECM. It will be discussed later in this thesis that our SCCC engine is going to be designed using common rail fuel delivery

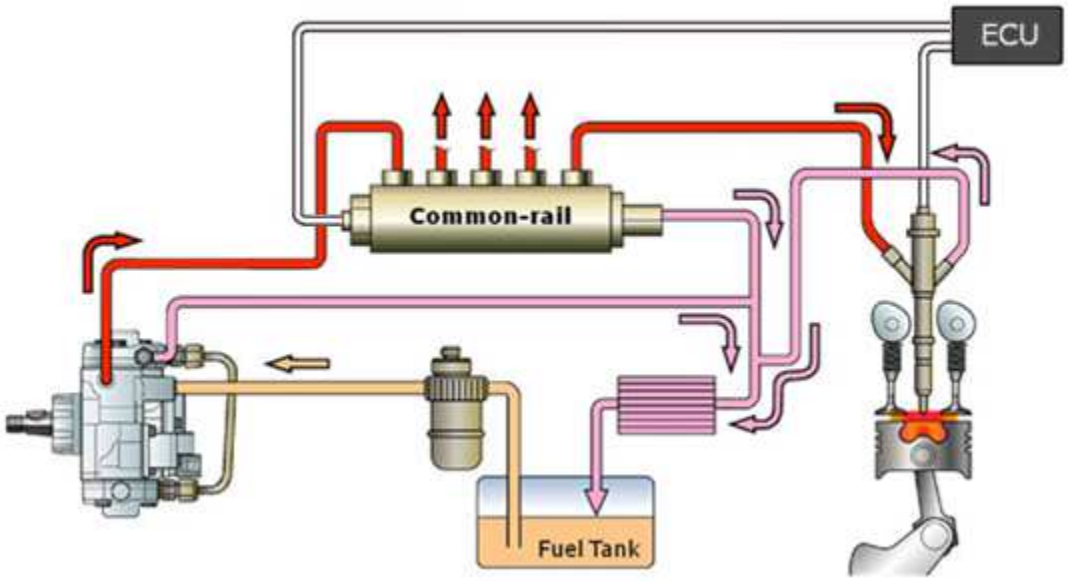

Fig. 43 Common rail fuel delivery schematic shown on a conventional compression ignition engine with a "W" bowl piston head. (Sourced from www.wikipedia.com)

The governor requests a particular amount of fuel at every sample interval to match either a targeted engine speed (incase of a full range governor) or a targeted torque (incase of a min-max governor) and tries to limit the equivalence ratio in the combustion chamber so as not produce a rich or lean combustion leading to excessive engine emissions or deteriorated engine performance. Fig. 43 illustrates a Common Rail Fuel Injection (CRFI) schematic.

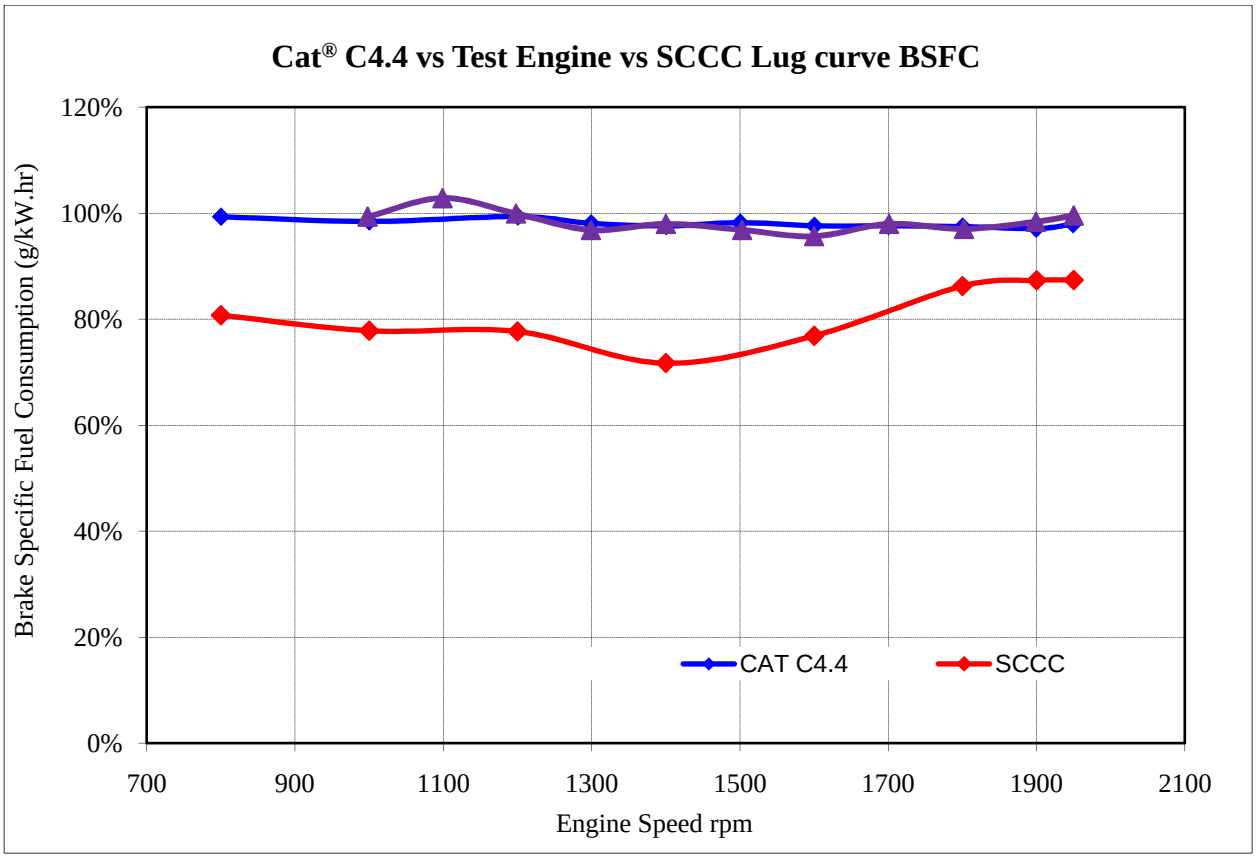

Fig. 44 Lug curve BSFC.

Fig. 44 shows the brake specific fuel consumption of Cat® C4.4 engine on its lug curve. We will evaluate our SCCC engine against C4.4 at all points on the lug curve and the area under it to identify SCCC's performance at all load conditions. 28 evaluating points were chosen for the steady state evaluation of the SCCC engine. Fig. 45 shows those 28 points with 7 points at each fuel rate but varying engine speeds. 35% of lug curve fuel was chosen as the minimum as BSFC for any engine increases at a very high rate and will eventually reach "infinity" as fuel rate decreases, this is because the power the engine is making at very low fuel rates vs the power needed to overcome the internal engine friction and pump losses almost cancels out, thus resulting in us with a "zero" net power at one point. As BSFC is a measure of fuel used per

power produced, BSFC becomes infinity at zero net power operation. At 35% lug curve fuel the BSFC of our engine can be accurately measured to produce meaningful correlation thus 35 % was the lowest point we chose.

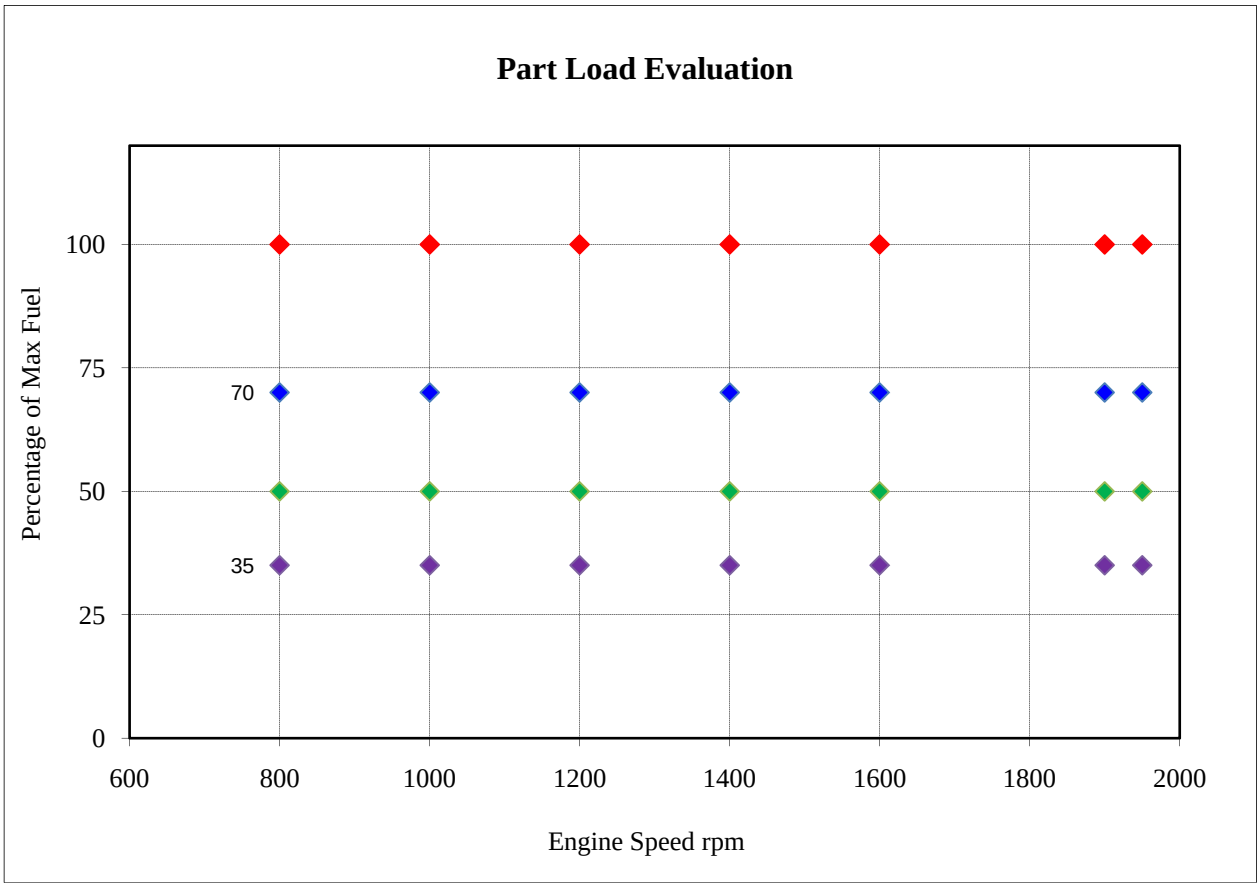

Fig. 45 Part load operating points.

After a good initial set of engine parameters were defined we started the improvement of our SCCC engine using "design of experiments" (DOE) methodology by varying the few parameters that were identified as key to improving SCCC engine BSFC and efficiency. Fig. 46 shows the efficiency comparison of our first guess model to Cat® C4.4. DOE yielded huge improvements.

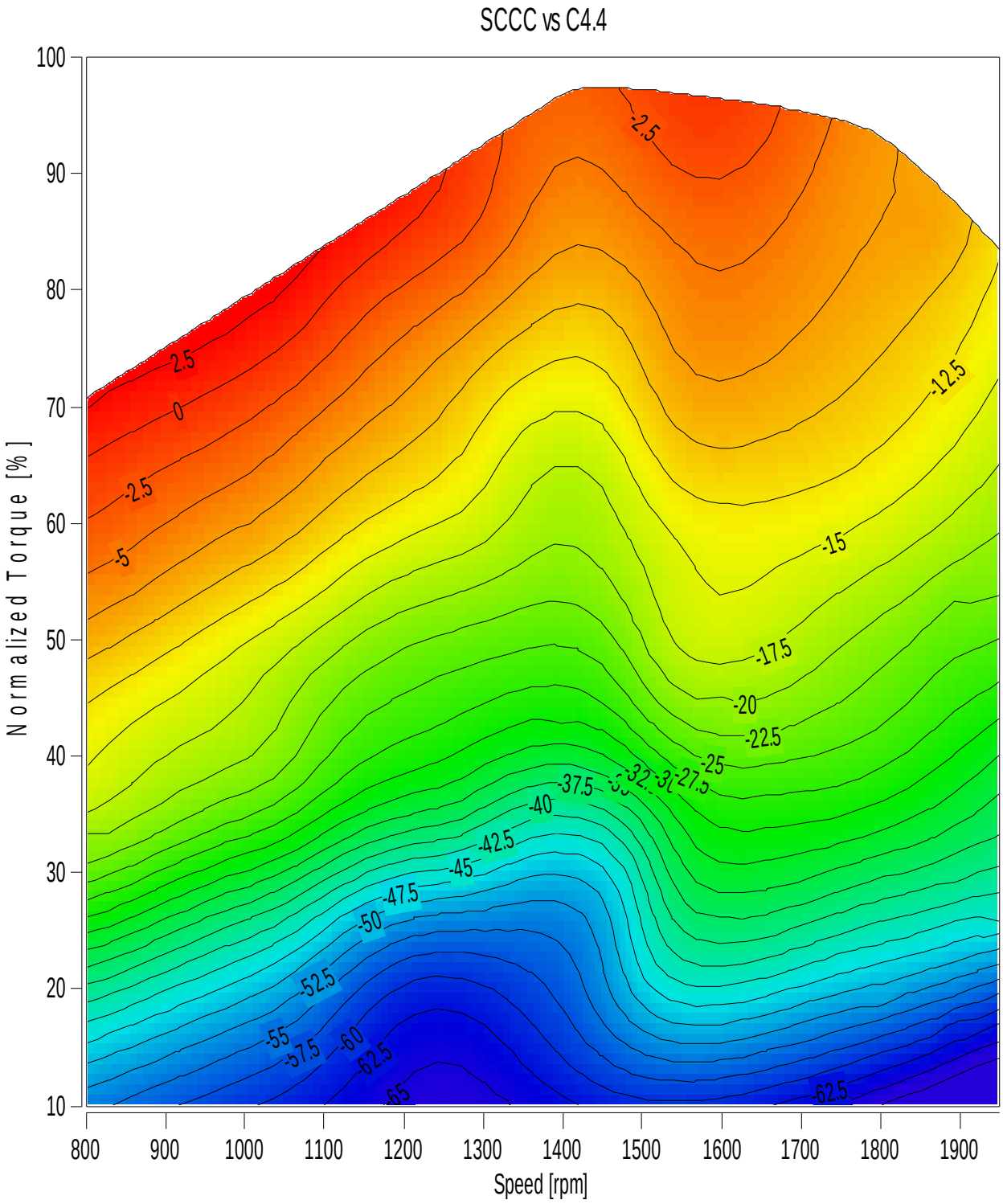

Fig. 46 SCCC first guess model BSFC comparison to Cat® C4.4.

Table 4 shows the parameters that were varied, their range of variance and highlighted in orange are the final selected values that yielded the best results.

The DOE was broken down into three steps to reduce the number of total simulations and dependant variables were clubbed under each set.

DOE 1		Value 1	Value 2	Value 3
1	Espd(rpm)	800	1400	1950
2	Fuel(lug curve fuel %)	100	50	
3	Main/Pilot Timing CA' BTDC	0/10	-5/5	-10/0
4	Compression Ratio of Combustor	85:1	92.5:1	100:1
5	Cylinder Phasing(CA')	22.5	30	37.5
6	Total number of Iterations	**3x2x3x3x3 = 162**		
DOE 2		Value 1	Value 2	Value 3
8	Espd(rpm)	800	1400	1950
9	Fuel(lug curve fuel %)	100	50	
10	Pilot Injection (% total fuel)	0.005	0.01	
11	Fuel Rail Pressure (KPa)	50000	100000	150000
12	Intake Valve Lift(mm)	9.33	25	
13	Exhaust Valve Lift(mm)	9.33	25	
14	Transfer Valve Lift(mm)	5	10	15
15	Total number of Iterations	**3x2x2x3x2x2x3 = 432**		

DOE 3		1	2	3	4	5	6	7	8
17	Espd(rpm)	800	1000	1200	1400	1600	1800	1900	1950
18	Fuel(lug curve fuel %)	100	70	50	35				
19	Transfer Valve Dia(mm)	25	27	30					
20	Total number of Iterations	**8x4x3 = 96**							

Table 4 DOE variables and their chosen values.

Rail Pressure Map (Kpa)		
RPM		
800	150000	50000
1400	100000	50000
1950	100000	50000
	50% Lug Curve Fuel	100% Lug Curve Fuel

Table 5 Fuel rail pressure map.

Once we had our initial set of parameters based on packaging and design constraints we attempted DOE 1 and DOE 2 at low, mid and high engine speeds only. All the results of DOE 1 and DOE 2 were set as a constant going into DOE 3 and then the engine was completely evaluated at all engine speeds. The fuel rail pressure map was made by analyzing the results and thus we can infer that a SCCC engine would benefit from a common rail design so we can vary the fuel rail pressure.

Fig. 46 Valve lift profiles were made by analyzing the results and it was inferred that variable valve timing is not needed at this time. The basic idea behind valve timing is to open the intake valve when there is enough vacuum inside the cylinder to provide efficient intake air flow through the manifold, but waiting too long to open the valve can cause engine choking and decrease the overall engine efficiency. The transfer valve timing was designed to achieve a pressure gradient across the compressor and combustor cylinders, reduce the turbulence of air and reduce velocity in the transfer duct. Exhaust valve timing was designed to use the input charge for scavenging while providing enough time for all burnt gas removal.

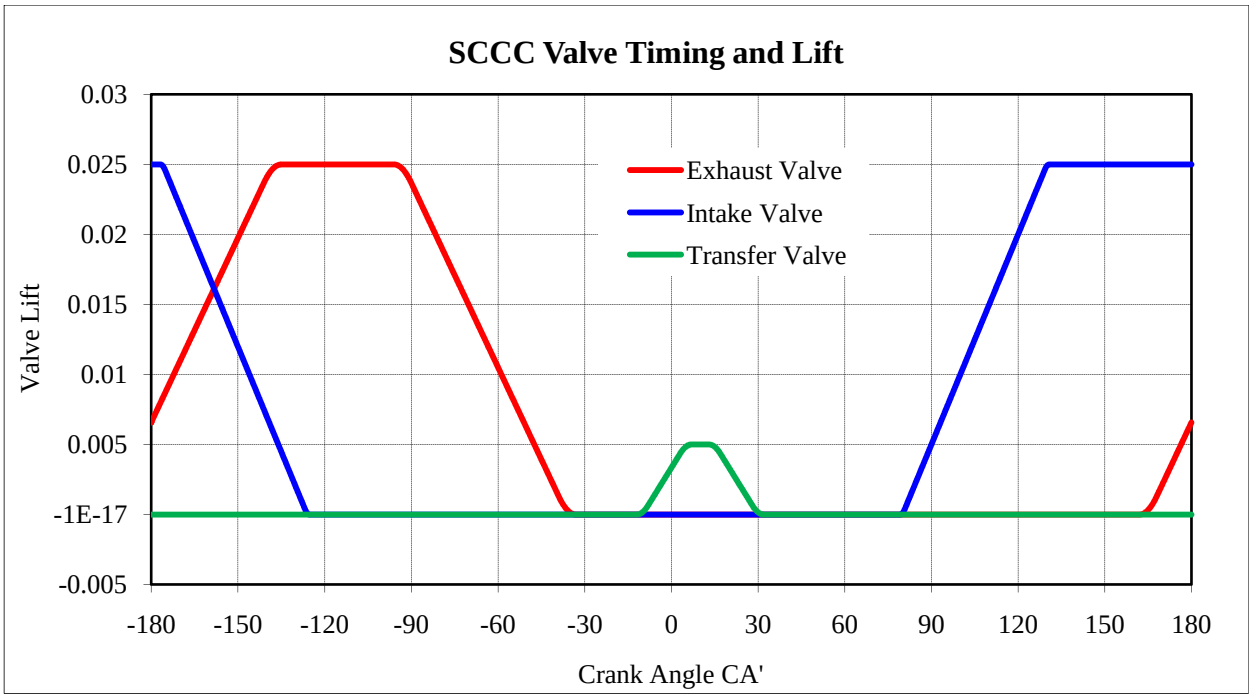

Fig. 47 Valve timing and lift.

Fig. 48 shows SCCC engine in-cylinder temperature and pressure rise and transfer duct charge transfer characteristic in motoring mode. During motoring the dynamometer is used to rotate the engine at a constant speed while no fuel is added to the engine, this helps us evaluate the gas dynamics of the system without the pulsation caused due to combustion. Fig. 48 also highlights the desirable pressure gradient created between the compressor and combustor cylinder by optimum valve timing. Transfer duct velocity and mass transfer rate are used to estimate the optimum time for fuel injection to achieve the best vaporization and mixing of fuel. The last two rows show no heat release rate and no main fuel injection profile as would it be expected while the engine is operated in motoring mode.

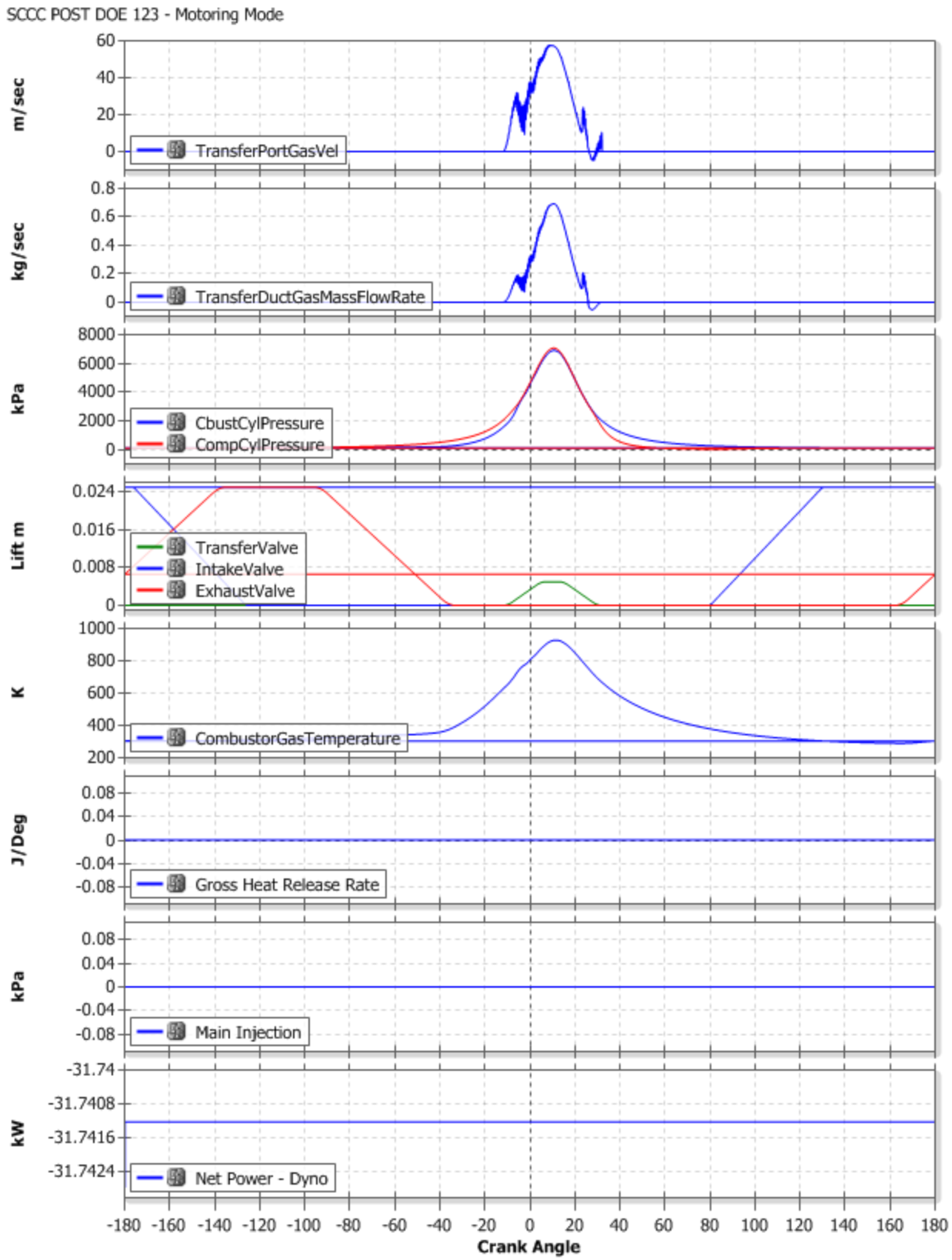

Fig. 48 SCCC C4.4 operating characteristic in motoring mode.

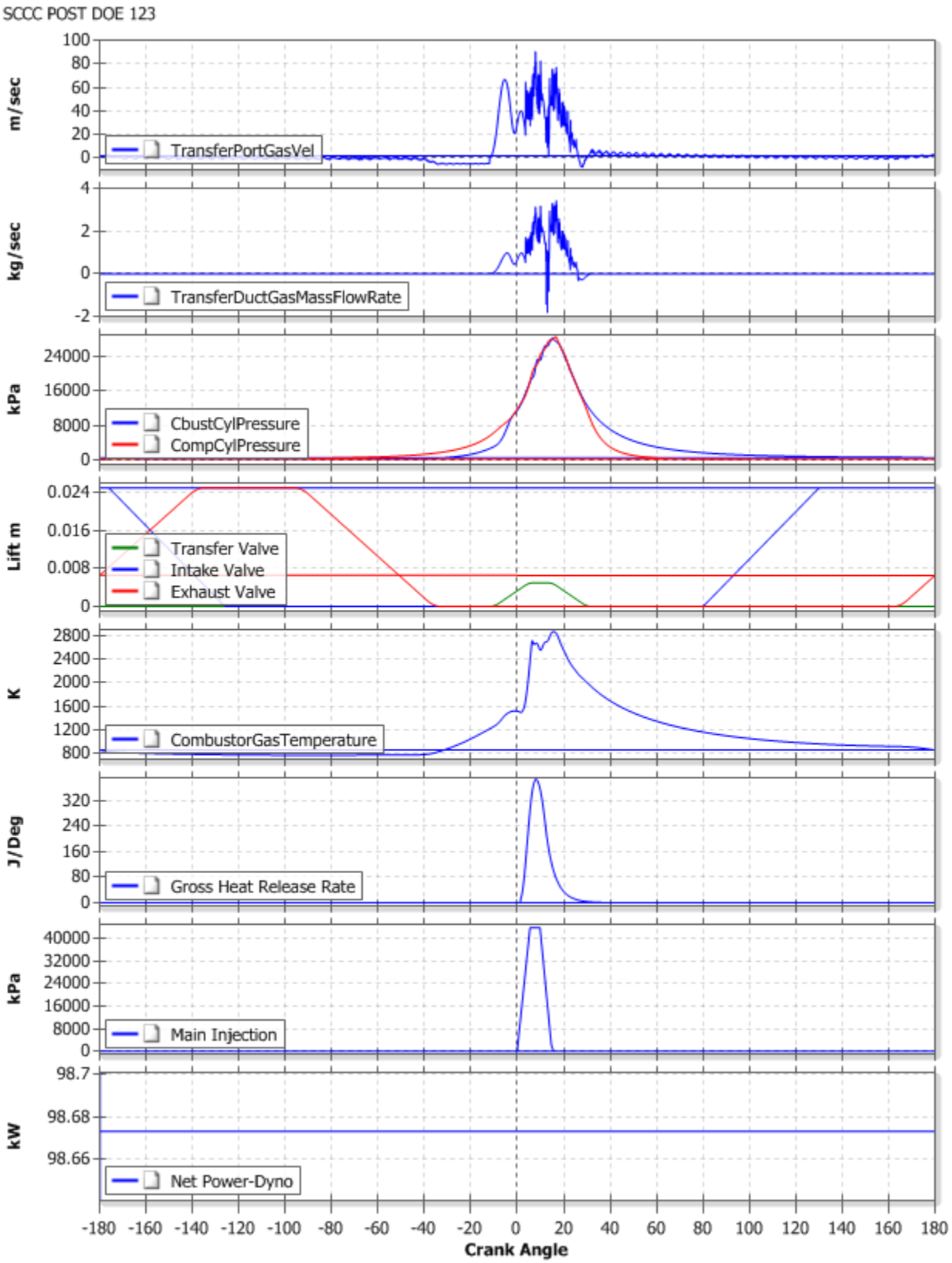

Fig. 49 SCCC C4.4 operating characteristic at full load and high idle.

Fig. 49 shows the operating characteristics of the SCCC engine in its plant model at high idle and 100% lug curve fuel. In comparison with fig. 48 one can clearly see the pulsation caused in the transfer duct due to combustion profile in the combustor cylinder. Injector geometry was designed to provide the short injection duration with optimum spray characteristics for swirl mixing. The injection is kept short and aligned with the transfer valve opening and closing to use the most out of the air velocity in the transfer duct that aids in mixing. Heat release completes over a very short crank angle span and displays characteristics of spontaneous combustion which indicates that split cycle clean combustion is primarily dependant on chemical kinetics. In an attempt to control the physical and chemical delays is combustion there is a very small pilot injection used 10 CA' prior to the main injection that could not be captured in the graph. It can also be seen that at the current operating point of 1950rpm and 100% lug curve fuel the SCCC engine makes 98.7kW of net power.

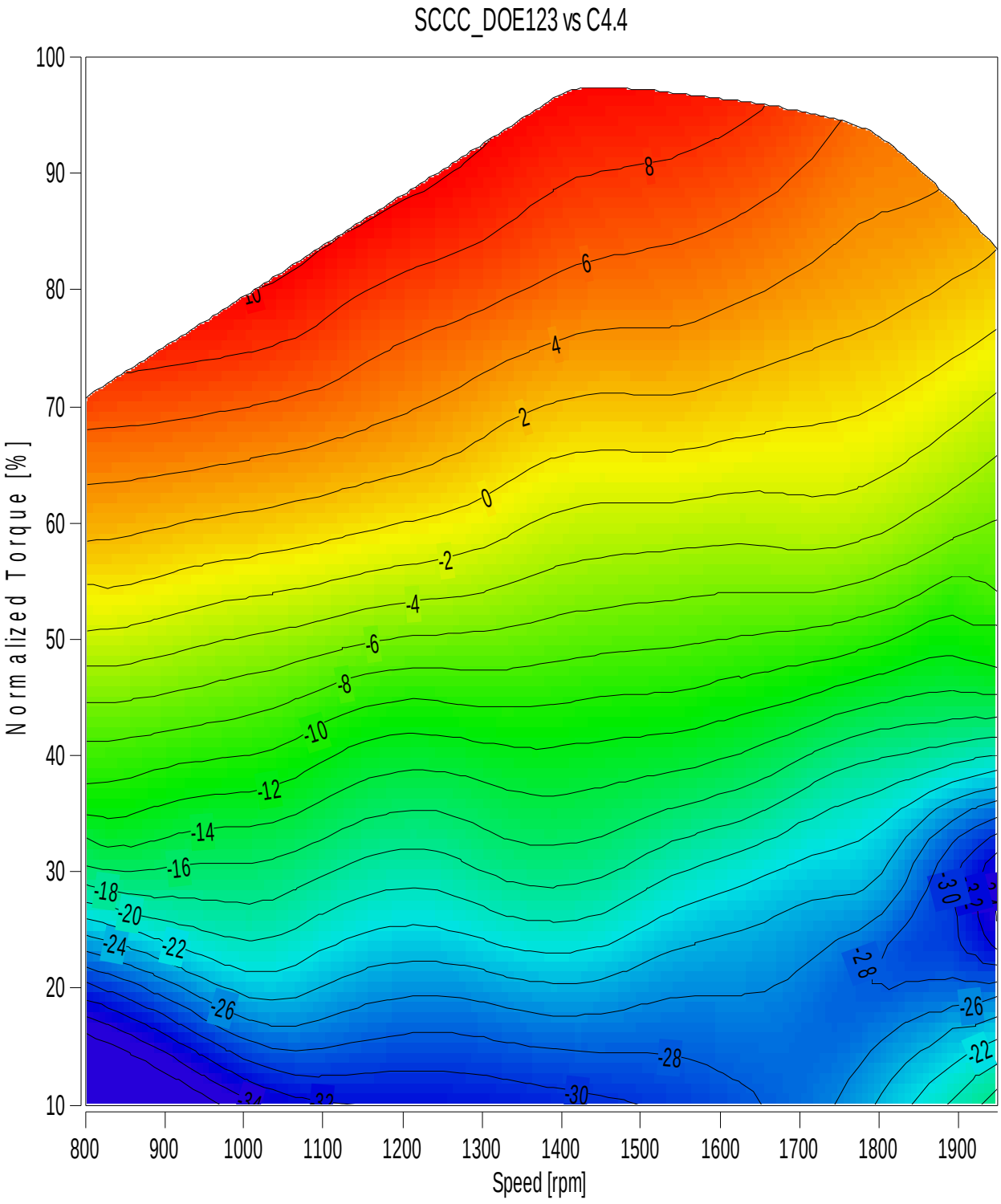

Fig. 50 Cat® C4.4 vs SCCC percent BSFC comparison.

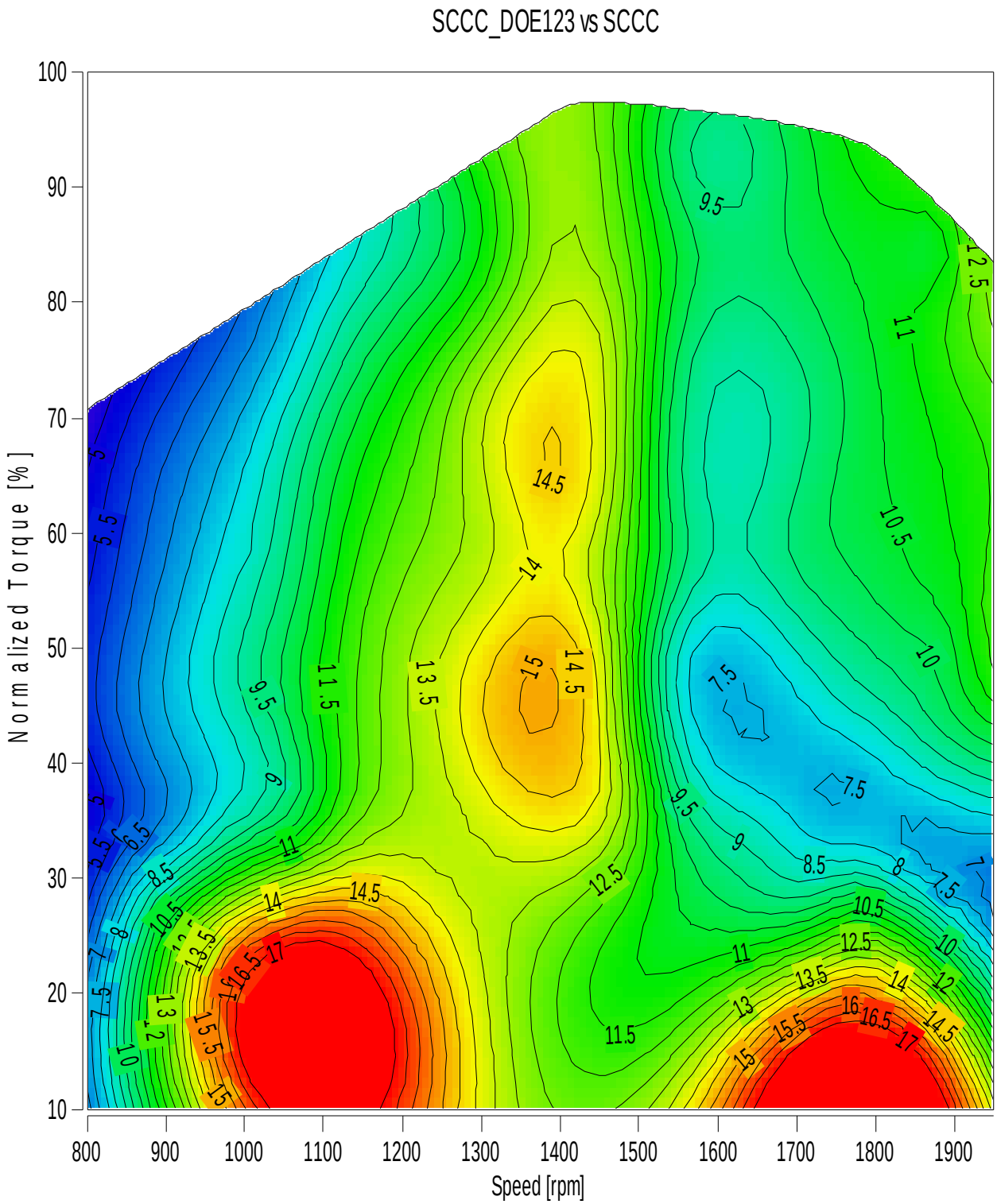

Fig. 51 SCCC first guess model to post DOE 1, 2 and 3 improvements in BSFC.

Fig. 50 is an important result of this study, it compares brake specific fuel consumption of the Cat® C4.4 to the SCCC engine with its entire plant model (air systems and crank etc.) for all possible engine operating points. It can be seen that for greater than 55% of max engine load (270 Nm and above) SCCC engine has up to 10% better BSFC than Cat® C4.4.

Below 55% of max engine load, SCCC engine BSFC is below Cat® C4.4 and it incrementally worsens as load is decreased. BSFC is worst at the low and high operating speeds and low load as shown by the region in red.

SCCC engine requires significantly more work in pumping than a conventional compression ignition engine and at low engine loads, pumping loss to power produced ratio increases significantly more than in a CI engine and the resultant net power is worse that worsens the BSFC as seen in table 6.

Percent Lugcurve Fuel	Engine Speed	SCCC DOE123	SCCC Initial Guess Model	CAT C4.4	SCCC DOE123 vs CAT C4.4	SCCC DOE123 vs SCCC Initial Guess Model	SCCC Initial Guess Model vs C4.4
Fuel	**rpm**	**BSFC**	**BSFC**	**BSFC**	**% Adv**	**% Adv**	**% Adv**
100.0%	800	203	212	218	7%	5%	3%
70.0%	800	217	230	216	-1%	6%	-6%
50.0%	800	255	269	223	-14%	5%	-20%
35.0%	800	334	360	250	-33%	7%	-44%
100.0%	1000	199	214	218	9%	7%	2%
70.0%	1000	211	231	213	1%	8%	-8%
50.0%	1000	248	273	220	-13%	9%	-24%
35.0%	1000	295	354	243	-21%	17%	-45%
100.0%	1200	200	220	219	9%	9%	0%
70.0%	1200	213	243	216	1%	12%	-13%
50.0%	1200	255	293	221	-15%	13%	-32%
35.0%	1200	298	376	243	-23%	21%	-55%
100.0%	1400	193	222	215	10%	13%	-3%
70.0%	1400	208	243	212	2%	14%	-14%
50.0%	1400	243	286	219	-11%	15%	-30%
35.0%	1400	278	355	237	-17%	22%	-50%
100.0%	1600	195	215	214	9%	9%	-1%
70.0%	1600	213	233	215	1%	9%	-8%
50.0%	1600	247	267	222	-11%	8%	-20%
35.0%	1600	307	343	249	-23%	10%	-38%
100.0%	1800	202	228	213	5%	11%	-7%
70.0%	1800	230	256	221	-4%	10%	-16%
50.0%	1800	290	314	238	-22%	8%	-32%
35.0%	1800	376	446	294	-28%	16%	-51%
100.0%	1900	209	236	216	4%	11%	-9%
70.0%	1900	243	272	223	-9%	11%	-22%
50.0%	1900	327	353	251	-30%	8%	-41%
35.0%	1900	435	563	350	-24%	23%	-61%
100.0%	1950	211	242	216	2%	13%	-12%
70.0%	1950	249	282	226	-10%	12%	-24%
50.0%	1950	349	375	259	-34%	7%	-45%
35.0%	1950	472	650	390	-21%	27%	-67%

Table 6 Cat® C4.4 vs SCCC %BSFC Comparison.

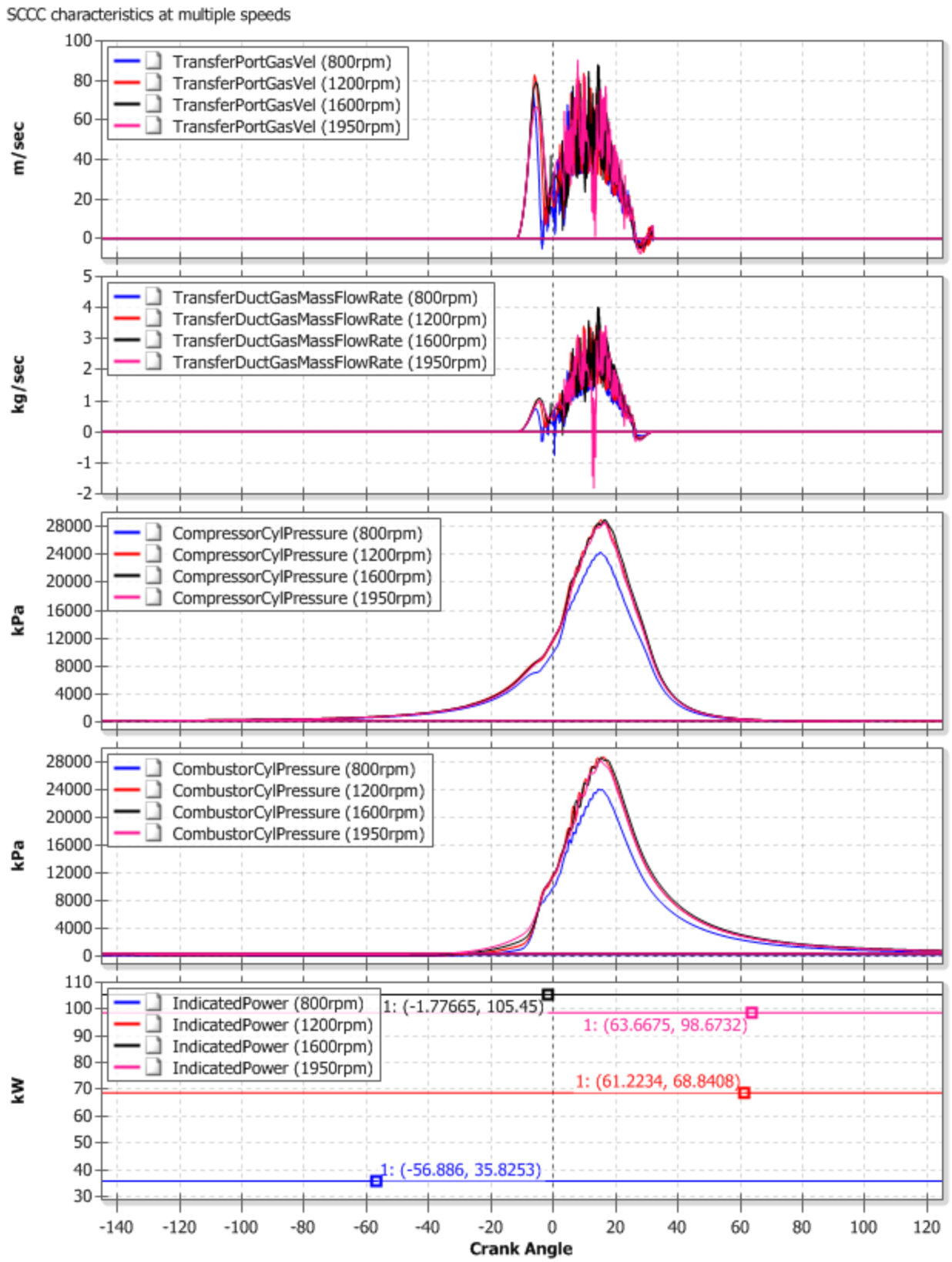

Fig. 52 a. SCCC C4.4 characteristics along multiple points on the lug curve.

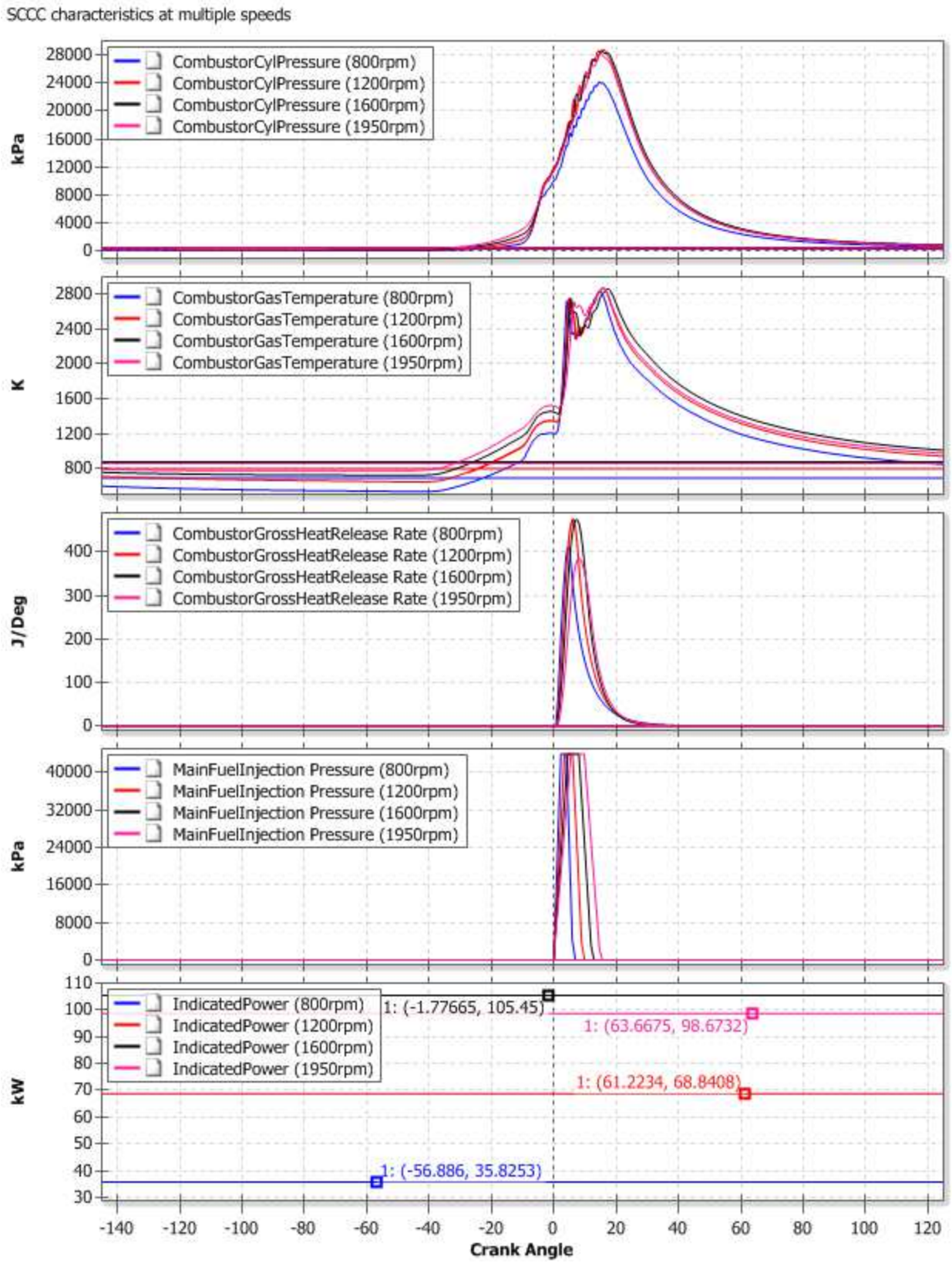

Fig. 52 b. SCCC C4.4 characteristics along multiple points on the lug curve.

Fig. 52 show the operating characteristics of SCCC operating at full load and running at 800, 1200, 1600 and 1950 rpm along the lug curve. The transfer valve mass flow rate, compressor and combustor pressure profiles and other variables as shows provide a good insight to SCCC operation.

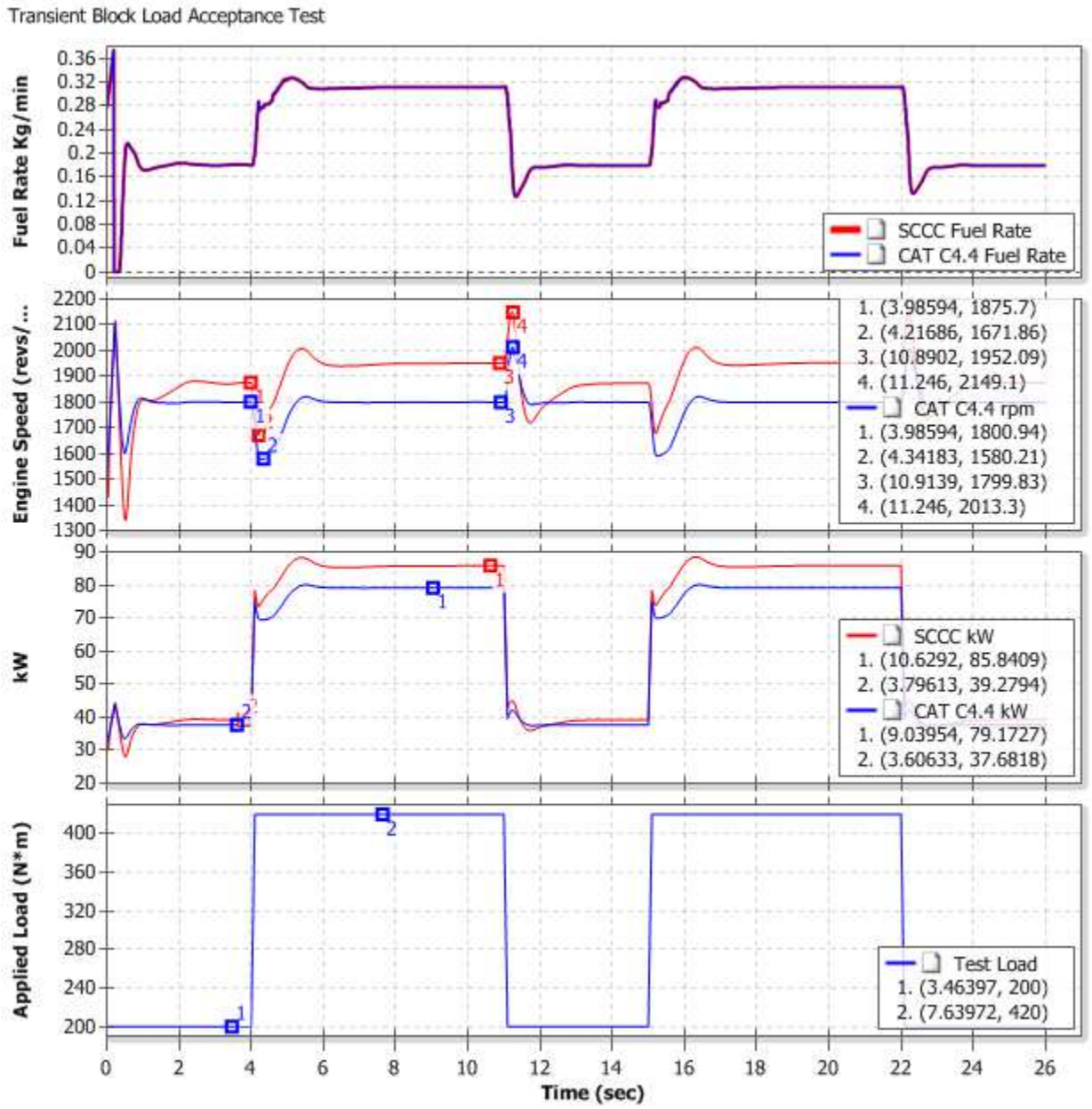

Fig 53. SCCC vs C4.4 Transient evaluation using block load.

Fig. 53 shows the industry standard test for evaluating an engines transient response by block load application and monitoring engine rpm droop and overshoot with reference to a steady state engine rpm upon sudden load application. The graph above does not show the conventional block load application as SCCC engine speed could not be held constant as we did not have a transient engine governor developed for it.

Block Load acceptance test was run at 1800 rpm with a instantaneous load of 85% of peak torque. Cat® C4.4 engine speed drooped by 12% upon load application before recovering and SCCC engine speed drooped by 11% and recovered to a different engine speed due to not being governed. Fig 53 row 1 shows the same fuel rate being fed to both engines and row 4 shows the change in load from 200 Nm to 420 Nm instantly. Overall the block load acceptance test shows that SCCC has a comparable transient response to a conventional compression ignition engine.

Cat® C4.4 governor fuel was used to drive both Cat® C4.4 and SCCC engine. The governor is based on a simple proportional integral control over engine speed of CAT C4.4 thus you can see that C4.4 is held at a constant 1800 engine rpm. As SCCC has a better BSFC the same fuel quantity provided by the governor (referred to as governor fuel) lets the SCCC engine to run at a higher engine speed than the C4.4. However if we look at percentage droop in engine speed upon block load application we can see the SCCC engine has good transient load acceptance characteristics.

Chapter 5

5.1 Conclusions

The study yielded successful results and expanded our understanding of the new Split Cycle Clean Combustion (SCCC) Engine using diesel fuel. There are many research studies that confirm the benefits of SCCC in reducing emission but prior to this study there is no evidence of the efficiency and performance characteristics of a SCCC engine being evaluated in a complete plant model that includes all important air systems. This study thus has been very significant in evaluating SCCC engine in its entire plant setup. This study also demonstrated the use of one-dimensional modeling to model and simulate SCCC with high accuracy along with providing the benefits of expanded component modeling, much faster computational times and opening opportunities for iterative modeling. This study thus has been very significant in evaluating 4.4 liter SCCC engine in its entire plant setup and comparing full load and part load performance to a similar size compression ignition engine using steady state and transient evaluation.

a) In this study a two cylinder Split Cycle Clean Combustion Diesel was successfully modeled and simulated using Caterpillar Inc's one dimensional modeling software Dynasty.
b) The engine, the entire intake and exhaust air system was modeled along with a dynamometer and engine performance was successfully evaluated on a wide range of equivalence ratios.
c) All results from the one dimensional SCCC model matched very well to the results published by University of Pisa using their CFD model thus validating the one-dimensional modeling methodology.

d) A turbocharged four cylinder Split Cycle Clean Combustion Diesel was successfully modeled and simulated using Caterpillar Inc.'s one dimensional modeling software Dynasty.

e) Steady state and transient performance of the engine was successfully evaluated at various engine loads and engine speeds.

f) Results show that the Split Cycle Clean Combustion engine has upto 10% better BSFC to a similar sized compression ignition engine for load factor greater then 55%.

g) Split Cycle Clean Combustion engine operating in 2-stroke cycle has an average volumetric efficiency of 75% throughout its operating range.

h) SCCC engine transient load acceptance characteristics are comparable to a CI engine.

i) SCCC engine can be successfully employed for power generation and on machines for steady state and transient applications.

j) The confidence gained by this study motivated the integration of more complex multi-cylinder turbocharged SCCC engine with varied duct configuration.

5.1 Future Work

5.1.1 Emissions Model Development in one-dimension for SCCC combustion.

One of the many next steps that would build this study would be to develop a soot and NOx emissions model in a parametric form that can be integrated into one-dimensional modeling and yield accurate bi-products during various stages in combustion. There are many studies published that would make for a good foundation for the parametric emissions model.

5.1.2 Engine Governor

There are 3 types of engine governors that commonly exist:

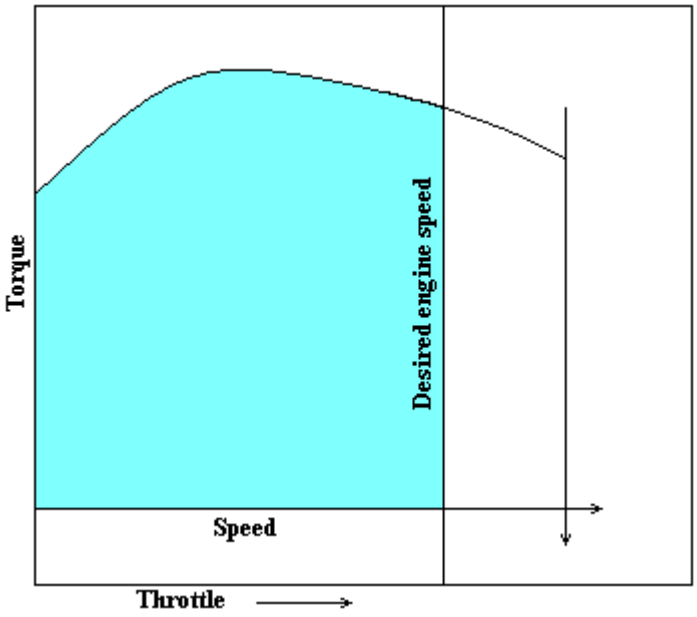

Fig. 54 Full range governor.

a.) Full range governor – it's a proportional integral control to maintain the engine at a desired engine speed. The throttle pedal basically sets a desired speed so as load conditions change on the engine, governor will vary fuel quantity to deliver the required torque to maintain the engine at the desired speed.

b.) Min-max governor – it's a proportional integral control to maintain the engine at a desired engine torque. The throttle pedal basically sets a desired torque so as load conditions change on the engine, governor will vary fuel quantity to keep operating at the desired torque and while engine speed can vary.

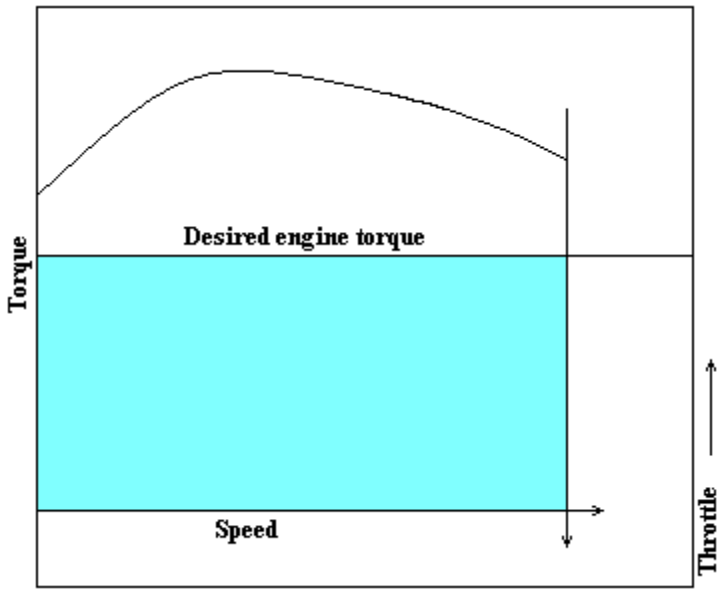

Fig. 55 Min-max governor.

c.) Speed torque governor – this type of a governor operates the engine in a boundary defined by upper and lower speed limits and upper and lower torque limits.

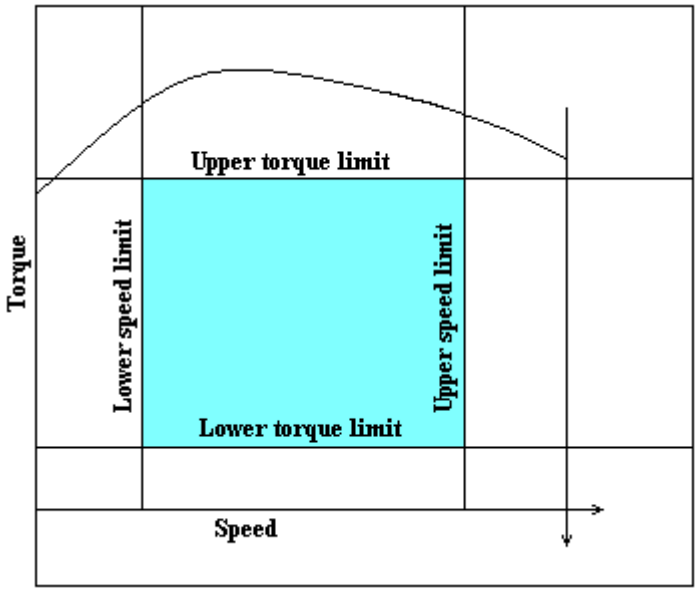

Fig. 56 Speed torque governor.

Engine governors have the job of controlling the engine to a desired operating point while monitoring emissions and working under the emissions limit. So once the emissions are modeled the next step would be to develop a governor control and do a back to back comparison again to a conventional diesel engine, so that a specified rating can be decided for the engine and the performance can be evaluated on a smaller region in focus based on the application requirements. Different applications my employ different types on engine governors based on their need to control engine speed or engine torque or both.

Cited Literature

1. Musu, E., Rossi, R., Gentili, R., and Reitz, R., (2010), “Clean Diesel Combustion by Means of the HCPC Concept”, SAE Paper 2010-01-1256.
2. Rao, S., Rutland, C. J., and Fiveland S. B., (2003), “A Computationally Efficient Method for the Solution of Methane - Air Chemical Kinetics With Application to HCCI Combustion”, SAE Paper 2003-01-1093.
3. Babajimopoulos, A., Assanis and D. N., and Fiveland S. B., (2002), “An Approach for Modeling the Effects of Gas Exchange Processes on HCCI Combustion and Its Application in Evaluating Variable Valve Timing Control Strategies”, SAE Paper 2002-01-0829.
4. Simescu, S., Fiveland S. B., and Dodge, L.G., (2003), “An Experimental Investigation of PCCI-DI Combustion and Emissions in a Heavy-Duty Diesel Engine”, SAE Paper 2003-01-0345.
5. Khalid, A., Yatsufusa, T., Miyamoto, T., Kawakami, J., and Kidoguchi, Y., (2009), “Analysis of Relation between Mixture Formation during Ignition Delay Period and Burning Process in Diesel Combustion”, SAE Paper 2009-32-0018/20097018.
6. Aradi, A. A., and Thomas, W. R. (1995), “Cetane Effect on Diesel Ignition Delay Times Measured in a Constant Volume Combustion Apparatus”, SAE Paper 952352.
7. Musu, E., Rossi, R., Gentili, R., and Reitz, R. (2010), “CFD Study of HCPC Turbocharged Engine”,SAE Paper 2010-01-2107.

8. Olsson, J., Tunestål, P., Johansson, B., Fiveland, S. B., Agama, R., Wili, M., and Assanis, D. (2002), "Compression Ratio Influence on Maximum Load of a Natural Gas Fueled HCCI Engine", SAE Paper 2002-01-0111.

9. Kang, JM., Chang, CF., Chen, JS., and Chang, MF. (2009), "Concept and Implementation of a Robust HCCI Engine Controller", SAE Paper 2009-01-1131.

10. Fiveland S. B., and Assanis, D. N., (2002), "Development and Validation of a Quasi-Dimensional Model for HCCI Engine Performance and Emissions Studies Under Turbocharged Conditions", SAE Paper 2002-01-1757.

11. Kim Y., Min, K., Kim, MS., Chung, SH., and Bae, C., (2007), "Development of a Reduced Chemical Kinetic Mechanism and Ignition Delay Measurement in a Rapid Compression Machine for CAI Combustion", SAE Paper 2007-01-0218.

12. Fiveland S. B., and Assanis, D. N., (2001), "Development of a Two-Zone HCCI Combustion Model Accounting for Boundary Layer Effects", SAE Paper 2001-01-1028.

13. Zaidi, K., and Andrews, G. E., (2011), "Diesel Fumigation Partial Premixing for Reducing Ignition Delay and Amplitude of Pressure Fluctuations", SAE Paper 980535.

14. Ladommatos, N., Abdelhalim, S. M., Zhao, H., and Hu, Z., (2011), "Effects of EGR on Heat Release in Diesel Combustion", SAE Paper 98018.

15. Fiveland S. B., Agama, R., Christensen, M., Johansson, B., Hiltner, J., Mauss, F., and Assanis, D. N., (2001), "Experimental and Simulated Results Detailing the Sensitivity of Natural Gas HCCI Engines to Fuel Composition", SAE Paper 2001-01-3609.

16. Yun, H., Wermuth, N., and Najt, P., (2011), "High Load HCCI Operation Using Different Valving Strategies in a Naturally-Aspirated Gasoline HCCI Engine", SAE Paper 2011-01-0899.

17. Gray, A.W., and Ryan, T. W., (1997), “Homogeneous Charge Compression Ignition (HCCI) of Diesel Fuel”, SAE Paper 971676.

18. Musu, E., Gentili, R., and Reitz, R. D., (2009), “Homogeneous Charge Progressive Combustion (HCPC): CFD Study of an Innovative Diesel HCCI Concept”, SAE Paper 2009-01-1344.

19. Shudo, T., Ono, Y., and Takahashi, T., (2003), “Ignition Control by DME-Reformed Gas in HCCI Combustion of DME”, SAE Paper 2003-01-1824.

20. Nishijima, Y., Asaumi, Y., and Aoyagi, Y., (2002), “Impingement Spray System with Direct Water Injection for Premixed Lean Diesel Combustion Control”, SAE Paper 2002-01-0109.

21. Santoso, H., Matthews, J., and Cheng, W. K., (2005), “Managing SI/HCCI Dual-Mode Engine Operation”, SAE Paper 2005-01-0162.

22. Wayne, W. S., Corrigan, E. R., Atkinson, R. J., Clark, N. N., and Lyons, D. W., (2001) “Measuring Diesel Emissions with a Split Exhaust Configuration”, SAE Paper 2001-01-1949.

23. Ayoub, N. S., and Reitz, R. D., (1995), “Multidimensional Modeling of Fuel Composition Effects on Combustion and Cold-Starting in Diesel Engines”, SAE Paper 952425.

24. Wang, Z., Shuai, SJ., and Wang, JX., (2008), “Multi-dimensional Simulation of HCCI Engine Using Parallel Computation and Chemical Kinetics”, SAE Paper 2008-01-0966.

25. Wiese, W., Pischinger, S., Adomeit, P., and Ewald, J., (2009), “Prediction of Combustion Delay and –Duration of Homogeneous Charge Gasoline Engines based on In-Cylinder Flow Simulation”, SAE Paper 2009-01-1796.

26. Kumar, R. H., and Antony, A. J., (2008), “Progressive Combustion in SI-Engines-Improved Empirical Models for Simulating and Optimizing Engine Performance”, SAE Paper 2008-01-1630.

27. Zhong, S., and Jin, G., Wyszynski, M. L., and Xu, H., (2006), “Promotive Effect of Diesel Fuel on Gasoline HCCI Engine Operated with Negative Valve Overlap (NVO)”, SAE Paper 2006-01-0633.

28. Wang, Z., Wang, JX., Tian, GH., Shuai, SJ., Zhang, Z., and Yang, J., (2008), “Research on Steady and Transient Performance of an HCCI Engine with Gasoline Direct Injection”, SAE Paper 2008-01-1723.

29. Kuleshov, A., Kozlov, A V., and Mahkamov, K., (2010), “Self-Ignition Delay Prediction in PCCI Direct Injection Diesel Engines Using Multi-Zone Spray Combustion Model and Detailed Chemistry”, SAE Paper 2010-01-1960.

30. Hiltner, J., Fiveland, S., Agama, R., and Willi, M., (2002), “System Efficiency Issues for Natural Gas Fueled HCCI Engines in Heavy-Duty Stationary Applications”, SAE Paper 2002-01-0417.

31. Shibata, G., Oyama, K., Urushihara, T., and Nakano, T., (2004), “The Effect of Fuel Properties on Low and High Temperature Heat Release and Resulting Performance of an HCCI Engine”, SAE Paper 2004-01-0533.

32. Bower, G. R., and Foster, D. E., (1993), “The Effect of Split Injection on Soot and NOx Production in an Engine-Fed Combustion Chamber”, SAE Paper 932655.

33. Agrell, F., Ångström, H. E., Eriksson, B., Wikander, J., and Linderyd, J., (2003), “Transient Control of HCCI through Combined Intake and Exhaust Valve Actuation”, SAE Paper 2003-01-3172.

34. Zhao, H., Peng Z., Williams, J., and Ladommatos, N., (2001), “Understanding the Effects of Recycled Burnt Gases on the Controlled Autoignition (CAI) Combustion in Four-Stroke Gasoline Engines”, SAE Paper 2001-01-3607.

35. Gong, W., Bell, S. R., Micklow, G. J., Fiveland, S. B., and Willi, M. L.,” (2002), “Using Pilot Diesel Injection in a Natural Gas Fueled HCCI Engine”, SAE Paper 2002-01-2866.

36. Bunting, B. G., Eaton, S. J., and Crawford, R. W., (2009) “Performance Evaluation and Optimization of Diesel Fuel Properties and Chemistry in an HCCI Engine”, SAE Paper 2009-01-2645.

37. Pedersen, P. S., and Qvale, B., (1974), “A Model for the Physical Part of the Ignition Delay in a Diesel Engine”, SAE Paper 740716.

38. Chen, C., and Veshagh, A., (1992), “A One-Dimensional Model for In-Cylinder Heat Convection Based on the Boundary Layer Theory”, SAE Paper 921733.

39. Sjöberg, M., Dec, J. E., Babajimopoulos, A., and Assanis, D., (2004), “Comparing Enhanced Natural Thermal Stratification Against Retarded Combustion Phasing for Smoothing of HCCI Heat-Release Rates”, SAE Paper 2004-01-2994.

40. Teng, H., McCandless, J. C., Schneyer, J. B., (2003), “Compression Ignition Delay (Physical + Chemical) of Dimethyl Ether – An Alternative Fuel for Compression-Ignition Engines”, SAE Paper 2003-01-0759.

41. Grose, D. J., and Austin, K., (2001), “Coupling of One Dimensional and Three Dimensional Simulation Models”, SAE Paper 2001-01-1770.

42. Bobba, M. K., Genzale, C, L., and Musculus, M. P. B., (2009), “Effect of Ignition Delay on In-Cylinder Soot Characteristics of a Heavy Duty Diesel Engine Operating at Low Temperature Conditions”, SAE Paper 2009-01-0946.

43. Patterson, M., and Hampson, G. J., (2008), “Heat Release Design Method for HCCI in Diesel Engines with Simulation”, SAE Paper 2008-28-0006.

44. Musu, E., Rossi, R., Gentili, R., and Reitz, R., (2011), “Heavy Duty HCPC”, SAE Paper 2011-01-1824.

45. Arias, D. A., and Shedd, T. A., (2006), “Implementation of a Theoretical Carburetor Model in One-Dimensional Engine Simulation Software”, SAE Paper 2006-01-1543.

46. Sendyka, B., and Filipczyk, J., (1995), “Simulation of the Characteristic of a Carburetor of an Internal Combustion Engine”, SAE Paper 950987.

47. Lyn, W. T., and Valdmanis, E., (1968), “The Effects of Physical Factors on Ignition Delay”, SAE paper 680102.

48. Rosseel, E., and Roger, S., (1996), “The Physical and the Chemical Part of the Ignition Delay in Diesel Engines”, SAE Paper 961123.

49. Assanis, D. N., Filipi, Z. S., Fiveland, S. B., and Syrimis, M., (2000), “A Methodology for Cycle-By-Cycle Transient Heat Release Analysis in a Turbocharged Direct Injection Diesel Engine”, SAE Paper 2000-01-1185.

50. Mo, Y., (2008), “HCCI Heat Release Rate and Combustion Efficiency: A coupled KIVA Multi-Zone Modeling Study”, University of Michigan Doctoral Thesis.

51. Etheridge, J. E., Mosbach, S., Kraft, M., Wu, H., Collings, N., (2010), “A Fast Detailed-Chemistry Modeling Approach for Simulating the SI-HCCI Transition”, SAE Paper 2010-01-1241.

52. Inventor Name.: Method for selecting fuel to both optimize the operating range and minimize the exhaust emissions of HCCI engines, US Patent 7,487,663.

53. US Patent 7,469,181, Caterpillar Inc.: High load operation in a homogeneous charge compression ignition engine.

54. US Patent 7,377,270, Caterpillar Inc.: Exhaust gas recirculation in a homogeneous charge compression ignition engine.

55. US Patent 7,377,254, Caterpillar Inc.: Extending operating range of a homogeneous charge compression ignition engine via cylinder deactivation.

56. US Patent 7,171,924, Caterpillar Inc.: Combustion control system of a homogeneous charge.

57. US Patent 7,131,402, Caterpillar Inc.: Method for controlling exhaust emissions from direct injection homogeneous charge compression ignition engines.

58. US Patent 6,752,104, Caterpillar Inc.: Simultaneous dual mode combustion engine operating on spark ignition and homogenous charge compression ignition.

59. US Patent 6,668,788, Caterpillar Inc.: Homogenous charge compression ignition engine having a cylinder including a high compression space.

60. US Patent 6,601,549, Caterpillar Inc.: Two stroke homogenous charge compression ignition engine with pulsed air supplier.

Vita

PERSONAL INFORMATION

Full name: Keshav Sud

E-mail address: keshav707@gmail.com

ACADEMIC BACKGROUND

Doctors of Philosophy, Mechanical Engineering, University of Illinois at Chicago, 2013.

Masters of Science, Mechanical Engineering, University of Illinois at Chicago, 2008.

Bachelors of Technology, Mechanical Engineering, Indraprastha University, 2007.

ACAMDEMIC/RESEARCH EXPERIENCE

Teaching Assistant, University of Illinois at Chicago, 2009.

Research Assistant, University of Illinois at Chicago, 2008.

PROFESSIONAL BACKGROUND

Caterpillar Inc., Peoria Illinois, 2010 – Current.

Caterpillar Inc., Peoria Illinois, Intern, 2008.

Honda, India, Intern, 2007.

Siemens, India, Intern, 2006.

LANGUAGES

English

PUBLICATIONS

1. Sud, K., Cetinkunt, S.,Fiveland, S. B.,Fluga, E. C., (2013), "A Simulation Based Comprehensive Performance Evaluation of CAT C4.4 Current Production Engine with its Split Cycle Clean Combustion Variant", SAE COMVEC 2013, Rosemont IL, Oct. 1st 2013, 13CV-0016.

2. Sud, K., Cetinkunt, S.,Fiveland, S. B.,Fluga, E. C.(2013), "Validating One-Dimensional Modeling Methodology of a Split Cycle Clean Combustion Diesel Engine", SAE COMVEC 2013, Rosemont IL, Oct. 1st 2013, 13CV-0017.

3. Sud, K., Cetinkunt, S.,Fiveland, S. B.,Fluga, E. C., (2013), "Steady State and Transient Performance Evaluation Between CAT C4.4 Engine and Its Split Cycle Clean Combustion Concept Variant", ASME Journal of Engineering for Gas Turbine and Power, GTP-13-1047, Submitted Feb. 10th, 2013.

4. Sud, K., Cetinkunt, S.,Fiveland, S. B.,Fluga, E. C., (2013), "Modeling and Validation of a Split Cycle Clean Combustion Diesel Engine Concept", ASME Journal of Engineering for Gas Turbine and Power, GTP-13-1045.